JOURNAL

OF

FOOD

PROCESS

ENGINEERING

FOOD & NUTRITION
PRESS, INC.

JOURNAL OF FOOD PROCESS ENGINEERING

JOURNAL OF FOOD PROCESS ENGINEERING

JOURNAL OF FOOD PROCESS ENGINEERING

Journal of
FOOD PROCESS
ENGINEERING

Printed in the United States of America

CONTENTS

ENZYMES IMMOBILIZED ON FORMED-IN-PLACE MEMBRANES FOR FOOD PROCESSING: PROCEDURES AND PROPERTIES

H. JEAN WANG[1], RONALD L. THOMAS[1], ANDRZEJ R. SZANIAWSKI[2,3]
and H. GARTH SPENCER[2,4]

[1]*Department of Food Science and* [2]*Department of Chemistry*
Clemson University, Clemson, SC 29634

ABSTRACT

The formation and properties of Formed-In-Place (FIP) membranes upon which enzymes had been immobilized were investigated to examine the potential of these reactive membranes in food processing applications. Enzymes were immobilized on two types of FIP membranes and their activities in appropriate fluids investigated. Flux was increased in the microfiltration of pectin solutions by immobilizing pectinase on titanium dioxide microfiltration membranes. A flux increase of 15% was obtained without permeate recycle and 112% with permeate recycle using a 0.1% solution of citrus pectin. Glucose production from dextrin was performed using glucoamylase (GA) immobilized on a zirconium hydrous oxide-polyacrylate nanofiltration membrane. Optimum activity occurred at pH 4.0 and 50C for the immobilized GA. The dextrose equivalent (DE) value of the membrane permeate was approximately ten times higher than the product obtained with free GA during the same time interval.

INTRODUCTION

Immobilized enzymes have been used for a variety of applications in food processing (Cheryan 1986). This report is concerned with the properties of Formed-In-Place (FIP) membranes containing immobilized enzymes as used in two potential food processing applications; immobilization of pectinase on a microfiltration membrane to improve the flux in separations of solutions containing pectin and immobilization of glucoamylase (GA) on a nanofiltration

---

membrane to form a membrane bioreactor for the conversion of dextrins to glucose. Preliminary results using different FIP membranes had indicated promise in these types of applications (Thomas *et al.* 1989a,b).

The FIP microfiltration membrane used for the pectin separation was a permanent titanium oxide microfiltration layer on a porous stainless steel tube, rather than the replaceable microfiltration layers on the stainless steel tube used in the previous investigations. The properties of the membrane used in the microfiltration of pectin solutions have been investigated without immobilized enzymes (Szaniawski and Spencer 1991). These membranes are very durable in most applications, including harsh washing conditions such as the normal clean-in-place (CIP) procedures used in the food processing industry (Spencer and Thomas 1991). The FIP membrane used in the investigation of the conversion of dextrins to glucose was a nanofiltration membrane that permits passage of glucose while rejecting the incompletely hydrolyzed dextrins better than the previously used microfiltration membrane.

The addition of enzymes has been considered for processes involving membrane separations or concentrations of fruit juices and other liquid food streams that contain pectin because pectin is often considered a major contributor to fouling in these systems. For example, Medina and Garcia (1988) report the use of pectinase as a pretreatment in the reverse osmosis concentration of orange juice. Although the flux was not improved in this application, the standard membrane cleaning procedure used after the concentration of the pectinase pretreated juice prevented the loss of productivity that was observed with repeated experiments with the membrane used without pectinase pretreatment. The pectin and cellulose layer accumulation on the membrane was avoided by the pretreatment with pectinase. However, the concentrate produced from the enzyme-treated juice exhibited some settling, apparently because the pectin had experienced partial degradation.

The use of pectinase immobilized on the membrane should affect the pectin in a concentrate less than pretreatment of the bulk solution. If its presence on the membrane increased flux or facilitated cleaning, the benefits of the degradation at the membrane surface could be realized with a minimum alteration of the concentrate.

Bioreactors can be made continuous in operation by using immobilized enzymes on a support in a column reactor or a membrane reactor. These continuous operation reactors are considered useful or potentially useful. Continuous bioreactors using membranes include several types:

(1)   membrane recycle reactors containing free or immobilized enzymes that can be retained by an ultrafiltration membrane that passes the product and usually other components of the reaction mixture,

(2)   hollow fiber reactors with the enzyme isolated from the substrate mixture

by an ultrafiltration membrane in which both substrate and product must pass through the membrane,

(3)   membrane immobilized enzyme recycle reactors with the enzyme immobilized on the reaction mixture side of a membrane that also provides separation of the product from the mixture, and

(4)   a combination of membrane recycle reactor and membrane immobilized enzyme recycle reactor.

This paper reports results of experiments associated with two food processing applications, ultrafiltration or microfiltration of pectin containing solutions and conversion of dextrin to glucose, utilizing enzymes immobilized on Formed-In-Place membranes. The microfiltration experiments were carried out with dilute pectin solutions using a microfiltration membrane with and without immobilized pectinase to determine the effect of the immobilized pectinase on the flux and the degradation of the pectin in the recycling solution. The experiments with glucoamylase (GA) immobilized on a hyperfiltration membrane operated as a membrane immobilized recycle reactor for the conversion of dextrin to glucose were run to investigate the immobilization procedures, the activity properties of the immobilized GA and the feasibility of the reactor system.

MATERIALS AND METHODS

Membranes

The substrates for the FIP membranes are titanium dioxide microfiltration (MF) membranes on the inside surface of porous sintered stainless steel tubes, supplied as AS microfiltration membranes by Du Pont Separation Systems, Inc. The AS microfiltration membrane was used as received in the experiments to separate pectin. The modules were 1.6 cm ID tubes providing areas of 0.025 m^2 enclosed in stainless steel housings. The membrane used in the dextrin-glucose bioreactor consisted of a zirconium (IV) hydrous oxide-polyacrylate layer formed on a module of like dimensions by the procedure described by Thomas et al. (1977) and provided hyperfiltration properties representative of the ZOPA membranes marketed by Du Pont Separation Systems, Inc. The rejection of a 0.02 M NaNO$_3$ solution was 0.80–0.95 at pH > 5, and the rejection of glucose was about 0.5 with less dependence on pH.

Materials

Citrus pectin obtained from U.S. Biochemical Corp. (Cleveland, OH) was used in the experiments. Polygalacturonase (pectinase) from *Aspergillus niger*

(EC 3.2.1.15), 3-9 U/mg protein (one unit liberates 1.0 mmol of galacturonic acid from polygalacturonic acid per min at pH 4.0 at 25C) obtained from Sigma Chemical Co. (St. Louis, MO) was used as the enzyme. Glucoamylase (GA) (EC 3.2.1.3, mixture of *Rhizopus mold*) with an activity of 12 U/mg and Type I dextrin (average MW 6,000) obtained from Sigma Chemical Co. (St. Louis, MO) were used in the experiments. The maltose, maltotriose, D glucose and other low molecular weight saccharides were also obtained from Sigma Chemical Co. (St. Louis, MO) for use as analysis standards.

Membrane System and Procedures

The membrane system consisted of a feed tank, high pressure triplex positive displacement pump, membrane module, pressure gauge at the inlet of the module (P), a letdown valve in the concentrate return line from the module to the feed tank (V2) and a control valve in the line bypassing the module (V3) (Fig. 1). The temperature was controlled with a cooling or heating coil in the feed tank. Flows were measured by timed volume collection. The pressure and crossflow velocity were established with the control valves. Zero recovery experiments were maintained by returning both permeate and concentrate flows to the feed reservoir.

The pectin microfiltration experiments were run at 45 ± 1C, crossflow velocity of 1.5 m/s and at various pressures with 0.1% citrus pectin solutions. Fresh fruit juices contain pectin concentrations that begin at about 0.2% (Fogarty and Ward 1972). Most of the dextrin hydrolysis experiments using immobilized GA were run by circulating a 10 L volume of a 1.0% dextrin solution in distilled water adjusted to pH 5.0 through the module with complete recycle of the permeate at 21 bar and 30 ± 1C.
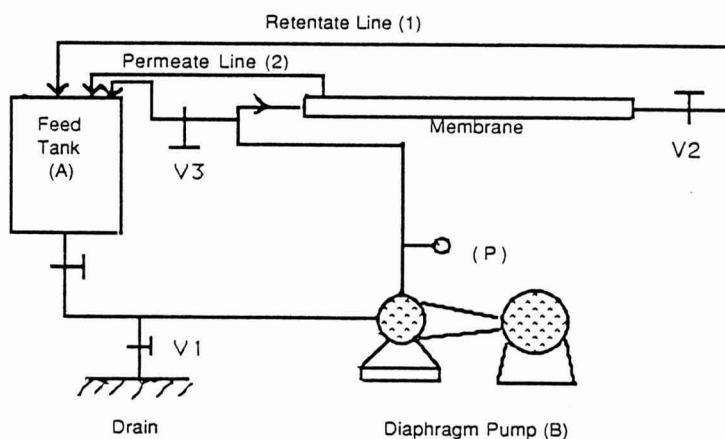
FIG. 1. SCHEMATIC OF THE FILTRATION SYSTEM

Analysis Procedures

The pectic substances concentration was determined by the Robertson (1979) colorimetric method with m-hydroxydiphenyl color reagent and the reducing sugar concentration by the Nelson (1944) colorimetric method with arsenomolybdate color reagent. The relative number average degree of polymerization of the permeate and feed, $<DP>_P$ / $<DP>_F$, were estimated from these measurements. The concentration of protein was determined using the Bio-Rad assay procedure. The total amount of protein as obtained in the crude enzyme reagent is reported for the pectinase experiments.

The GA concentration was determined in the presence of the other proteins in the enzyme solution by high performance size exclusion chromatography (HPSEC), the low molecular weight oligosaccharides were resolved by HPLC as reported by Wang and Thomas (1991) and the total carbohydrate concentration by the method described by Brooks *et al.* (1986).

The HPSEC analysis for GA was determined with a Beckman TSK 3000SW column (300 × 7.5 mm), connected to a TSK precolumn (75 × 7.5 mm). The mobile phase was a 0.1 M potassium phosphate buffer (pH 6.0), which had been filtered through a 0.45 μm filter before HPSEC analysis. A 20 μl sample of GA solution was eluted at a flow rate of 0.5 ml/min and detected with a Waters Model 440 absorbance detector at a wave length of 280 nm. The GA concentration calculated with reference to peak height standard curves, which were integrated with a Waters Model 740 data module, attenuated at 128X.

Low molecular weight oligosaccharides (DP 1–10) were resolved by HPLC using a 10 cm × 8 mm ID C_{18} cartridge installed in a rubber sleeve within a RCM-100 radial compression module. The rubber sleeve was surrounded by a hydraulic fluid (glycerine); pressure was generated by moving three lever-driven pistons in the glycerine. The pressure was transmitted through the flexible sleeve to the wall of the cartridge, as well as to the particles of the packed bed. A modified inlet connector was used to fit the Guard-PAK precolumn inserts directly into the Radial-PAK C_{18} cartridge (Waters Associates, Milford, MA). HPLC-grade water as the mobile phase was filtered through a 0.22 μm filter and degassed under vacuum. Sugar standards for DP were prepared from 1.0 mg/ml glucose, maltose and maltotriose. Standard solutions were used to determine the retention time and concentration. The sugars were passed through a 0.45 μm filter prior to injection. The concentration of each saccharide (DP 4 to DP 10) was determined relative to a glucose standard. A 15 μl volume of the dextrin hydrolysate was eluted with water at a flow rate of 1.0 ml/min and detected with a Waters Model 410 differential refractive index detector.

Immobilization of Enzymes on the Membranes

The pectinase was adsorbed on the microfiltration module by circulating a dilute solution of the crude enzyme (about 55 mg/l) buffered at pH 3.5 through the apparatus under 7.0 bar pressure for 60 min. The amount of protein adsorbed was determined by analysis of the decrease in protein content of the solution corrected for the amount adsorbed by the apparatus without the module. The adsorption of protein was approximately 5.0 g/m^2 after 60 min, with about 90% of this amount adsorbed in 5 min.

The immobilization of GA on the nanofiltration membrane was accomplished using the procedures of Thomas *et al.* (1989a). A 10 L volume of 0.1% (w/v) GA in 0.05 M sodium acetate buffer at pH 5.0 was recirculated through the coated module at pressures up to 50 bar. The maximum GA immobilization was achieved in 20 min. The amount of GA immobilized on the membrane was determined from the decrease of its concentration in the buffer solution by the HPSEC analysis. A 10 L volume of distilled water, adjusted to pH 5.0 was circulated through the module to remove free GA and the other proteins in the enzyme solution.

Catalytic Activity of Free and Immobilized Glucoamylase

The catalytic activity of both free (soluble) and immobilized GA was determined by measuring the amount of glucose liberated from a 1.0% dextrin solution. The immobilized GA activity was evaluated by a once-through or single pass experiment using the membrane with immobilized GA. Prior to dextrin hydrolysis after GA immobilization, the enzymatic zirconium hydrous oxide-polyacrylate membrane was washed with 20 L of distilled water and 10 L of sodium acetate buffer (pH 4.0) for 30 min at 14 bar and again with 10 L of distilled water to remove the free GA. To determine the catalytic activity of the immobilized GA, 10 L of 1.0% dextrin was circulated through the membrane for 20 min at 30C with a trans-membrane pressure of 14 bar. The permeate was analyzed for low molecular weight saccharides by HPLC, reducing sugars (Thomas *et al.* 1989a), and total carbohydrates. The dextrose equivalent (DE) was calculated as the ratio of the reducing sugar content to the total carbohydrate content times 100. The free GA activity was determined by preparing 2.0 ml of 1.0% dextrin solution in a capped test tube and adding 27.5 ml of 0.1% crude GA and incubating in a water bath. The reaction mixtures were inactivated at 100C for 1 min.

Membrane Cleaning

The ability to restore UF or MF membrane productivity after a period of use on process streams that foul is necessary for the successful use of mem-

branes in most applications. The water permeability was measured before and after the experiments with pectin solutions. Cleaning after the pectin experiments was attempted by first washing with water without recycle of permeate or concentrate at minimum pressure, maximum crossflow velocity, and 45 ± 1C. The water permeability was again measured. The object was to determine the extent of the water permeability reduction resulting from the exposure to the pectin that was reversible to a water wash. The membrane was then cleaned by a CIP procedure consisting of circulating a pH 11.5 NaOH solution for about 10 min, flushing out this solution and washing with about 50 L of water, circulating a dilute (about 0.2%) hydrogen peroxide solution for about 30 min, flushing out this solution, washing with about 50 L of water, and determining the water permeability again. This CIP treatment restored the original permeability to the MF membrane over a series of many experiments. The object was to determine the extent of the water permeability reduction by the pectin that could be considered permanent or requiring chemical removal. As a last step of cleaning and preparation for immobilization of the enzyme, the membrane was washed with a HNO_3 solution at pH 2.5 for 30 min and rinsed with water. In contrast to the harsh treatment of the UF membrane, the nanofiltration membrane used in the immobilized GA experiments was normally only washed with water and sodium bicarbonate solutions between experiments to avoid altering the nanofiltration layer by harsh cleaning methods.

RESULTS AND DISCUSSION

Microfiltration of Pectin Solutions

The effects of the immobilized pectinase were determined by comparing flux, rejection and other properties of the membrane with and without immobilized pectinase in the microfiltration of a 0.1% citrus pectin solution at pH 3.5. Results of three sequences of ultrafiltration experiments are presented:

(1) without immobilized pectinase and with permeate recycle,
(2) with immobilized pectinase and without permeate recycle, and
(3) with immobilized pectinase and permeate recycle.

A new pectin solution was used at each pressure in experiment sequence (2). The pectin solution was not changed for the series of pressures in experiment sequences (1) and (3).

The dependence of flux on pressure is shown in Fig. 2. The typical gel-polarized behavior of ultrafiltration of macromolecules, i.e., a dependence of flux on pressure at low pressure followed by a transition to flux independent
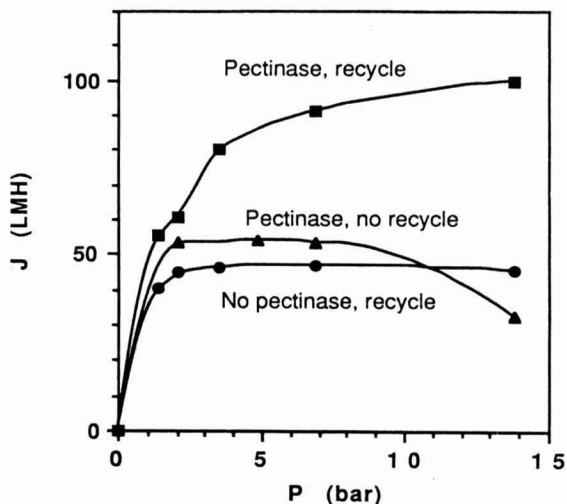
FIG. 2. FLUX OF 0.1% PECTIN SOLUTION VERSUS PRESSURE
●, Without pectinase and with permeate recycle; ▲, with pectinase
and without permeate recycle; and ■, with pectinase and
permeate recycle.

of pressure at higher pressure, was exhibited in experiment sequence (1). The experiment with the immobilized enzyme without permeate recycle, experiment sequence (2), gave a similar pressure dependence of the flux but exhibited an apparent small decline in flux at high pressure. The flux in the range of 3–7 bar for the experiments with immobilized pectinase (2) is about 15% greater than the flux in the experiments without immobilized enzyme (1). The flux for the experiment sequence with immobilized enzyme and permeate recycle (3) exhibited a strong dependence on pressure followed by a weak dependence, attaining about a 112% increase over the experiment without immobilized enzyme (1) at 14 bar.

The flux and other results of the three series of experiments are summarized in Table 1. The pectin rejection in the three experiment sequences was 0.85 for (1), 0.89 for (2) and 0.99 for (3) and independent of the pressure. The ratio of $<DP>$ of the permeate to the feed (or concentrate) as determined by the analysis of reducing sugar and pectin was 0.83 for the experiments without immobilized pectinase and with permeate recycle (1), 0.05 for the experiments with immobilized pectinase and without permeate recycle (2), and 0.007 for the experiments with immobilized pectinase and permeate recycle (3).

TABLE 1.
SUMMARY OF RESULTS OF THE THREE SERIES OF MICROFILTRATION
EXPERIMENTS USING 0.1 g/L PECTIN SOLUTIONS WITH THE AS MEMBRANE

Procedures and Results	Experiment Sequence		
	1	2	3
Immobilized Pectinase	No	Yes	Yes
Permeate Recycle	Yes	No	Yes
Maximum Flux (LMH)	47	54	100
Pectin Rejection	0.85	0.89	0.99
Ratio of <DP> in permeate to <DP> in feed	0.83	0.05	0.007
Flux loss irreversible to water wash, %	89	93	95

These large reductions in $<DP>$ of the permeates of the membranes with immobilized pectinase suggest that the enzyme remained active when immobilized. No protein was detected in the feed or permeate solutions of experiment sequences (2) and (3), indicating that the enzyme remained immobilized during the experiments using the pectin solutions. Although the decrease in the average degree of polymerization ($<DP>$) of the pectin in the feed in experiment sequence (3) was only 3.5%, the flux increase in this experiment was greater by a factor of about seven over the increase in flux in the experiment without permeate recycle.

The cleaning experiments following the pectin experiments implied that the permeability reduction resulting from the exposure to the pectin could be largely attributed to fouling that was irreversible to washing with water; 89% in experiment sequence (1), 93% in experiment sequence (2) and 95% in experiment sequence (3).

The much larger flux obtained in experiment sequence (3) than in experiment sequence (2), where immobilized enzyme was present in both but the permeate was recycled only in experiment sequence (3), is striking. The immobilized enzyme should primarily alter the molecular mass only of the pectin on the membrane surface and in its pores. The recycled permeate resulted in only a small, about 3.5%, reduction of the molecular mass of the feed.

Mechanisms accounting for the additional increase resulting from the recycle remain speculative.

Adsorption of larger amounts of pectinase than the usual 5.0 g/m^2 resulted in fluxes during microfiltration of the pectin solution that were less than the flux of the membrane without immobilized pectinase. More enzyme is not necessarily better in this case.

No systematic reduction in flux was observed in the extended series of experiments. In fact the water permeability increased slightly with use. This was observed for sequences of experiments with and without immobilized enzymes because complete cleaning was accomplished with the FIP microfiltration membranes.

These results suggest methods of modifying the flux of these MF membranes in separations of feed streams in which pectin contributes significantly to limiting the flux. If a small reduction in viscosity of the concentrate product by pectin hydrolysis can be tolerated, a partial recycle of the permeate in the process with a controlled amount of pectinase immobilized on the membrane, or a very small amount of pectinase in the bulk that is later deactivated, could significantly enhance the flux. If absolutely no pectin hydrolysis can be tolerated in the concentrate product, the processing flux might be increased modestly through the use of pectinase immobilized on the membrane without any recycle of the permeate.

Glucose from Dextrins

The optimum pH for immobilization of GA on the zirconium hydrous oxide-polyacrylate membrane was approximately 5. No GA was detected by HPLC in the membrane permeate during the immobilization process, indicating its complete rejection. The amount of GA adsorbed at pH 5 appeared to be pressure dependent, with the optimum occurring at approximately 14 bar (Fig. 3). However, glucose production was only slightly higher when the enzyme was immobilized at 14 bar (Fig. 4), indicating that a substantial portion of the additional enzyme being adsorbed at that pressure did not retain as high a fraction of its activity as that adsorbed at lower pressures. The total carbohydrate rejection was 0.97–0.99 in these experiments.

Figure 5 shows the pH dependence of the catalytic activity of the immobilized and free GA relative to the maximum activity for each. The optimum activity occurred near pH 5 for the free GA but was shifted to 4 or less for the immobilized GA. The cause of the shift has not been determined. However, the influence of the interaction between the membrane and the immobilized GA and the dependence of the interaction on pH that could be related to the pH dependence of the fixed charge concentration in the zirconium hydrous oxide-polyacrylate membrane, i.e., uncharged below about pH 4–5 and
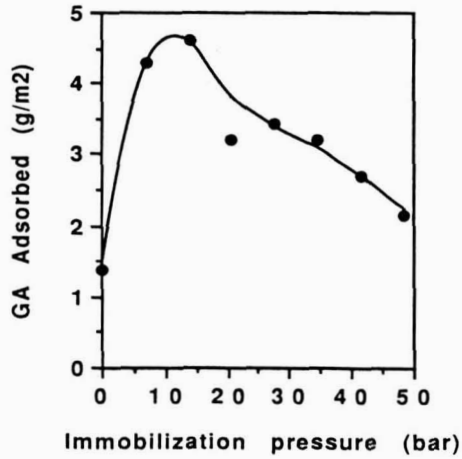
FIG. 3. EFFECT OF PRESSURE APPLIED DURING IMMOBILIZATION
OF THE GLUCOAMYLASE ON THE AMOUNT OF ENZYME
IMMOBILIZED ON THE ZIRCONIUM HYDROUS
OXIDE-POLYACRYLATE MEMBRANE
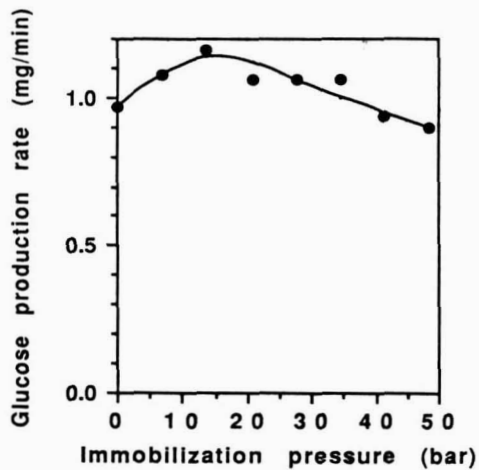
FIG. 4. EFFECT OF PRESSURE APPLIED DURING IMMOBILIZATION
OF THE GLUCOAMYLASE ON THE GLUCOSE PRODUCTION
RATE BY AN ENZYMATIC ZIRCONIUM HYDROUS
OXIDE-POLYACRYLATE MEMBRANE
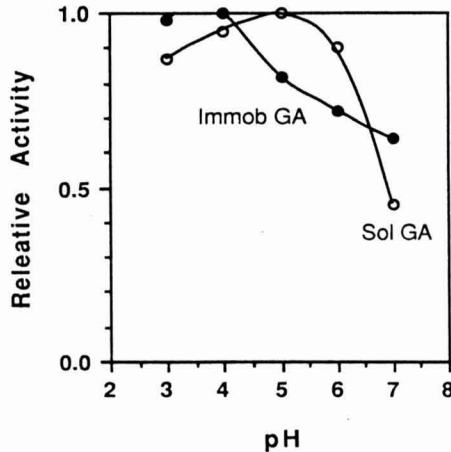
FIG. 5. DEPENDENCE OF THE RATE OF GLUCOSE PRODUCTION
ON pH, RELATIVE TO THE MAXIMUM RATE OF EACH TYPE
OF CATALYZED REACTION
○, Free GA and ●, immobilized GA.

negatively charged at higher pH, should be considered as a possible source of
the difference in the pH dependence of the activity.

The difference in the effect of temperature on the catalytic activity
observed for the immobilized and free GA is especially significant. Figure 6
shows the temperature dependence of the initial catalytic activity relative to the
maximum obtained for each system operating at the pH of its maximum activity,
i.e., 4 for the immobilized GA and 5 for the free GA. The catalytic activity
maximum occurred near 50C for the immobilized GA and near 60C for the free
GA. The temperature dependence of the catalytic activity stability is very
important in determining the use of immobilized enzymes. Figure 6 also shows
the temperature dependence of the relative activity after 60 min. There is a
strong dependence of the activity decline on the operating temperature. The
results indicate that the immobilized GA system must be operated at less than
30C, to obtain a reasonable time interval between removal of the inactive GA
and redeposition of active GA.

The HPLC results of hydrolysis of the 10 mg/ml dextrin solutions for 20
min in the immobilized GA and free GA experiments (Fig. 7 and 8) show that
the glucose concentration was significantly higher ($p < 0.05$) in the immobilized
GA permeate than in the free GA reaction solution. Equal samples from each
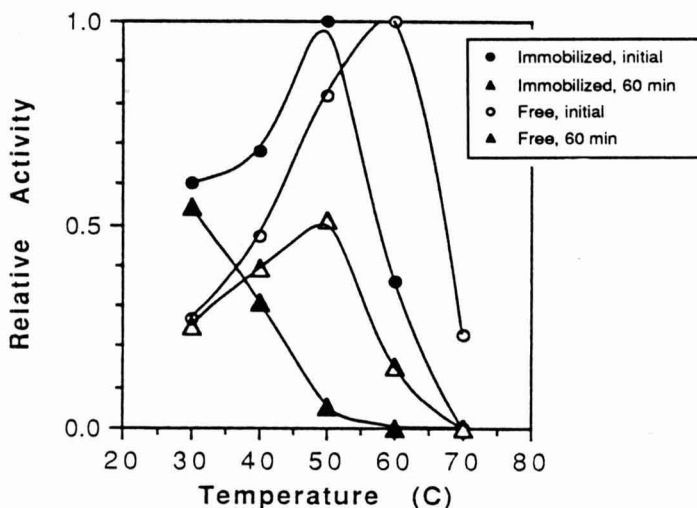
FIG. 6. TEMPERATURE DEPENDENCE OF THE RATES OF GLUCOSE
PRODUCTION RELATIVE TO THE MAXIMUM RATE OF EACH TYPE
OF CATALYZED REACTION
●, Initial relative rate by immobilized GA, ▲, relative rate after 60 min
by immobilized GA, ○, initial relative rate by free GA, and △, relative
rate after 60 min by free GA.

experiment were injected undiluted into the HPLC and analyzed at the same
attenuation for composition comparison. The DE value in the permeate product
of the immobilized GA experiment (55.0) was also significantly higher (p <
0.05) than the product of the free GA experiment (4.7). The reduction of high
as well as the low molecular weight saccharides (DP 2-7) resulting from both
higher conversion and rejection of these oligomers by the nanofiltration
membrane produced a purer product, i.e., higher DE, than the free GA
experiment. Kinetic data from the two types of experiments (Fig. 9) show that
the rate of glucose production increased as the substrate concentration increased
with immobilized GA, whereas the rate of glucose production remained constant
as the substrate concentration increased with free GA, indicating that the rate of
hydrolysis with immobilized GA is limited by the dextrin concentration while the
rate with free GA is limited by the enzyme concentration. The rate of hydrolysis
with free enzyme requires adding more enzyme. The potential for higher
production rates by the immobilized GA system over the free enzyme system for
this limited amount of enzyme is indicated.
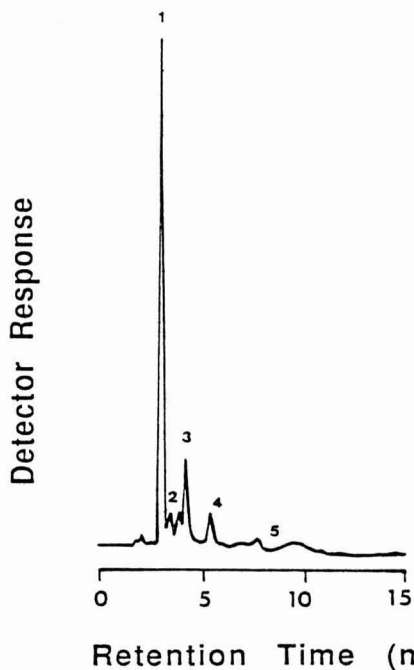
FIG. 7. HPLC CHROMATOGRAM OF LOW MOLECULAR MASS
OLIGOSACCHARIDES PRESENT IN THE DEXTRIN (10 mg/ml)
HYDROLYSATE WITH IMMOBILIZED GA TREATMENT
Numbers indicate degree of polymerization
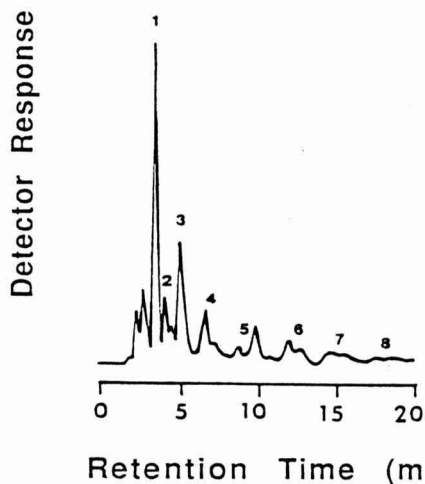
FIG. 8. HPLC CHROMATOGRAM OF LOW MOLECULAR MASS
OLIGOSACCHARIDES PRESENT IN THE DEXTRIN (10 mg/ml)
HYDROLYSATE WITH FREE GA TREATMENT
Numbers indicate degree of polymerization
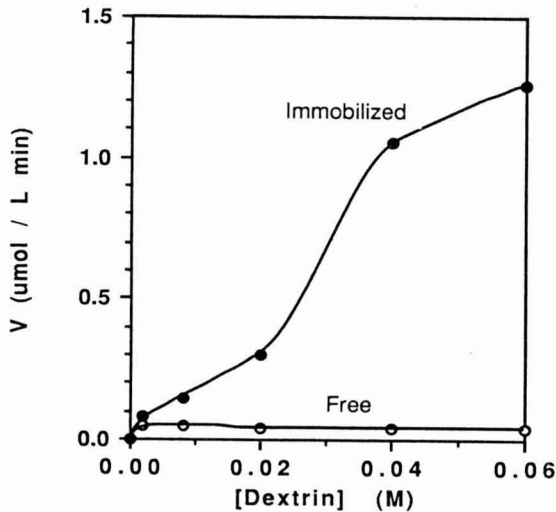
FIG. 9. INITIAL RATE OF GLUCOSE PRODUCTION VERSUS DEXTRIN
CONCENTRATION
○, Free GA and ●, immobilized GA

Useful enzyme activity was obtained with the immobilized GA, even though its activity properties are modified by the immobilization on this substrate. The reduction of temperature stability of the activity may indicate a modification that is definitely a process disadvantage because it restricts the operating temperature well below the optimum temperature for the free enzyme and reduces the permeability of the membrane by requiring a lower temperature. However, the higher DE and the accompanying reduction in the concentration of the oligosaccharides obtained in the dextrin hydrolysates from the immobilized GA experiment compared to the free GA experiment product constitutes an advantage for the immobilized GA process. The potential for use of membrane immobilized enzymes would be improved significantly by the use of enzymes that possess greater temperature stability when immobilized than the one used in these experiments.

Diffusion controlled kinetics are well documented for immobilized enzyme systems with increased Michaelis constants being commonly observed (Godfrey 1983). Increasing substrate flow and mixing with the enzyme and reducing layer thickness can counter reduced reaction rates caused by diffusion limitations. This condition can be achieved with immobilization of the enzymes on a membrane

surface where the convective flow to the enzyme can be controlled, allowing a higher substrate feed concentration than could normally be used in packed bed reactors. Also, clarification of the dextrinized feedstocks might not be required under the crossflow conditions. Furthermore, back diffusion problems might also be reduced by removing the glucose as it was formed. This work indicates that GA immobilized on a membrane could be configured as a continuous hydrolysis reactor for the production of high dextrose equivalent glucose syrup.

ACKNOWLEDGMENTS

REFERENCES

BROOKS, J.R., GRIFFIN, V.K. and KATTAN, M.W. 1986. A modified method for total carbohydrate analysis of glucose syrups, maltodextrins, and other starch hydrolysis products. Cereal Chem. *63*, 465.

CHERYAN, M. 1986. *Ultrafiltration Handbook*, Technomic Publishing Co., Lancaster, PA.

FOGARTY, W.M. and WARD, O.P. 1972. Pectic substances and pectinolytic enzymes. Proc. Biochem. *7*, 13–17.

GODFREY, T. 1983. Ch. 4.21. In *Industrial Enzymology*, (T. Godfrey and J. Reichelt, eds.) p. 444, Nature Press, New York.

MEDINA, B.G. and GARCIA, A., III. 1988. Concentration of orange juice by reverse osmosis. J. Food. Proc. Engr. *10*, 217–228.

NELSON, N. 1944. A photometric adaption of the Somogye method for the determination of glucose. J. Biol. Chem. *153*, 375–380.

ROBERTSON, G.L. 1979. The fractional extraction and quantitative determination of pectic substances in grapes and musts. Am. J. Enol. Vitic. *30*, 182–186.

SPENCER, H.G. and THOMAS, R.L. 1991. Fouling, cleaning and rejuvenation of Formed-In-Place membranes. Food Technol. *45*, 98.

SZANIAWSKI, A.R. and SPENCER, H.G. 1991. Microfiltration of pectin solutions by a titanium dioxide membrane. Key Engr. Mater. *61 & 62*, 243–248.

THOMAS, D.G. 1977. Dynamic membranes: Their technology and engineering aspects. In *Reverse Osmosis and Synthetic Membranes*, (S. Sourirajan, ed.) pp. 295–312, National Research Council of Canada, Ottawa.

THOMAS, R.L., McKAMY, D.L. and SPENCER, H.G. 1989a. Applications of immobilized enzymes on Formed-In-Place membranes in food processing. In *Advances in Reverse Osmosis and Ultrafiltration*, (T. Matsuura and S. Sourirajan, ed.) pp. 563–574, National Research Council of Canada, Ottawa.

THOMAS, R.L., McKAMY, D.L., ZHANG, L. and SPENCER, H.G. 1989b. Interactions of inorganic Formed-In-Place membranes with proteins. In *Proceedings of the First International Conference on Inorganic Membranes*, (L. Cot and J. Charpin, eds.) pp. 453–456, Montpellier, France.

WANG, H.J. and THOMAS, R.L. 1991. HPLC for the assessment of glucoamylase immobilized on metallic membranes. J. Chromatogr. *536*, 107–111.

A RESEARCH NOTE
COMPRESSIVE STRESS-STRAIN RELATIONSHIPS OF AGGLOMERATED INSTANT COFFEE[1]

CHRISTOPH NUEBEL and MICHA PELEG[2]

Department of Food Science
University of Massachusetts
Amherst, MA 01003 USA

ABSTRACT

Shallow beds (3-9 mm) of two commercial agglomerated spray dried instant coffees were compressed using a Universal testing machine. The stress-stress relationships had the sigmoid shape characteristic of cellular solids and could be described by a four parameter model originally developed for solid foams. The magnitude of the model parameters was less sensitive to the relative humidity level at storage in the range of 11-65% than to the bed's thickness. The jaggedness of the stress-strain relationship is a manifestation of the particles brittleness and crumbliness and it is considerably reduced when they are plasticized, as a result of moisture uptake, for example. The degree of jaggedness, determined in the normalized (dimensionless) stress-strain relationships, could be qualified and compared in terms of an apparent ("natural") fractal dimension. It was calculated from the linear region of the corresponding Richardson plots using the "blanket" algorithm. This apparent fractal dimension, however, was only a relative measure of jaggedness, since both the scales and resolution of the mechanical signatures were arbitrarily selected. The jaggedness of the individual agglomerates signatures could not be directly inferred from those of their assemblies, primarily because the effects of averaging and the bed's cushioning could not be separated.

INTRODUCTION

Brittle, fragile particulates have jagged compressive stress-strain relationships when tested individually or in bulk. The jaggedness can be

---

attributed, at least partly, to fracture, which is also evident in fines formation. The degree of jaggedness, therefore, serves as a measure of brittleness and fragility, which are prime factors in the agglomerates mechanical stability and hence the product quality. With the availability of fast microcomputers and algorithms analysis of jagged signatures has been greatly facilitated. The best example is the Fast Fourier Transform or FFT (Ramirez 1985), which is now a standard option in most mathematical and statistical software packages. The mere transformation of a time series into a power spectrum can identify frequencies of a particular significance and, the general shape of the spectrum can be indicative of the kinetics or mechanism that produced the signature. The jaggedness of the signature can also be characteristic of the specimen's material and/or the process by which it was formed. The degree of jaggedness of fractal objects can be expressed quantitatively in terms of the magnitude of their fractal dimension. If, however, an object or signature does not have self-similarity properties and is therefore not truly fractal, its jaggedness can still be character- ized by a "natural" or an apparent fractal dimension determined by the same methods that are applicable to truly fractal objects (Kaye 1981, 1989). Such jaggedness measures were extensively used to characterize the morphology of particulates silhouettes (Kaye 1989) instant coffee agglomerates included (Peleg and Normand 1985; Normand and Peleg 1986a; Barletta and Barbosa-Canovas 1993). Recently it has also been used to characterize mechanical signatures of brittle foods and particulates (Barrett *et al.* 1992; Rohde *et al.* 1993a,b; Peleg and Normand 1993). The magnitude of the fractal or apparent fractal dimension, of a signature can be determined by various algorithms (Peitgen and Saupe 1988; Barnsley 1988; S. Peleg *et al.* 1984; Barletta and Barbosa-Canovas 1993). When applied to a line signature it always gives a measure of jaggedness on a scale from one, Eucledian, and therefore smooth, to two, the theoretical upper limit. (The upper limit if it could be reached would signify that the line is so convoluted that it occupies an area).

Because of their smallness, mechanical evaluation of coffee agglomerates individually with a standard Universal Testing Machine is very difficult and can be judged impractical. Consequently, it would be much easier to assess their mechanical properties by testing them in bulk. In such a case, however, any measurement will be influenced, simultaneously, by both the breakage properties of the individual particles and the deformability of their assembly as a whole. It has been shown recently with puffed cereal particles, which are much larger than instant coffee agglomerates (5-8 mm in diameter as compared to < 3 mm), that the analysis of brittle food particulates in bulk can be done by combining algorithms to assess jaggedness with models of cellular solids deformation (Nuebel and Peleg 1993). The objective of this work is to assess the applicabili- ty of this combined approach to spray dried instant coffee agglomerates and to test whether the resulting jaggedness and deformability parameters can be used

to monitor textural changes in the coffee agglomerates exposed to various levels of relative humidity.

EXPERIMENTAL

Several jars of two national brands of agglomerated spray dried instant coffee were purchased at a local supermarket. The agglomerates were removed from the jars and sieved gently by hand to collect a size fraction $1.7 < d < 3.1$ mm. The sieved agglomerates were then stored at an ambient temperature of about 25C in evacuated glass desiccators over saturated solutions of LiCl, R_2CO_3, $Mg(NO_3)_2$ and $NaNO_2$ to produce equilibrium relative humidities of about 11, 43, 52 and 65%, respectively (Greenspan 1977). They were tested after about 48 h of storage, sufficient time to reach a constant weight. Samples were compressed in a metal compression cell with a 5 cm internal diameter (Moreyra and Peleg 1980) using an Instron Universal Testing machine model 1000. The crosshead speed was 10 mm/min in all the experiments. The Instron was interfaced with a Macintosh II Computer (4MB RAM and 80 MB hard disk) through a Strawberry Tree ACM2-12 interface board. Computer software developed by M.D. Normand was used to control the machine during the data acquisition and for subsequent data processing. The latter included conversion of the machine's continuous voltage versus real time output into digitized stress-strain relationships, curve fitting through nonlinear regression using the Systat package 5.2.1 and other mathematical operations and transformations (see below).

All the mechanical tests were performed in duplicate, and their results are reported as mean values unless otherwise stated.

Mathematical Treatment of the Results

The stress-strain data were sampled at a rate that produced more than 128 points in a strain range of up to about 40%. These were reduced to about 60 data points at equal time intervals and then fitted with a four parameter empirical mathematical model that was developed for the description of the sigmoid stress-strain relationships of cellular solids (Swyngedau et al. 1991 a,b):

$$\sigma = k_1 \varepsilon^{n1} + k_2 \varepsilon^{n2} \tag{1}$$

where σ is the engineering stress, ε the engineering strain and the k's and n's constants ($n_1 < 1$ and $n_2 > 1$). The reason for the reduction of the data to about 60 points is that nonlinear regression with a much larger number of "noisy" data points usually takes a very long time, even when performed with

a fast microcomputer, while its effect on the magnitude of the computed parameters is negligible.

The complete data set of each stress-strain relationship was used to calculate a normalized dimensionless stress $Y(\varepsilon)$ using the transformation (Barrett et al. 1992; Rohde et al. 1993a):

$$Y(\varepsilon) = [\sigma(\varepsilon)-\sigma^*(\varepsilon)]/\sigma^*(\varepsilon) \tag{2}$$

where $\sigma^*(\varepsilon)$ is the fitted value calculated by Eq. 1.

The jaggedness of the normalized stress-strain relationships so created, in terms of an apparent or "natural" fractal dimension (Kaye 1981), was determined using the "blanket" algorithm (Peleg et al. 1984; Normand and Peleg 1986b; Barrett et al. 1992). It is based on the construction of a Richardson plot, a logarithmic relationship between a series of calculated line lengths and their corresponding length scales. The apparent fractal dimension D_f, is calculated from the slope of the plot's linear region by:

$$D_f = 1 + \mid \tan \delta \mid \tag{3}$$

where $\tan \delta$ is the slope (see below). The apparent fractal dimension, as previously mentioned, can vary between one for a perfectly smooth curve and two, the theoretical upper limit of a line whose jaggedness is so great as to almost occupy an area that is two dimensional.

The power spectrum of the harmonics of the normalized stress-strain relationships was determined using the Fast Fourier Transform (FFT) algorithm, which is a standard option of the Systat package.

RESULTS AND DISCUSSION

The typical general shape of the compressive stress-strain relationships of agglomerated instant coffee is demonstrated in Fig. 1 and 2. It has a characteristic almost linear region, at very small strains ending abruptly and followed by a concave upward continuation. These features of the stress-strain relationships are very common in cellular solids (Gibson and Ashby 1988). The first region represents the deformability of the still intact structure, and the slope is a measure of the intact structure's stiffness. At a certain strain level, some of the cell walls start to buckle, fold and/or fracture and therefore the stress level remains fairly constant or increases at only a moderate rate. Cellular materials used for cushioning are especially designed to have this region extended, with the stress kept at an almost constant level. Consequently, they can absorb a lot of mechanical energy (the area under the curve) without
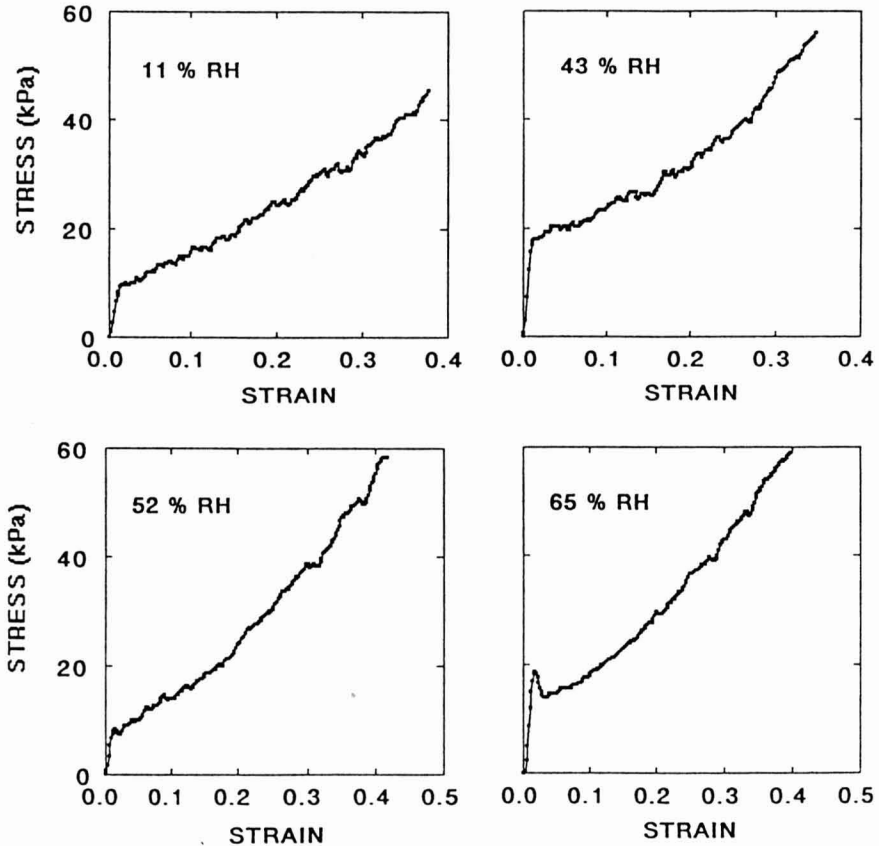
FIG. 1. COMPRESSIVE STRESS-STRAIN RELATIONSHIPS OF AGGLOMERATED
INSTANT COFFEE AT FOUR ERH LEVELS
Brand A (bed's depth ~ 3 mm).

inducing or transmitting stress. Further compression and the accumulation of
the cell wall solid material, however, increases the density and stiffness of the
compact, causing the stress to rise sharply and hence the concave upward shape
of the stress-strain curve at the higher strains region.

As previously mentioned, the overall shape of such relationships over the
entire strain range can be described by Eq. 1 (Swyngedau et al. 1991a,b). The
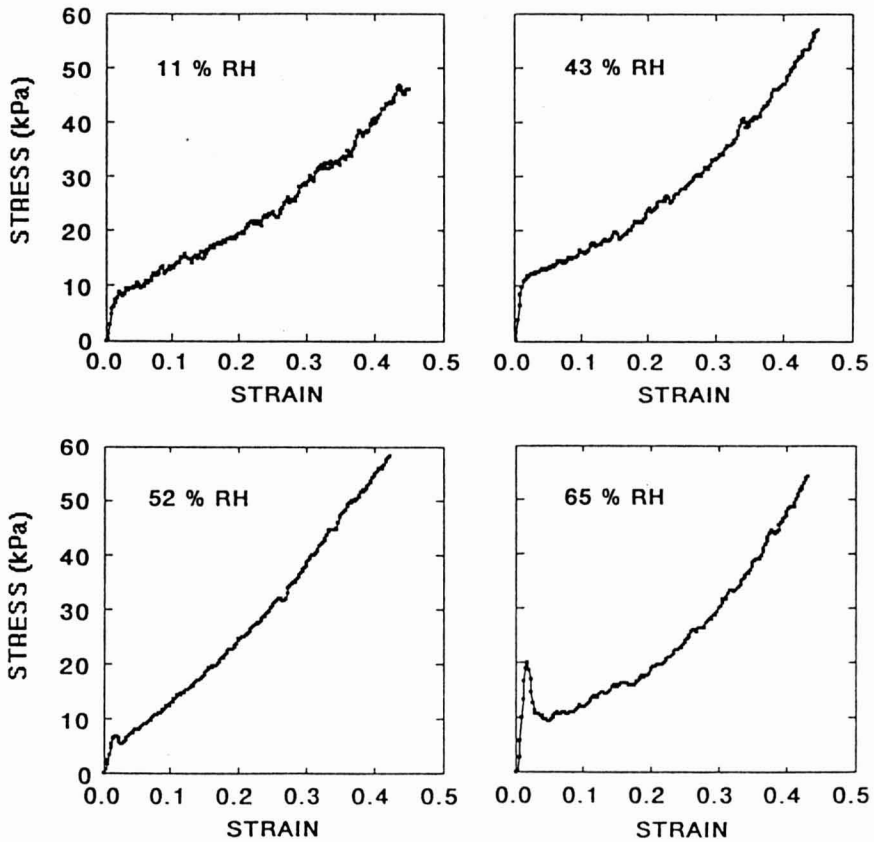
FIG. 2. COMPRESSIVE STRESS-STRAIN RELATIONSHIPS OF AGGLOMERATED
INSTANT COFFEE AT FOUR ERH LEVELS
Brand B (bed's depth ~ 3 mm).

regression parameters of the equation are presented in Table 1 and its fit demonstrated graphically in Fig. 3. It appears, therefore, that the overall deformability of the coffee agglomerates bed follows that of brittle solid foams. Thus, at least in principle, assessment of differences between coffees or monitoring changes in stored samples (see below), can be done using the same type of models.

Another characteristic of the stress-strain relationships of the coffee agglomerates especially when dry is their ruggedness. It becomes more clearly evident in the plot of the normalized (dimensionless) stress versus strain

TABLE 1.

MECHANICAL PROPERTIES OF INSTANT COFFEE
AGGLOMERATES TESTED IN BULK[1]

| Brand | ERH (%) | Constants of Eq. 1[2] | | | | | Apparent Fractal Dimension, D_f[3] (-) |
		k_1 (kPa)	n_1 (-)	k_2 (kPa)	n_2 (-)	r^2	
A	11	41	0.35	206	2.3	0.994	1.42
	43	36	0.27	223	2.4	0.993	1.34
	52	36	0.32	272	2.5	0.994	1.24
	65	20	0.24	229	2.4	0.992	1.18
B	11	32	0.37	229	2.6	0.996	1.46
	43	24	0.27	208	2.7	0.993	1.41
	52	16	0.28	195	1.7	0.999	1.20
	65	14	0.1	325	2.3	0.996	1.30

1) Bed depth 3 mm.
2) Of the original stress-strain relationships.
3) Of the normalized signatures.

relationships shown in Fig. 4 and 5. Application of the "blanket" algorithm (Peleg *et al.* 1984; Barrett *et al.* 1992) to the normalized data resulted in Richardson plots with a clearly identifiable linear region, Fig. 6-7, from which an apparent or "natural" fractal dimension, D_f, could be calculated using Eq. 3. The curvature at the left end of the plot is a result of the fact that a real signature, unlike a mathematical fractal object, has a finite length. At the other end, the curvature is an artifact of the algorithm, produced when the number of iterations becomes excessive and the "blanket" too "thick". In this situation the calculated line length approaches asymptotically that of the original signature's overall span, (Normand and Peleg 1986b; Peleg and Normand 1993).
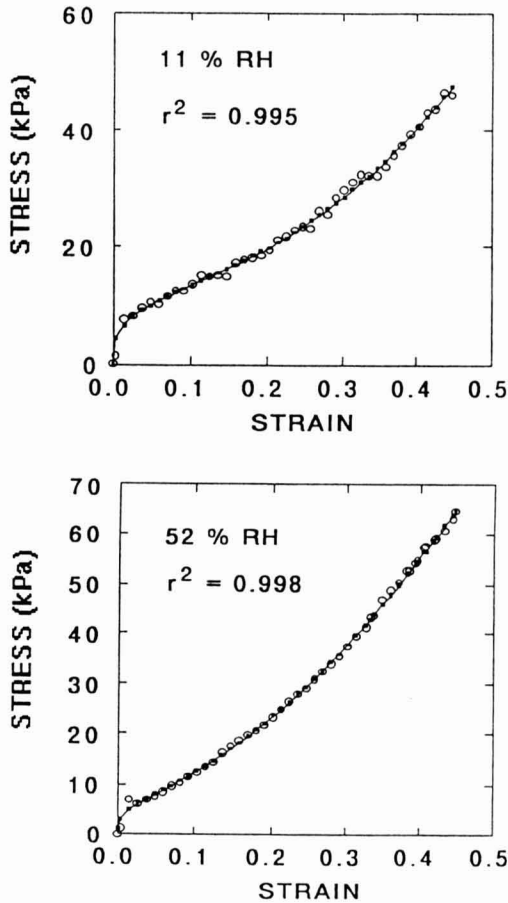
FIG. 3. GRAPHICAL DEMONSTRATION OF THE FIT OF EQ. 1 TO
THE STRESS-STRAIN RELATIONSHIPS OF AGGLOMERATED
INSTANT COFFEE

Since both the scale and the resolution of the normalized signature's two axes were arbitrary, the apparent or "natural" fractal dimension so determined is only a relative measure of jaggedness. Consequently, it can only be used to compare the jaggedness of normalized signatures with the same number of points and presented in the same coordinates. Or in other words, the degree of jaggedness in terms of an apparent fractal dimension as reported in Table 1 is indicative of differences between the coffee samples tested in this work, but
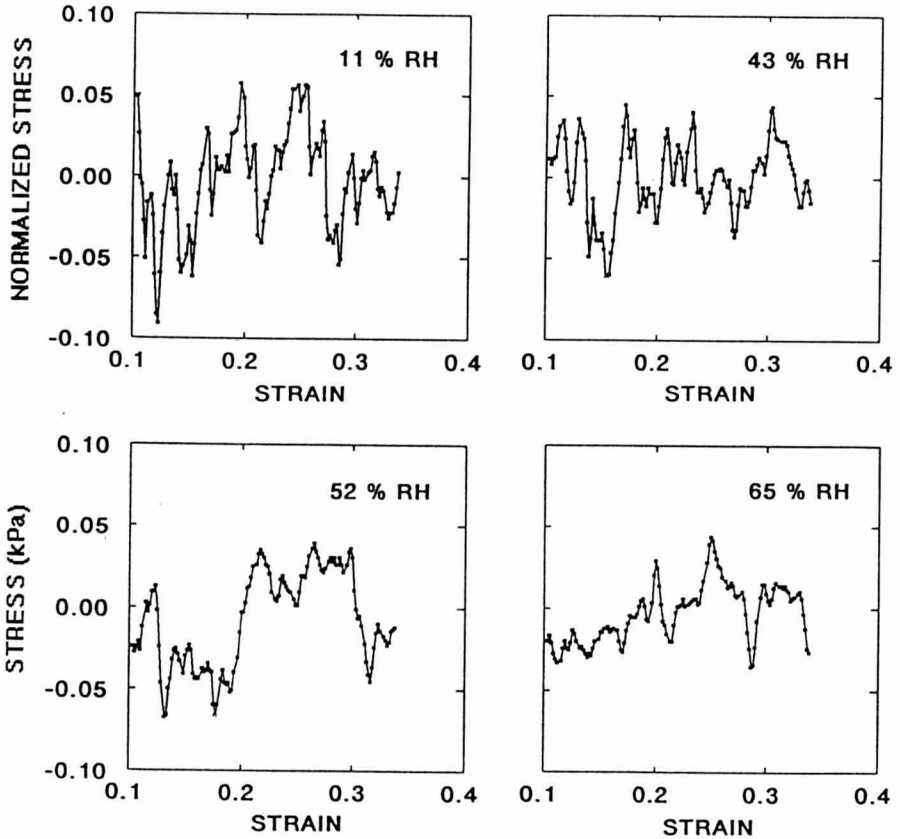
FIG. 4. NORMALIZED SIGNATURES OF AGGLOMERATED INSTANT COFFEE
AT FOUR ERH LEVELS: BRAND A

cannot be used for comparison with other brittle particulates whose signatures are given on a different scale. In fact, the absolute amplitude of the normalized signatures was only on the order of 0.05 as compared with about 0.4, which was observed in individual brittle food particulate at a comparable strain (Peleg and Normand 1993; see below).
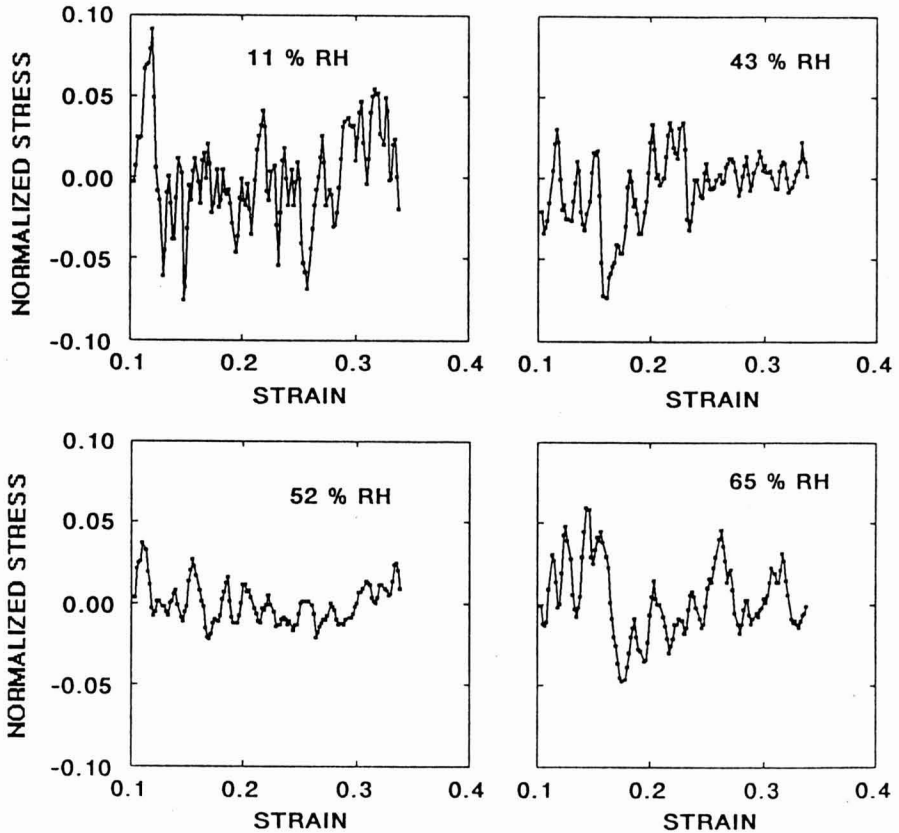
FIG. 5. NORMALIZED SIGNATURES OF AGGLOMERATED INSTANT COFFEE
AT FOUR ERH LEVELS: BRAND B

Smoothing Effects

Since, as previously mentioned, it is difficult to test coffee agglomerates individually, testing in bulk is a technical compromise. Its major drawback is that the test's output is a record not only of the breakage of individual agglomerates but also that of the deformability of the bed. This has two main effects on the signature's morphology.
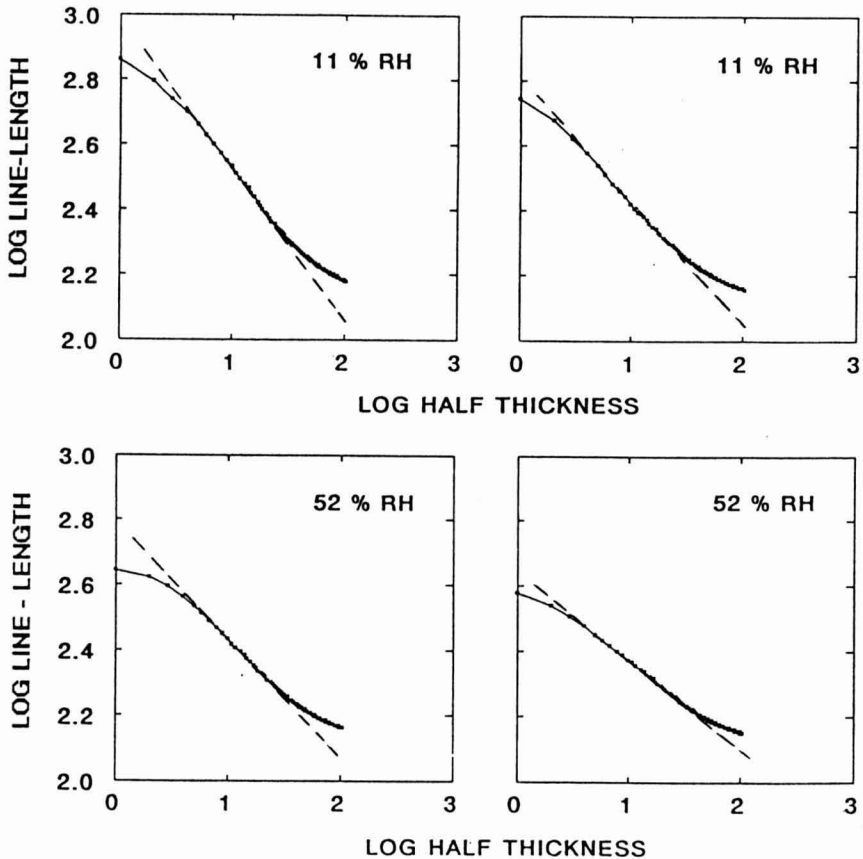
FIG. 6. EXAMPLES OF RICHARDSON PLOTS OF NORMALIZED MECHANICAL
SIGNATURES OF AGGLOMERATED INSTANT COFFEE BRAND A, PRODUCED
BY THE BLANKET ALGORITHM
Note the linear region that enabled the calculation of D_f using Eq. 3.

It causes its smoothing in the same manner that averaging noisy
"random" signatures produces a record that is smoother than that of the
individual signatures. It is a result of mutual cancellation of the contributions
of maxima in one signature by smaller values and/or minima in the other
signatures. This effect is clearly reflected in the relatively small absolute
amplitude of the coffees when tested in bulk. The signature of the individual
agglomerates therefore is expected to be much more jagged than that of their
bulk. According to basic statistical principles the amplitude of a signature
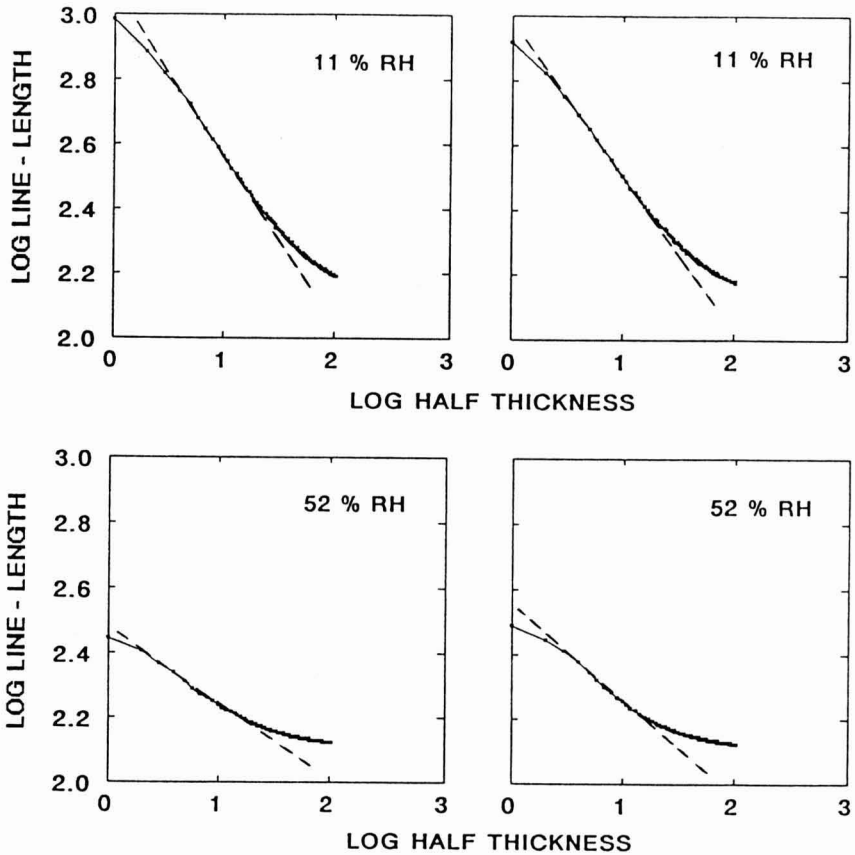
FIG. 7. EXAMPLES OF RICHARDSON PLOTS OF NORMALIZED MECHANICAL
SIGNATURES OF AGGLOMERATED INSTANT COFFEE BRAND F,
PRODUCED BY THE BLANKET ALGORITHM
Note the linear region that enables the calculation of D_f using Eq. 3.

obtained by averaging the amplitudes of a large number of random signatures
is expected to be inversely proportional to the square root of the number of
signatures averaged. In our case the number of individual particles is unknown
and can only be estimated. Thus, by how much the jaggedness of the individual
particles signatures differs from that of their bed is a question that can be only
satisfactorily answered when a method to test individual instant coffee
agglomerates is developed. (In principle an estimate can be reached by testing
powder specimens in cells with various diameters, thus having a certain control
over the agglomerates number.)

The other smoothing effect stems from the bed's ability to act as a cushion and thus reduce the amount of fracture of at least some of the agglomerates. The bed deformation also has its own characteristic "frequencies" produced by the particles' reorientation and interparticle friction for example. If these become significant factors, (see below) then increasing the bed's depth will cause an appreciable smoothing of the mechanical signature.

As shown in Table 2 the bed's depth had a major difference on its overall mechanical behavior. The increase in the magnitude of the k's of Eq. 1 is a clear indication of stiffening. It means that the deeper bed became more compact and that an agglomerate's tendency to break down was probably reduced to some extent when placed on other agglomerates instead of on the hard flat bottom of the cell. The bed's signature jaggedness, however, did not change dramatically with depth (Table 2). This suggests that the signatures of even the 3 mm deep beds, the thinnest practically possible, are already smoothed to a great extent as a result of the averaging effect.

Effect of Equilibrium Relative Humidity (ERH)

As can be seen in Fig. 1,2,3 and 5 and Table 1, exposure of the agglomerates to various levels of relative humidity in the range of 11–65% did not have a dramatic effect on their stress-strain relationships. Or, in other words, the bed depth (Table 2) had a much stronger effect than the moisture loss or gain experienced by the instant coffee powders at the reported levels of

TABLE 2.
EFFECT OF BED DEPTH ON THE DETERMINED CHARACTERISTIC
OF INSTANT COFFEE AGGLOMERATES[1]

Bed depth (mm)	k_1 (kPa)	Constants of Eq. 1[2] n_1 (-)	k_2 (kPa)	n_2 (-)	r^2	Apparent Fractal Dimension, D_f[3] (-)
3	25	0.35	271	2.6	0.995	1.44
6	37	0.40	564	3.1	0.996	1.42
9	55	0.53	1330	3.5	0.997	1.36

1) Brand A tested as is.
2) Of the original stress-strain relationships.
3) Of the normalized signatures.

relative humidity. However, the powders of both brands were already sticky at 65% ERH (see below) and they could not be tested by the described procedure after exposure to higher humidity levels. What could clearly be observed though was a decrease in the magnitude of the apparent fractal dimension, with moisture sorption (Table 1) indicating smoothing of the stress-strain curve. This was quite expected, since the material of which the coffee particles is made of is known to become plasticized as a result of glass transition at a water activity range that corresponds to the reported ERH levels.

An anomaly of sort was observed in the signature of the brand B coffee exposed to 65% ERH (Table 1). Its jaggedness was higher than that of samples stored at 52% (D_f = 1.3 vs. 1.2). This jaggedness, however, was not due to stiffening of the particles but to a "slip stick" effect. Support for this explanation can be found in the appreciable stress drop (Fig. 1 and 2) that was only observed in the wet powders, of both brands.

The combined effects of the changes in the agglomerate's texture and the bed's deformability produced power spectra that were not always easy to interpret. Examples are shown in Fig. 8 and 9. Although the decrease in jaggedness as a result of exposure to 52% RH, as compared to 11 and 43% RH, is clearly evident in the corresponding spectra, the "slip-stick" effect at 65% ERH is practically indistinguishable from that produced by higher particle brittleness. Consequently, and unlike in the case of brittle particulates tested individually (Rohde *et al.* 1993 a,b), no correlation could be found between quantitative parameters derived from the power spectrum and the apparent fractal dimension of the signature. It is possible, however, that such a correlation will emerge when a larger number of samples is tested. Or, alternatively, that harmonics associated with agglomerates breakage and the bed's deformability can be identified and separated. This, however, requires a more elaborate set of experiments, outside the scope of the reported work.

CONCLUSIONS

The compressive stress-strain relationships of instant coffee agglomerates have a characteristic sigmoid shape that can be described by a model originally developed for cellular solids. The magnitude of the model parameters strongly depends on the bed depth and to a lesser extent on the equilibrium relative humidity, as long as the particles remain solid (ERH < ~ 65%). Because of an averaging effect the degree of jaggedness of the stress-strain relationship of the bulk must have been much lower than that of the individual agglomerates, although the latter could not be determined directly. The degree of jaggedness can be conveniently assessed by transforming the original stress-strain relationship into a normalized (dimensionless) signature and constructing its
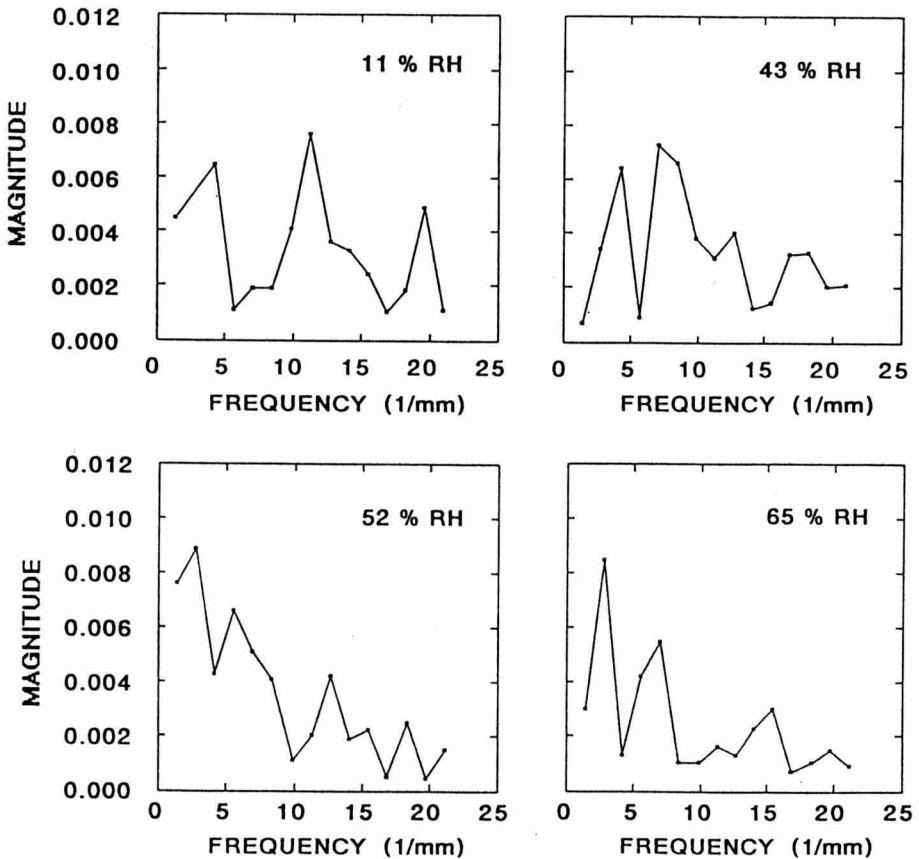
FIG. 8. POWER SPECTRA OF NORMALIZED MECHANICAL SIGNATURES
OF AGGLOMERATED INSTANT COFFEE, BRAND A, STORED AT FOUR
ERH LEVELS

Richardson plot using the blanket algorithm. Although it is very doubtful that
the normalized, or the original, signature is a truly fractal object, its Richardson
plot has a clearly recognizable linear region from which an *apparent* fractal
dimension can be calculated and used as a ruggedness measure on a scale from
1 to 2. Since the normalized signature's resolution and scales were arbitrarily
selected, the apparent fractal dimension so determined provides only a relative
measure of jaggedness. It is, however, a sensitive parameter to monitor the
effects of relative humidity on the agglomerates texture, which were not
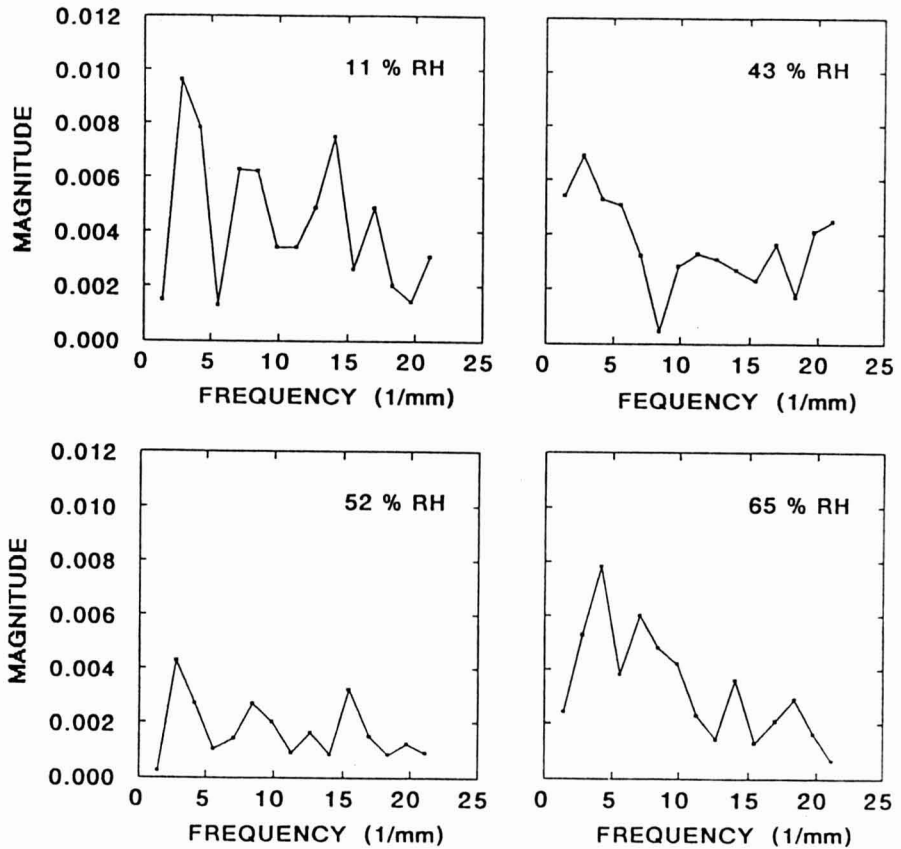
FIG. 9. POWER SPECTRA OF NORMALIZED MECHANICAL SIGNATURES OF
AGGLOMERATED INSTANT COFFEE, BRAND B, STORED AT FOUR
ERH LEVELS

sufficiently large to drastically alter the general shape of the stress-strain
relationship of their beds.

ACKNOWLEDGMENT

REFERENCES

BARLETTA, B.J. and BARBOSA-CANOVAS, G.V. 1993. Fractal analysis to characterize ruggedness changes in tapped agglomerated food powders. J. Food Sci. *58*, 1030–1035, 1046.

BARNSLEY, M. 1988. *Fractals Everywhere*, Academic Press, New York.

BARRETT, A.M., NORMAND, M.D., PELEG, M. and ROSS, E. 1992. Characterization of the jagged stress-strain relationships of puffed extrudates using Fast Fourier Transform and fractal analysis. J. Food Sci. *57*, 227–232.

GIBSON, L.J. and ASHBY, M.F. 1988. *Cellular Solids*, Pergamon Press, Oxford.

GREENSPAN, L. 1977. Humidity fixed points of binary saturated aqueous solutions. J. Res. (Natl.) Bur. Stand. *81A*, 89–96.

KAYE, B.H. 1981. *Direct Characterization of Fine Particles*, John Wiley & Sons, New York.

KAYE, B.H. 1989. *Random Walk Through Fractal Dimensions*, VCH, New York.

MOREYRA, R. and PELEG, M. 1980. Compressive deformation patterns of selected food powders. J. Food Sci. *45*, 864–868.

NORMAND, M.D. and PELEG, M. 1986a. Determination of the fractal dimension of particle silhouette using image processing techniques. Powder Technol. *46*, 209–214.

NORMAND, M.D. and PELEG, M. 1986b. Evaluation of the blanket algorithm for ruggedness assessment. Powder Technol. *54*, 255–259.

NUEBEL, C. and PELEG, M. 1993. Characterization of the stress-strain relationship of puffed cereals tested in bulk. J. Food Sci. *58*, 1356–1360, 1374.

PEITGEN, H-O. and SAUPE, D. (eds.). 1988. The *Science of Fractal Images*, Springer-Verlag, New York.

PELEG, M. and NORMAND, M.D. 1993. Determination of the fractal dimension of the irregular compressive stress-strain relationships of brittle crumbly particulates. Part. Part. Syst. Charact. *10*, 301–307.

PELEG, M. and NORMAND, M. D. 1985. Characterization of the ruggedness of instant coffee particles by natural fractals. J. Food Sci. 50, 829-831.

PELEG, S., NAOR, J., HARTLEY, R. and AVNIR, D. 1984. Multiple resolution texture analysis and classification. IEEE Trans. Patterns Anal. Mach. Intelligence *6*, 518–523.

RAMIREZ, R. 1985. *The FFT: Fundamentals and Concepts*, Prentice-Hall, Englewood Cliffs, NJ.

ROHDE, F., NORMAND, M.D. and PELEG, M. 1993a. Characterization of the power spectrum of force-deformation relationships of crunchy foods. J. Texture Studies *24*, 45–62.

ROHDE, F., NORMAND, M.D. and PELEG, M. 1993b. Effect of equilibrium relative humidity on the mechanical signatures of brittle foods. Biotechnol. Prog. *9*, 497–503.

SWYNGEDAU, S., NUSSINOVITCH, A. and PELEG, M. 1991a. Models for the compressibility of layered polymeric sponges. Polym. Eng. Sci. *31*, 140–144.

SWYNGEDAU,S., NUSSINOVITCH, A., ROY, I., PELEG, M. and HUANG, V. 1991b. Comparison of four models for the compressibility of breads and plastic foams. J. Food Sci. *56*, 756–759.

DETERMINATION OF RESIDENCE TIME DISTRIBUTION OF NONSETTLING FOOD PARTICLES IN VISCOUS FOOD CARRIER FLUIDS USING HALL EFFECT SENSORS

GARY S. TUCKER and PETER M. WITHERS

Department Food Process Engineering
Campden Food and Drink Research Association
Chipping Campden
Glos, GL55 6LD, UK

ABSTRACT

Hall effect sensors were used to determine residence time distributions for diced carrot particles in 4% Colflo 67 carrier fluid. Four sensors at either end of a 3.2 m long 2 in. IDF tube viscometer allowed residence times to be measured for carrot particles incorporating a ceramic magnet. Mean particle residence times were greater than mean bulk residence time for 8 mm diced carrots, whereas 15 mm carrots showed trials in which particles travelled faster than the bulk fluid. Increasing concentration of 15 mm diced carrots from 3.25, 6.30, 9.16 to 11.85% w/w resulted in decreasing mean particle residence times from 17.6, 17.0, 15.9 to 14.3 s, with minimum residence times of 16.4, 16.2, 14.8 and 13.4 s, respectively. This sensing technique operates through stainless steel, providing applications for UHT foods containing particles. In addition, the technique was not affected by high particle concentration, and will operate for any distribution of particle size, shape or type.

INTRODUCTION

The development of continuous sterilization processes for food products containing particulate matter has been limited by a number of fundamental problems that have to be solved before commercial advantage can be taken. Without over-simplification of the technology these can be broken down into three areas: high temperature and pressure rheology of the heterogeneous food, prediction/measurement of heat transfer into the particles, and residence time distribution for both solid and liquid phases. This paper deals with residence

time distribution, and a system for making appropriate measurements is described.

The difficulty introduced by including particles into a continuous heat process is related to the existence of a distribution in exposure times for the different fractions comprising the complete product. In conventional canning processes the time-temperature profile experienced by the can during sterilization is identical for each can during the process. This allows heat penetration measurements to be taken on a small number of cans that are representative of the entire load. For a continuous heat process it is necessary to measure the exposure time of the liquid fraction in addition to that of the particles.

The techniques for determining residence time distributions (RTD) for liquids were covered in detail by Danckwerts (1953), and in many other publications since. The RTD was determined by injecting a plug of tracer dye into the fluid at the entrance to the holding tube, and measuring the variation of tracer concentration with time at the outlet. The area under the curve of the graph of tracer concentration (y axis) against time (x axis) was normalized by dividing the concentration values by the total area under the curve. These new values were designated as E(t) values and plotted against time to give the residence time distribution graph.

Current industrial practice for processing liquid foods continuously assumes the worst case, in that under laminar flow in a holding tube the fastest moving product travels at twice the speed of the average moving product (Pflug *et al.* 1990). However, the relationship between the maximum fluid velocity and average fluid velocity is a function of the velocity profile, which can be determined from the rheological properties of the food under UHT conditions.

The velocity characteristics of a pseudoplastic fluid (Power Law fluid with $n < 1$) can be described in terms of the mean fluid velocity (v), the flow behavior index (n) and the radius of the holding tube (R), as quoted in Manson and Cullen (1974):

$$v_x = v \cdot \left(\frac{3n+1}{n+1} \right) \left[1 - \left(\frac{r}{R} \right)^{(n+1)/n} \right] \tag{1}$$

where v_x is the fluid velocity (m.s^{-1}) at a radial distance, r (m).

In terms of the maximum fluid velocity (v_{max}), which occurs along the center line of the tube, Eq. (1) simplifies to:

$$\frac{v_{max}}{v} = \frac{3n+1}{n+1} \tag{2}$$

Hence, reliable rheological data is required when using a tube viscometer to predict flow patterns at high temperatures and pressures (Tucker 1992). From these data it is possible to calculate the theoretical maximum velocity along the center line of the pipe, and thus determine the minimum fluid residence time.

Heterogeneous foods contain large discrete particles, which are of a size such that the residence times for the particles may differ from that of the carrier fluid. To prevent settling of the particulate matter, highly viscous carrier fluids are required to create the effect of neutral buoyancy of the particles. For these food products it is important to understand the residence time behavior of the discrete particles, in addition to that of the liquid portion.

The area for concern when processing such products is the holding tube and the prediction of residence time distribution within this length of pipe section. Pflug et al. (1990) stated that "...tests should be conducted using the actual food product flowing steadily through the system. Establishing flow through the system using only the carrier medium and then introducing one or several particles may lead to residence time distribution results, for the fastest particle, that are not applicable to the commercial product." Thus a system is needed that permits the measurement of residence times in foods containing up to 60% w/w solids within opaque carrier fluids. Any other apparatus will not provide the desired results.

The literature on solid-liquid flows in pipes is considerable, but most concern the handling of slurries, suspensions and isolated particles from chemical engineering sources. None of these situations are relevant to aseptic processing of heterogeneous foods and more specifically, the time spent during holding tubes involving nonsettling particles in non-Newtonian carrier fluids.

Taeymans et al. (1985) carried out a study of the RTD of 6 mm alginate beads in water, and found that the residence time (RT) of the beads increased and approached that of the fluid as the blade speed of the scraped surface heat exchanger (SSHE) was increased. Increasing the alginate bead concentration from 4% to 8% was found to reduce the RT, but the relevance of this work to higher solid concentrations in viscous non-Newtonian carrier media is unclear.

An interesting theoretical study by Manson and Cullen (1974) used the velocity profile for Power Law fluids to predict the RTD for particles flowing along streamlines. This was combined with a finite difference model for heat transfer into a cylindrical particle to illustrate the importance of various aseptic processing parameters.

Dutta and Sastry (1990) used sodium carboxymethylcellulose (CMC) solutions to represent typical pseudoplastic food materials, with 0.95 cm spherical particles of polystyrene as simulated food particles. The density of both phases was similar, therefore this study was more representative of nonsettling particles expected with viscous carrier fluids. Average velocities of the model food particles were investigated by video-taping them during their passage

through a transparent holding section (4.7 cm i.d.) similar in dimension to that of commercial equipment. All experiments were conducted at room temperature and atmospheric pressure, and the analysis of results was in terms of the mean particle velocity, mathematics of particle activity, and the application of the Froude number.

A study using water as the carrier fluid was reported by Hong et al. (1991). Their work used 5 mm diameter alginate beads injected before the 35.6 mm i.d. holding tube, and subsequently collected using a rotating basket arrangement on exit from the holding tube. Residence times for the solid fractions were found to be 1.032 times that of the fluid. A Reynolds number of 13,800 indicated turbulent flow, hence the results were not applicable to the laminar flow systems reported in this document. The temperature used by Hong et al. (1991) was 25C but the equipment was designed such that high temperatures (>100C) could be studied, although no work has been reported to date using this system at elevated temperatures.

Two further papers using visual detection systems (Lee and Singh 1991; Yang and Swartzel 1991) concerned the measurement of residence times for particles, but neither were relevant to actual SSHE operating conditions. Lee and Singh (1991) presented a report for different sized potato cubes from 1.0 to 2.0 cm in CMC solutions of varying concentration. The application was for vertical flows such as those encountered in ohmic heating, although the results presented were taken at 23C. Dyed potato cubes were introduced as the tracer particles and individual residence times between the inlet and outlet port of the SSHE recorded. Potato concentrations of 0–40% w/v were investigated, and the normalized residence times for the particles were found to be greater than those for the mean fluid residence time (measured from the volumetric flow rate). Yang and Swartzel (1991) developed a method for determining residence time distributions of particles using photosensors to detect single particles in holding tubes. The carrier fluid was water and 19.1 mm diameter polystyrene spheres were used as tracer particles. A glass holding tube 50.8 mm i.d. allowed detection of the opaque particles with the optical grid formed from multiple photosensor pairs installed around the tube. A normal distribution was obtained from 75 replicated runs, performed at room temperature under turbulent flow conditions (Re = 34,000).

The only study reported to date using non-Newtonian carrier fluids, nonsettling particles and conducted at high temperature was that of Alcairo and Zuritz (1990). Both of the solid and liquid materials were the same as those used by Dutta and Sastry (1990), but the analysis was performed using residence time distributions through the SSHE. Polystyrene spheres were introduced to the system at the inlet to the SSHE, and the total residence times were measured through the heater, holding section, and cooler, for the complete unit. The

effects of particle diameter, fluid viscosity, fluid mass flow rate and SSHE rotational blade speed were investigated in terms of the residence times and RTDs. However, the particles were individually introduced to the fluid, hence no particle-particle interaction occurred, and also the residence times in the holding tube alone could not be evaluated using this apparatus.

A magnetic particle technique similar to that presented here was devised by Segner *et al.* (1989). Two copper coils of about 80 turns were used, one at the entrance and one at the exit of the holding tube, to detect the presence of a moving magnetic field. Turkey cubes (12.7 mm) containing a 3 mm ceramic magnet were pumped around a SSHE using a starch/sugar/water solution as the carrier fluid. Calculated holding times based on laminar flow assumptions were found to give conservative estimates of particle flow rate through the holding tube. In all cases, the fastest magnetic particles were much slower that those based on presumed laminar flow for each product flow rate investigated. In addition, the variation in residence times increased as the holding tube was lengthened from 6.9 m to 58.2 m and also as the flow rate decreased from 47.7 L.min^{-1} to 28.0 L.min^{-1} (for the 6.9 m length) and from 64.7 L.min^{-1} to 24.2 L.min^{-1} (for the 58.2 m length). This technique was applied in an actual SSHE using high flow rates but one possible restriction may be in the minimum particle velocity required to generate an e.m.f. in the copper coils.

The most recently published work (Palmieri *et al.* 1992) used 1 cm potato cubes dyed with iodine, but the carrier fluid was a 10% w/w sodium chloride solution and therefore the particles were significantly more dense than the liquid. The RTD of the potato cubes was evaluated by video recording through a transparent window, and that of the liquid by measuring the outlet pH at 10 s intervals following injection of a pulse of citric acid into the pipe. The variables studied were flow rate and particle concentration from 10% to 30% using room temperature (15C) as the operating temperature. However, the Reynolds numbers (Re) for this work were in excess of 10,000, indicating turbulent flow, and therefore the results would not be applicable to nonsettling particles in viscous carrier fluids which exhibit laminar flow.

An experimental technique was described which has applications in the measurement of particle residence times under aseptic processing conditions: high temperatures and pressures, viscous carrier fluids (providing nonsettling conditions for particulate matter), stainless steel holding sections, opaque carrier fluids flowing in laminar flow situations, and a distribution of particle shapes and sizes. The technique described has potential applications for these conditions, and the development and testing of the system was detailed for trials conducted at room temperature. It was also anticipated that a similar experimental technique could be applied to liquid residence times, but the target for this initial study was particle RTD. Two variables affecting RTD were investigated:

the effect of changing the bulk flow rate and the effect of changing particle concentration. The objective of this work was the development of a practical residence time sensing technique for food particles.

MATERIALS AND METHODS

Measurement of Particle Residence Times

In order to measure the velocity of food particles in a pumped system a method was required to detect a specific particle without interfering with the product flow. The sensing technique had to operate through the stainless steel walls of the pipe, otherwise the system could not be applied to actual processes. The method chosen used Hall effect sensors (Bueche 1986), which were able to detect a particle containing a small magnet travelling in a 2 in. IDF pipe. The sensors were found to operate reliably through the pipe wall (2–3 mm thick stainless steel) at a range of up to 40 mm, using pieces of ceramic magnetic material approximately $5 \times 5 \times 2$ mm. The magnets were embedded in a variety of materials including pieces of carrot, adhesive tape, silicone elastomers and heat shrink sleeving. None of these materials were found to adversely affect the sensors; thus the particles containing the magnets could be tailored to closely match the food particles in terms of physical size and density.

To determine the residence time of a particle in the system, two Hall effect sensor arrays were required, each consisting of 4 individual sensor devices, mounted on the pipe a fixed distance apart (Fig. 1). The time taken for the magnetic particle to reach the second sensor array, having passed the first, allowed the residence time of the particle to be calculated. For the purposes of the experimental work an electronic circuit and sensor system using multiple sensors was devised. This provided visual indication of the sensor array outputs and a timer triggered by the sensor arrays to display the time taken to a 0.1 s resolution.

The 4 Hall effect sensors were set at 90 degree intervals around the circumference of the tube viscometer pipe and in the same radial plane. The sensitive surfaces of the devices were clamped directly to the pipe surface. Two such sensor arrays were mounted 3.2 m apart on a straight length of pipe in the system. The devices used were linear Hall effect integrated circuits (IC's) (RS Components Ltd., P.O. Box 99, Corby, Northants, NN17 9RS, U.K.). These had differential outputs that produced a voltage that varied linearly with magnetic flux. The arrays were connected to the sensing electronics via screened multi-core cables. The differential output from each sensor was fed to a unity gain differential amplifier (1/4 of TL084), which provided good noise rejection.

The output signal passed through a passive first order high pass filter with a 1 Hz cutoff to remove any drift and DC voltage offset from the signal. The filter
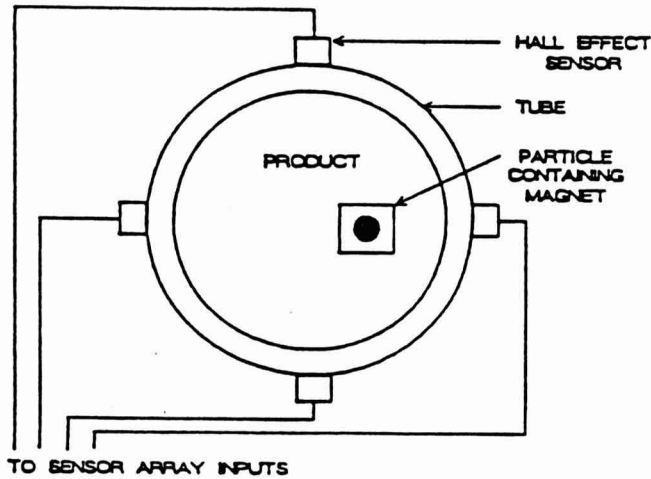
FIG. 1. ARRANGEMENT OF HALL EFFECT SENSORS

output was buffered by a field effect transistor (FET) op-amp (1/4 of TL084) configured as a noninverting amplifier with a gain of 200. The feedback resistor was bypassed by a capacitor to prevent instability, and the output from this amplifier fed to the positive input of a voltage comparator (1/4 of LM339N). The reference voltage fed to the negative input was derived from a potentiometer which the potentiometer clamped to $\pm$ 0.6V above and below ground by two diodes. The output from the comparator was fed via a diode to an open-collector driver (ULN2803A), which drove an light emitting diode (LED) to indicate the state of the comparator. The driver output was also used to match the bipolar comparator output to complementary metal-oxide semiconductor (CMOS) logic levels. The above circuitry was repeated eight times in total, four circuits for the first or "start" sensor array and four for the second or "stop" array. The CMOS signals for each array were "ORed" together to provide single start and stop signals. These were fed to the SET and RESET inputs of a D-type flip-flop (CD4013). The Q output of the flip-flop was used to enable a programmable crystal oscillator (PXO1000) with an output frequency of 10Hz. The oscillator signal was used to drive a 4 decade counter/driver (ZN1040E). The counter outputs drove a multiplexed 4 digit LED display to indicate seconds to 1 decimal place.

The circuit and sensors were powered by a ± 9V dual-rail regulated power supply with further regulation to provide a +5V rail for the CMOS circuitry. The power rails were heavily decoupled to prevent instability and reduce noise. The circuit was shown in block diagram form, as shown in Fig. 2.
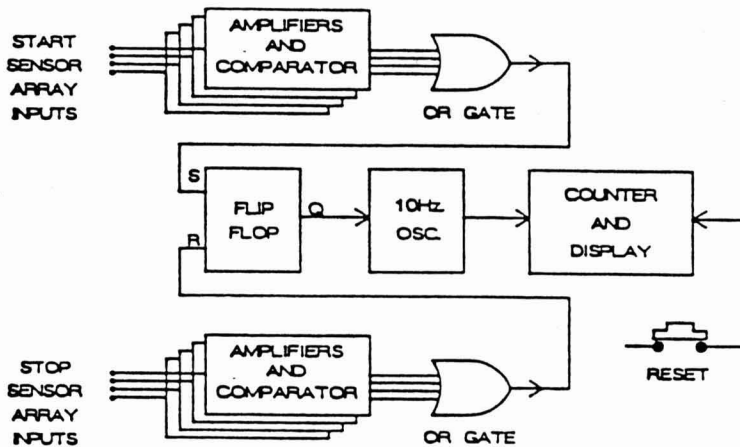
FIG. 2. ELECTRONIC CIRCUITRY FOR HALL EFFECT SENSORS

During operation, one or more of the sensors produced a change in output voltage in response to a magnetic particle passing the start sensor array. This was buffered by the differential amplifier into the high pass filter, and then amplified by the noninverting amplifier to produce a voltage pulse of typically 0.5–2.0V. The voltage was compared by the comparator to the reference voltage from the potentiometer. This reference was set to just prevent noise from operating the comparator. The bipolar output from the comparator had the negative voltage removed by the diode before driving the LED's via the open collector drivers. The "ORed" start and stop signals set and reset the flip-flop respectively, thus enabling the oscillator and hence the counter/display for the time the particle takes to pass from the start to the stop sensor array. Since the

oscillator ran at 10 Hz, the counter showed elapsed time to a resolution of 0.1 s. The counter was reset via a push-button after each pass.

Characterization of Flow Properties

Measurement of the pressure drop over a 3.2 m pipe section for a series of volumetric flow rates allowed the shear stress at the pipe wall to be related to the shear rate. Using this data the flow properties were characterized using the Power Law, to obtain the general consistency coefficient (k) and the flow behavior index (n). To measure the pressure at either end of the 3.2 m of 2 in. IDF pipe, miniature prototype Druck DPCR81 transducers were used. These were specially designed to operate and remain linear at temperatures as high as 130C. This meant that they could be mounted directly into the tube with the diaphragm directly in contact with the product, without the need for capillary legs. The pressure range of each transducer was 0–50 psig, and each were connected to Druck DPI2600 digital displays giving a resolution of 0.01 psi. Errors on pressure drop measurement were calculated to be $\pm$ 2.0%. The pressure could also be read via a 4–20 mA current loop output, and this was used to provide the signal for the differential display circuit described below. Because of their small size special gland assemblies were constructed to clamp the transducers into the bosses in the tube.

The differential pressure was measured using an electronic circuit, shown in Fig. 3. Current loop outputs from the Druck displays were converted to voltages, subtracted to produce a difference and thus displayed as differential pressure. The difference voltage was scaled and output to a digital display, which showed differential pressure measured in psi to a display resolution of two decimal places.

Each current loop signal from the Druck displays was fed through a precision 250 ohm resistor (0.1% tolerance). The voltages across these were fed to unity gain differential amplifiers (1/4 of LF347), which removed noise and common mode components of the signal. Following this, the voltages were fed to either input of a third unity gain differential amplifier (1/4 of LF347), and the output of this amplifier was the difference between the input signals. In order to minimize the effects of rapid pressure fluctuations caused by the pump the signal was fed through a passive first order low pass filter with a time constant of 2–3 s. This had the effect of smoothing out the fluctuations to give a more stable display. The filter was buffered by a noninverting amplifier (1/4 of LF347) whose output drove a potential divider, which was scaled to give 10 mV per psi. The scaled voltage drove a liquid crystal display (LCD) voltmeter with a full scale range of $\pm$ 199.9mV, which in turn generated a differential pressure range of $\pm$ 19.99 psi.
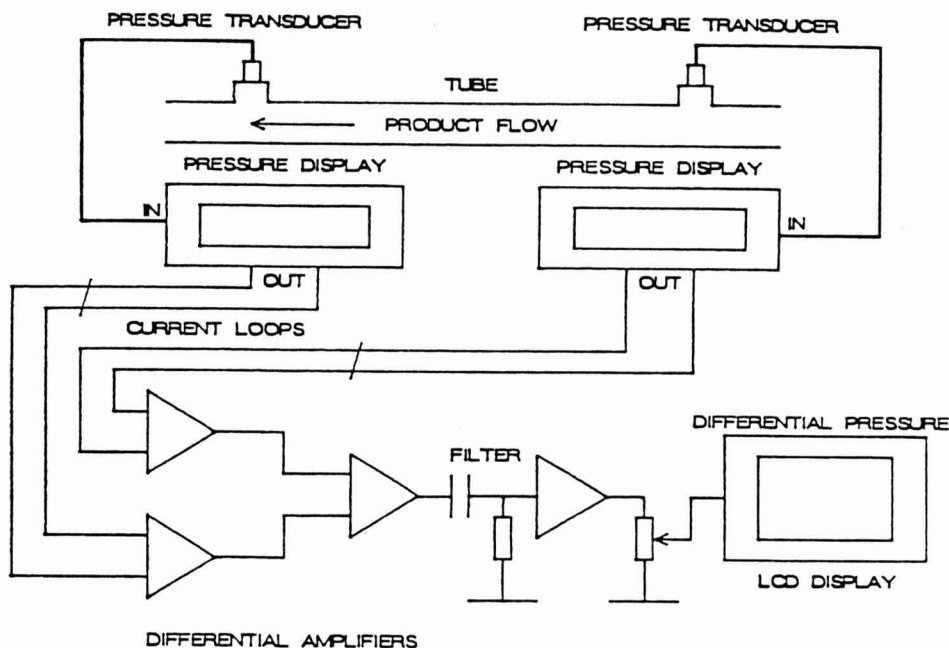
FIG. 3. ELECTRONIC ARRANGEMENT FOR MEASURING THE
DIFFERENTIAL PRESSURE

The circuit used precision resistors throughout in order to minimize inaccuracies. Power was provided by a heavily regulated main power supply with extra decoupling capacitors at the LF347 to ensure good noise rejection. During use, the 4–20 mA current signal, equivalent to 0–50 psig, from the Druck displays was fed through the 250 ohm input resistors giving a voltage across these of 1–5 V. This voltage was fed to unity gain differential amplifiers whose outputs in turn drove the third differential amplifier. The voltage at the output of this amplifier was equivalent to the difference between the two input currents and hence the pressures at the two transducers. The output voltage was from −8V to +8V depending on the input signals, although in practice it was much smaller due to the small pressure differential experienced in the tube. The filter removed rapid fluctuations from the signal and the potential divider reduced the voltage swing to ± 199.9mV, equivalent to ± 19.99 psi. This was used to drive the LCD display module whose decimal point was programmed to give two decimal places, that is to read pressure to 0.01 psi.

The system used to measure volumetric flow rate was a 10 L bucket and a stopwatch with 0.1 s resolution. This provided a sufficiently accurate flow rate measurement ($\pm$ 0.2 L.min^{-1}), which could not have been metered to the desired accuracy using conventional flow meters. In fact, Coriolis flow meters had been investigated as a means to determine mass flow rates, but the low flow rates required for aseptic processing ($<$50 L.min^{-1} in 2 in. IDF pipe) restricted the measurement range of the flow meter to the bottom of the scale. Unfortunately the accuracy obtained in this operational region was poor and unreliable; therefore Coriolis flow meters could not be used.

Experimental Methodology for Taking Residence Times

A schematic diagram of the tube viscometer with residence time adaptations is shown in Fig. 4. Fresh batches comprising 150 L of 4% Colflo 67 (National Starch and Chemical GmbH; 6730 Neustadt a.d.W., Bundesrepublik, Deutschland) were gelatinized in a steam pan and were used as the carrier fluid for the residence time studies. Unfortunately one of the disadvantages of using food materials as carrier fluids was that, unlike water, there was a time-dependent factor associated with intermolecular breakdown during continuous pumping for starch-based foods. This resulted in a reduction in the viscosity, as the shear on the fluid continued. To overcome this problem large volumes of starch (150 L) were made up fresh for each trial, and used for the duration of the residence time studies. In this way there was a limited amount of recirculation of the starch, and this helped to retain the flow characteristics throughout the experiments. However, to ensure that the fluid was not breaking down due to excessive shear, the rheological characteristics were assessed at the start and end of the residence time trials. To make this assessment of rheological properties a series of six pressure drop and flow rate readings were taken and the natural logarithm (flow rate) was plotted against the natural logarithm (pressure drop). The results are reported in the tables of data for residence times, as Power Law constants.

The Hall effect sensors easily detected single particles containing a magnet, in several different concentrations of carrots and through a 2 in. IDF stainless steel pipe. To introduce the magnetized carrot into the pump suction piping, a particle dosing tube was built. This involved a high density polyethylene tube 16 mm i.d. into which a 7 mm diameter stainless steel rod with a 13 mm nut passed. The small clearance between nut and tube allowed starch carrier fluid to pass but not the magnetic carrot, so that the carrot was slowly pushed into the pump suction piping. To prevent a bubble of air becoming trapped with the carrot, it was essential that the magnetic carrot was pushed slowly down the tube to allow the air to escape.
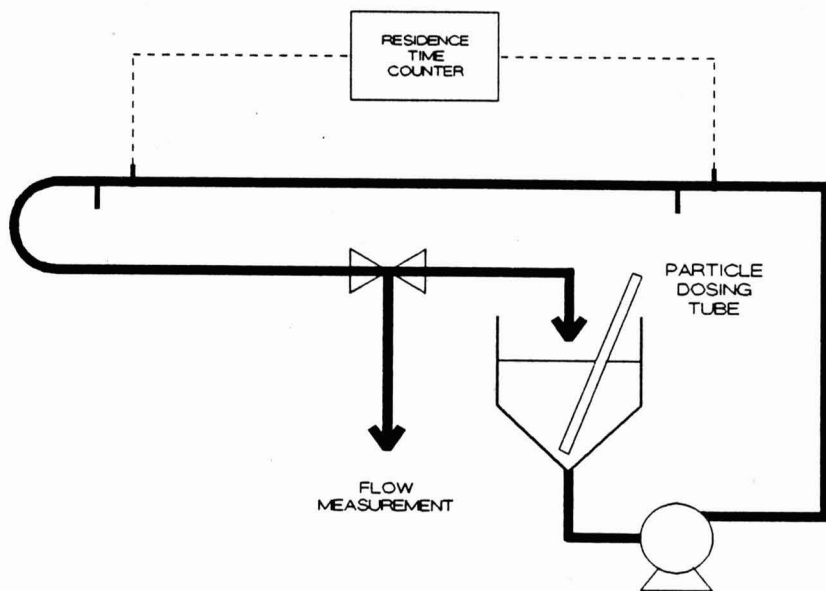
FIG. 4. SCHEMATIC DIAGRAM OF THE RESIDENCE TIME APPARATUS

On exit from the tube viscometer the magnetic particle was caught using a sieve. The approximate time of exit was calculated on the basis of the tube length after the holding section, so that the sieve did not collect too many carrots. Thus the mixture in the feed tank was not adversely affected by removing significant quantities of carrots. Blue shrink-wrap was used to enclose the magnet within the carrot; therefore it was a simple task to retrieve the magnetic carrot from the sieve containing other similar sized carrots by visual inspection. Once separated from the other carrots, the magnetic carrot was put back into the particle dosing tube and sent recirculating around the tube viscometer to record another residence time. Sample populations of 20 or 50 residence times were taken depending on the trial, and residence time distributions plotted for each trial.

Statistical Analysis Techniques

A total of 50 residence times (RT) were measured for each trial concerning the effect of three different flow rates and 20 RT per trial for the effect of four different particle concentrations. These were analyzed in terms of the mean RT, standard deviation, minimum RT, and via a plot of the residence time

distribution (RTD). The RTD was calculated from the Gaussian density function, which modelled the relative frequency distribution of errors (Mendenhall and Sincich 1989). This has also been referred to as the normal probability distribution (Alcairo and Zuritz 1990) and was calculated for the residence times as follows:

$$f(t) = \frac{1}{\sigma(2\pi)^{1/2}} \cdot e^{-(t-\mu)^2/2\sigma^2} \quad for \ -\infty < t < \infty$$

where t is the measured residence time (s)
   σ is the standard deviation (s)
   σ^2 is the variance (s^2)
   μ is the mean residence time (s)

Figures 5 and 6 show the Gaussian density function plotted against residence times for effect of bulk flow rate (Fig. 5) and particle concentration (Fig. 6).
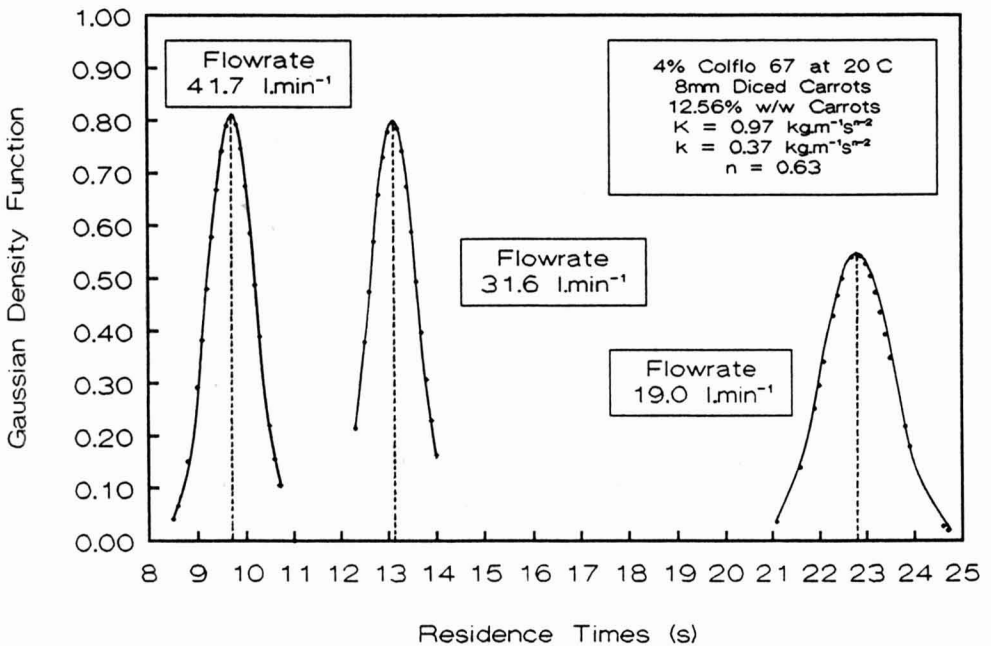
FIG. 5. THE EFFECT OF BULK FLOW RATE ON THE RESIDENCE TIME
DISTRIBUTION E(t)

G.S. TUCKER and P.M. WITHERS
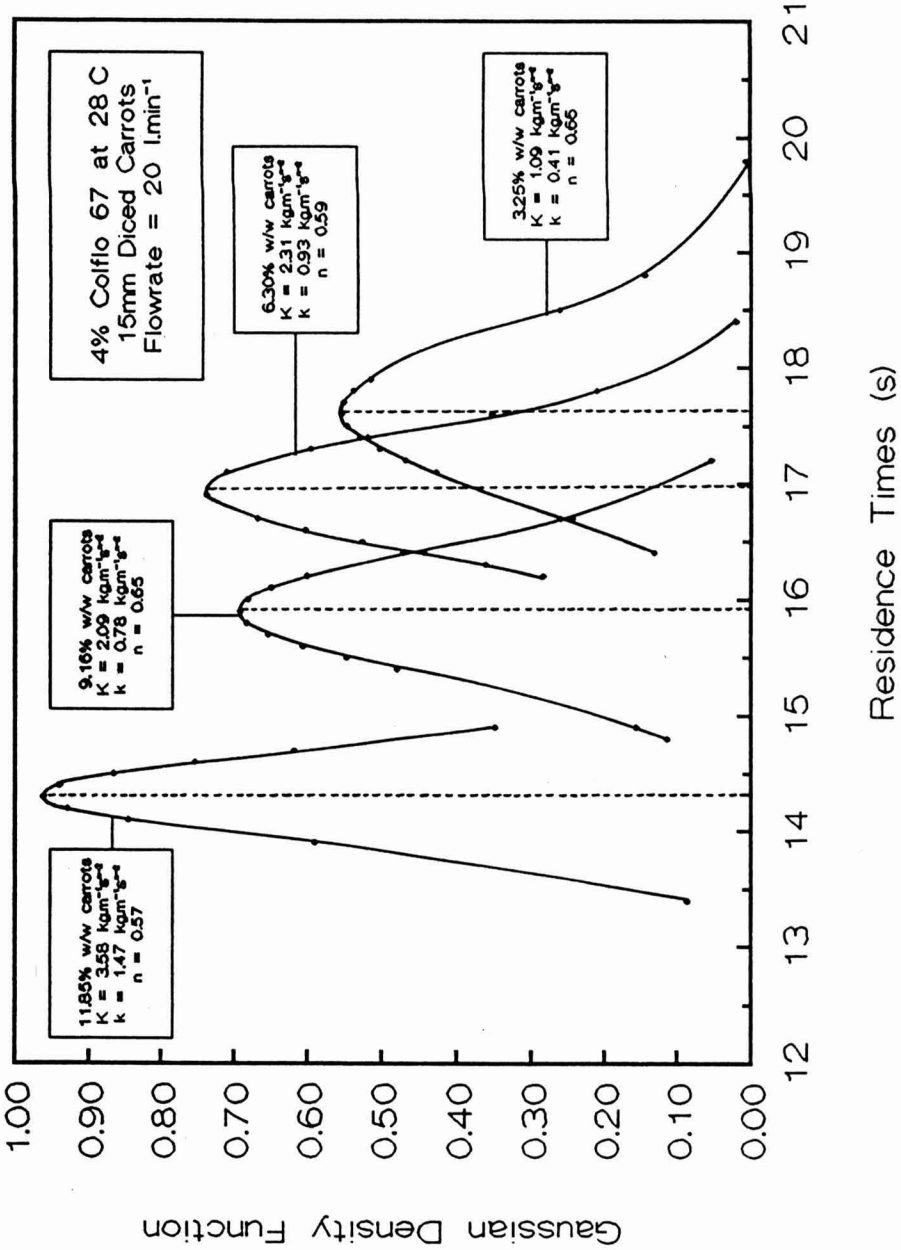
FIG. 6. THE EFFECT OF PARTICLE CONCENTRATION ON THE RESIDENCE TIME DISTRIBUTION E(t)

RESULTS AND DISCUSSIONS

Tube Reynolds numbers were calculated for each trial to confirm that the flow regime was laminar. For Power Law fluids, the tube Reynolds number can be defined as (Tucker 1992):

$$Re = \frac{4^n \rho . v . D}{K.(8v/D)^{n-1}}$$

or,

$$Re = \frac{8\rho . v^{2-n}. D^n}{2^n . K}$$

where ρ is the food density (kg. m^{-3})

v is the mean flow velocity (m. s^{-1})

D is the inside pipe diameter (m)

K is the consistency coefficient for pipe flow
[K = k(3n+1/n)^n] (kg. m^{-1}.s^{n-2})

k is the general consistency coefficient (kg. m^{-1}.s^{n-2})

n is the flow behavior index

The tube Reynolds numbers for the trials at three different flow rates were calculated from the following data, and presented in Table 1.

Density of the 8 mm diced carrot/starch mixture (ρ) was 1,009 kg.m^{-3}, inside pipe diameter (D) 0.0476 m, the consistency coefficient for pipe flow (K) 0.97 kg.m^{-1}.s^{n-2} and the flow behavior index (n) 0.63. Using the mean fluid velocity (v), as calculated from the volumetric flow rates for the three trials at 19.0, 31.6 and 41.7 L.min^{-1}, tube Reynolds numbers of were calculated from the values in Table 1.

TABLE 1.
FLOW DATA FOR DIFFERENT FLOW RATES OF 8 MM DICED CARROT
IN 4% COLFLO 67 at 20C

Flow rate (L.min^{-1})	Mean velocity (m.s^{-1})	Tube Reynolds numbers
19.0	0.18	74.2
31.6	0.30	149.0
41.7	0.39	218.1

These values were below that for the transition zone from laminar flow to turbulent flow, generally taken for liquids to be at Re = 2,100 (Skelland 1967) and it was therefore a safe assumption that the flow was laminar for the trials.

The tube Reynolds numbers for the trials at four different carrot concentrations, for 15 mm diced carrots, were calculated from the data given in Table 2. For each of these trials the flow characteristics calculated using the Power Law were different, hence these values were included in the table. The values for tube Reynolds number were also below 2,100; hence the flow behavior was laminar in each trial.

TABLE 2.
FLOW DATA FOR DIFFERENT CONCENTRATIONS
OF 15 MM DICED CARROT IN 4% COLFLO 67

Carrots % w/w (15mm diced)	Mean flow rate (L.min⁻¹)	Mean velocity (m.s⁻¹)	Consistency coefficient (K) (kg.m⁻¹.s^{n-2})	Flow behavior index (n)	Tube Reynolds number
03.25	19.9	0.19	1.09	0.65	67.3
06.30	19.9	0.19	2.31	0.59	35.9
09.16	19.6	0.18	2.09	0.65	34.6
11.85	20.1	0.19	3.58	0.57	24.5

Effect of Flow Rate on RTD

Table 3 presents the mean RT, minimum RT and standard deviation for three different flow rates of 12.5% w/w 8 mm diced carrot in 4% Colflo 67 carrier fluid calculated from 50 residence time measurements.

TABLE 3.
STATISTICAL DATA FOR RESIDENCE TIMES OF 8 MM
DICED CARROTS IN 4% COLFLO 67 AT 20C

Flow rate (L.min⁻¹)	Mean RT (s)	Minimum RT (s)	Standard deviation, σ (s)
19.0	22.8	21.1	0.73
31.6	13.1	11.0	0.50
41.7	9.7	8.5	0.49

Standard deviation was found to decrease from 0.73 to 0.49 s as the volumetric flow rate increased from 19.0 L.min^{-1} to 41.7 L.min^{-1}, indicating a narrower residence time distribution. The velocities of the 8 mm carrot particles were compared to the mean flow velocity (as measured with a calibrated bucket and stopwatch), and the results are shown in Table 4. These values indicated that the mean particle velocities were lower than the mean flow velocity of the heterogeneous mixture. It was also found that the velocity of the fastest moving particle was less than the mean flow velocity.

TABLE 4.
VELOCITIES OF PARTICLES AND FLUID FOR 8 MM DICED CARROTS
IN 4% COLFLO 67 AT 20C

Flow rate (L.min^{-1})	Mean flow velocity (m.s^{-1})	Mean particle velocity (m.s^{-1})	Maximum particle velocity (m.s^{-1})
19.0	0.18	0.14	0.15
31.6	0.30	0.24	0.29
41.7	0.39	0.33	0.38

Effect of Particle Concentration on RTD

Table 5 presents the mean RT, minimum RT and standard deviation for four concentrations, 3.25, 6.30, 9.16 and 11.85% w/w of 15 mm diced carrot in 4% Colflo 67 carrier fluid, calculated from 20 residence time measurements. Standard deviation decreased from 0.72 s at 3.25% w/w carrots to 0.42 s at 11.85% w/w carrots, indicating a narrower RTD as carrot concentration increased. The mean values for residence time decreased from 17.6 s to 14.3 s with the higher concentrations of particles.

TABLE 5.
STATISTICAL DATA FOR RESIDENCE TIMES OF
15 MM DICED CARROTS IN 4% COLFLO 67 AT 28C

15mm diced carrot concentration (%w/w)	Mean RT (s)	Minimum RT (s)	Standard deviation (s)
03.25	17.6	16.4	0.72
06.30	17.0	16.2	0.54
09.16	15.9	14.8	0.58
11.85	14.3	13.4	0.42

Table 6 presents data for the mean and maximum particle velocities, together with the mean flow velocity of the heterogeneous mixture. With reference to Eq. (1) for Power Law fluids it was possible to predict the maximum velocity of the heterogeneous mixture. This occurred along the center line, and was related to the flow behavior index (n), which dictated the shape of the velocity profile. Table 7 contains the normalized maximum flow velocity for the heterogeneous fluid as predicted using Eq. (1) together with the normalized particle flow velocities for the mean and fastest particles, as measured using the Hall effect sensors. The normalized velocities were obtained by dividing the respective velocities by the mean flow velocity of the mixture obtained from the volumetric flow rate readings.

TABLE 6.
VELOCITIES OF PARTICLES AND FLUID FOR
15 MM DICED CARROTS IN 4% COLFLO 67 AT 28C

Carrot concentration (% w/w)	Mean flow velocity $(m.s^{-1})$	Mean particle velocity $(m.s^{-1})$	Maximum particle velocity $(m.s^{-1})$
3.25	0.19	0.18	0.20
6.30	0.19	0.19	0.20
9.16	0.18	0.20	0.22
11.85	0.19	0.22	0.24

TABLE 7.
NORMALIZED FLOW VELOCITIES (NFV) AS
INFLUENCED BY CARROT CONCENTRATION

Carrot concentration (% w/w)	Theoretical NFV (equation 1)	Maximum particle NFV (measured)	Mean particle NFV (measured)
3.25	1.79	1.05	0.98
6.30	1.74	1.07	1.01
9.16	1.79	1.17	1.09
11.85	1.73	1.27	1.19

The NFV values in Table 7 clearly highlighted the trend in increasing particle flow velocities (decreasing residence times) as a function of increasing particle concentration. In this case the flow rate was 20.0 L.min^{-1} $\pm$ 0.2 L.min^{-1}

through a 2 in. IDF tube viscometer, using 15 mm diced carrots (with swarf) in a 4% Colflo 67 viscous carrier fluid, and the readings taken at room temperature of 28C.

Using comparable flow rates to those in this study, Alcairo and Zuritz (1990) reported that mean particle residence times were equal to mean fluid residence times, for single particles suspended in a viscous CMC carrier fluid. However, as the flow rate was increased it was found that the mean particle residence times decreased in relation to the mean fluid residence times. These results would appear to contradict those presented in this paper, but Alcairo and Zuritz (1990) used a single suspended particle only and did not consider the potential effects of particle-particle interactions. Lee and Singh (1991) presented data for potato cubes in CMC solutions travelling up a vertical pipe. The particle residence times were divided by the mean fluid residence times to normalize the residence times. It was found that the mean normalized particle residence times were between 6.1% and 14.7% longer, indicating that the particles spent longer travelling up the vertical tube than the liquid. These results were for particle concentrations up to 40% w/v and were therefore relevant to our work.

Similar results to those presented here were reported by Segner *et al.* (1989) using 12.7 mm turkey cubes in horizontal flow. It was found that the fastest magnetic turkey cubes were much slower than the theoretical calculations for laminar flow suggested. These results were taken at UHT conditions in a SSHE, and are therefore highly relevant.

CONCLUSIONS

The use of Hall effect sensors for residence time measurements of magnetic particles was demonstrated at room temperature. The technique has applications to pipe flow of large discrete particles at high temperatures and was proven to work through a stainless steel tube. In addition the Hall effect sensors were used in conjunction with pressure drop measurements from a tube viscometer. Therefore both rheological and residence time data were collected simultaneously, which provides information for the calculation of the fluid-particle surface heat transfer coefficient from relative velocity measurements. Using this it will be possible to design holding tube lengths using mathematical models, to ensure that safe sterilization processes are established. It should be noted, however, that the true relative velocity may be different from that calculated by this subtraction because of channelling effects around particles. Mean and fastest particle residence times were found to be less than the theoretical values predicted from laminar flow assumptions. Thus the industry practice of doubling the holding tube length based on mean velocity calculations was proven to be conservative, for the cases investigated.

The Hall effect sensors used in this system offer an output that varies linearly with magnetic field strength: that is, the closer the magnet is to the sensor the greater the output voltage. If a number of sensors were used in an array fitted to a tube as described in this report, the relative output signals from the sensors could be tuned to give an indication of the position of a magnetic particle as it passed the sensor array. If a number of arrays were fitted at regular intervals along the tube it may be possible to deduce the path of the particle. This information would be useful in determining the mechanism by which the particle moves in the product flow, in terms of the relative position of the particle at regular intervals. The information from the sensors would most likely need analysis within a computer, but the simplest approach would be to use the computer to interrogate the sensors directly via a suitable analogue interface card. It may then be possible to produce a real time indication of particle position as it passes each sensor array.

A sensor system such as this may find applications other than pumped systems as described here. For example the technique could be used to monitor the movement of food particles inside containers being agitated as part of a process or even particle movement due to convection currents within containers during heating.

In the short term it is planned that the tube viscometer with the two sets of four Hall effect sensors be attached to a SSHE. Thus, information could be obtained about heterogeneous flow systems at high temperatures applicable to UHT operations. The first work will use a SSHE under pasteurization conditions (<100C) and use the tube viscometer as one leg of the holding tube. Following on from this, the SSHE would be operated at sterilization temperatures (>110C). At such elevated temperatures the tube surfaces would be too hot for the Hall effect sensors to operate; therefore, the sensors could be mounted a small distance from the tube surface. The output signal is not affected by an air gap, other than that the distance for sensing a magnetic particle would be reduced. However, for a 2 in. IDF pipe this would not represent a problem.

ACKNOWLEDGMENT

REFERENCES

ALCAIRO, E.R. and ZURITZ, C.A. 1990. Residence time distributions of spherical particles suspended in non-Newtonian flow in a scraped-surface heat exchanger. Trans. ASAE *33*(5), 1621–1628.

BUECHE, F.J. 1986. *Introduction to Physics for Scientists and Engineers*, 4th Ed., pp. 450–452, McGraw-Hill Book Co., Singapore.

DANKWERTS, P.V. 1953. Continuous flow systems, distribution of residence times. Chem. Eng. Sci. *2*(1), 1–18.

DUTTA, B. and SASTRY, S.K. 1990. Velocity distributions of food particle suspensions in holding tube flow: experimental and modelling studies on average particle velocities. J. Food Sci. *55*(5), 1448–1453.

HONG, C.W., SUN PAN, B., TOLEDO, R.T. and CHIOU, K.M. 1991. Measurement of residence time distribution of fluid and particles in turbulent flow. J. Food Sci. *56*(1), 255–256, 259.

LEE, J.H. and SINGH, R.K. 1991. Process parameter effects on particle residence time in a vertical scraped surface heat exchanger. J. Food Sci. *56*(3), 869–870.

MANSON, J.E. and CULLEN, J.F. 1974. Thermal process simulation for aseptic processing of foods containing discrete particulate matter. J. Food Sci. *39*, 1084–1089.

MENDENHALL, W. and SINCICH, T. 1989. *Statistics for the Engineering and Computer Sciences*, 2nd Ed., pp. 190–191, Dellen Publishing Co., San Francisco.

PALMIERI, L., CACACE, D., DIPOLLINA, G. and DALL'AGLIO, G. 1992. Residence time distribution of food suspensions containing large particles when flowing in tubular systems. J. Food Eng. *17*, 225–239.

PFLUG, I.J., BERRY, M.R. and DIGNAN, D.M. 1990. Establishing the heat preservation process for aseptically packaged low-acid food containing large particulates, sterilized in a continuous heat-hold-cool system. J. Food Prot. *53*(4), 312–321.

SEGNER, W.P., RAGUSA, T.J., MARCUS, C.L. and SOUTTER, E.A. 1989. Biological evaluation of a heat transfer simulation for sterilising low-acid large particulate foods for aseptic processing. J. Food Processing Preservation *13*, 257–274.

SKELLAND, A.H.P. 1967. *Non-Newtonian Flow and Heat Transfer*, John Wiley & Sons, New York.

TAEYMANS, D., ROELANS, E. and LENGES, J. 1985. Influence of residence time distribution on the sterilization effect in a scraped-surface heat exchanger used for processing liquids containing solid particles. Int. Union of Food Sci. and Technol. Symp., Proc. of *Aseptic Processing and Packaging of Foods*, pp. 100–107, Tylosand, Sweden, Sept. 9–12, 1985.

TUCKER, G.S. 1992. Determining the rheological properties of liquid foods containing particulate matter during continuous processing. Technical Memorandum No. 668, Campden Food and Drink Research Assoc., Chipping Campden, Glos, UK.

YANG, B.B. and SWARTZEL, K.R. 1991. Photo-sensor methodology for determining residence time distributions of particles in continuous flow thermal processing systems. J. Food Sci. *56*(4), 1076–1081, 1086.

TEMPERATURE MAPPING IN A POTATO USING HALF FOURIER TRANSFORM MRI OF DIFFUSION

XIUZHI SUN[1], SHELLY J. SCHMIDT[2,3], and J. BRUCE LITCHFIELD

[1]Department of Agricultural Engineering
[2]Division of Foods and Nutrition
University of Illinois
Urbana, IL 61801

ABSTRACT

Two dimensional temperature maps of a potato during heating were obtained using magnetic resonance imaging (MRI) techniques. The molecular pseudo self-diffusion coefficient of the water in the potato was used as a temperature indicator. Two dimensional half Fourier transform spin-echo and Generalized Series reconstruction techniques were used to reduce data acquisition time to about 10 s/image and to improve temperature mapping resolution. Thermocouples were implanted into the sample so that temperature and MRI data were acquired simultaneously. The error in MRI measurements caused by noise and the time delay required to collect each data set was less than 0.84C with 0.75 mm^2 resolution. The average variation between MRI and thermocouple measurements was less than 0.5C. This is a promising new technique to noninvasively study heat transfer and to measure thermal properties of food materials.

INTRODUCTION

Temperature is an important parameter in food processes such as pasteurization, freezing, and drying. Temperature is also important in determining thermal properties of foods, such as specific heat, thermal conductivity, thermal diffusivity, and the convective heat transfer coefficient. These properties are needed to design and control food processes. A new approach to measure temperature noninvasively uses magnetic resonance imaging (MRI) techniques. The spin-lattice relaxation time (T_1) has been used as a temperature indicator since 1982 (Parker *et al.* 1982; Suits 1986; Dickinson *et al.* 1986; Howe 1988).

---

[3] Correspondent: Shelly J. Schmidt, 367 Bevier Hall, MC-180, Urbana, IL 61801, Phone 217-333-6369.

However, recently the self-diffusion coefficient (D) was reported to be more temperature sensitive than T_1 for a model food gel system (Le Bihan *et al.* 1989).

In previous work (Sun *et al.* 1993), a two dimensional temperature map of a model food gel (agar:microcrystalline cellulose:water at concentrations of 1.95:6.55:200, respectively) was obtained by MRI techniques using a pseudo self-diffusion coefficient (D*) method. The sample was heated and cooled by circulating water. The initial temperature of the sample for heating was 18C, and the heating water temperature was 35C. The initial temperature of the sample for cooling was 35C, and the cooling water temperature was 18C. The D* was found to be more sensitive to temperature than the self-diffusion coefficient (D). The temperature coefficient of the gel was approximately 13.0%/C. The error in the MRI measurements was found to be less than 1C with 1.5 mm² resolution. The average variation between MRI and thermocouple measurements was less than 1.3C. However, the data acquisition time for each self-diffusion mapping data set for the gel was about 30 s. Changes in temperature during data acquisition introduced error into the temperature mapping data obtained. The slower the data acquisition time and the larger the temperature difference between the particle and the liquid, the larger the error caused by the temperature change during data acquisition. Recently, a variety of fast MRI pulse sequences have been developed that can be used to decrease the data acquisition time (Le Bihan 1991; Wehrli 1991). However, whether these pulse sequences can be used depends largely on the composition of the sample and the capacity of the available MRI hardware.

The objectives of this study were to obtain 2D self-diffusion images of a potato using half Fourier transform MRI scanning and generalized series reconstruction techniques to decrease the data acquisition time, and compare the resultant MRI temperature images to those obtained simultaneously with thermocouples.

THEORY

When placed in a static magnetic field, the randomly oriented magnetic dipoles of selected nuclei line up with or opposite to the magnetic field to yield a magnetic moment. The simplified signal intensities given off from nuclei (i.e., proton) in a static magnetic field after a radio frequency excitation are given by Eq. 1:

$$S = K(T)\rho[1-\exp(-\frac{T_R}{T_1})]\exp(-\frac{T_E}{T_2})\exp(-bD) \qquad (1)$$

where S is the signal intensity, ρ is the proton density, T_R is the repetition time, T_1 is the spin-lattice relaxation time, T_E is the echo delay time, T_2 is the spin-spin relaxation time, b is the gradient factor (Eq. 2), D is the molecular self-diffusion coefficient, and K(T) is a constant at a constant temperature. The b factor is defined by Eq. 2:

$$b = \gamma^2 \int_0^{T_E} \sum_{j=1}^{n} [\int_0^{t'} G_j(t'') \, dt'']^2 \, dt' \qquad (2)$$

where $n = 1, 2, \ldots$, G_j is the gradient applied along a coordinate direction, t' is the gradient delay time, t'' is the gradient duration time, γ is the gyromagnetic ratio, and j is the number of gradients along the coordinate direction.

If the parameters in Eq. 1 are kept constant except for the b factor, a diffusion weighted image can be obtained. In the presence of a magnetic field gradient, as the molecules move randomly in space, they cause random phase shifts. This causes a reduction in the signal intensity, or so-called "signal attenuation" (Taylor and Bushell 1985). The faster the diffusion, the more signal attenuation. Therefore, the D image can be obtained by quantifying the signal attenuation.

Several different approaches can be used to obtain self-diffusion weighted images. They include increasing the following parameters: the number of echoes, the strength of the encoding gradient, the strength of the nonencoding (self-diffusion) gradient, and the duration time of gradients. All of these approaches require a minimum of two diffusion weighted images for the determination of a D image (Le Bihan 1988), as shown in Eq. 3:

$$\frac{1}{b_2-b_1} \ln(\frac{S_1}{S_2}) = \ln[\frac{\rho(1-\exp(-T_R/T_1))\exp(-T_E/T_2)\exp(-b_1 D)}{\rho(1-\exp(-T_R/T_1))\exp(-T_E/T_2)\exp(-b_2 D)}] = D \qquad (3)$$

where S_1 and S_2 are the signal intensities corresponding to b_1 and b_2. The approach of changing the strength of the nonencoding gradient to obtain the self-diffusion images was used in this study.

Assuming the Stokes-Einstein relation between viscosity and diffusion, the temperature dependence of the diffusion coefficient can be described by Eq. 4 (Simpson and Carr 1958; Cussler 1984; Le Bihan et al. 1989):

$$\frac{d\,D}{D} = (\frac{E_a}{K\,T}) \frac{d\,T}{T} \tag{4}$$

where E_a is the activation energy for translational molecular diffusion (erg), K is the Boltzmann constant (erg/mol K), and T is the temperature (K). By substituting dD and dT with ΔD and ΔT, and if the diffusion images D_r and D_i can be obtained at two different temperatures (T_r and T_i), the temperature image can be calculated using Eq. 5:

$$\Delta T = (T_i - T_r) = (\frac{KT_r^2}{E_a}) [\frac{D_i - D_r}{D_r}] \tag{5}$$

where T_r is the reference temperature, T_i is the temperature at a time later than the reference temperature, D_r is the diffusion coefficient at temperature T_r, and D_i is the diffusion coefficient at temperature T_i. The term KT_r^2/E_a, in Eq. 5 is referred to as the temperature coefficient.

The D described by Eq. 3, 4, and 5 can be considered the true D if the effects of macromotions are neglected. If one of the two images is acquired by turning off the diffusion gradient, the b factor is almost equal to zero, and the term e^{-bD} is close to one. Thus D can be obtained by Eq. 6:

$$D = \frac{1}{b}\ln(\frac{S_1}{S_2}) = \ln[\frac{e^{A_1}}{e^{A_2}e^{-bD}}] \tag{6}$$

where $A_1 = A_2$ (where $e^A = k(T)[1 - \exp(-T_R/T_1)]\exp(-T_E/T_2)$) and it is assumed that the temperature change is very small during data acquisition.

By assuming that the signal intensity is temperature independent if the b factor is close to zero, S_1 can be considered constant so that S_1 can be acquired at the reference temperature. Therefore, only one diffusion weighted image (S_2) is needed at any time during processing. However, the signal intensity is not temperature independent (Ruan 1991) so the D obtained by this method is in error by a factor D_1 (Eq. 7):

$$D^* = D_1 + D \tag{7}$$

where $D_1 = (A_1 - A_2)/b$ caused by temperature effects, and D* is defined as

the pseudo diffusion coefficient. The relative change of D and D* per unit temperature is defined by Eq. 8 and 9, respectively:

$$\frac{\Delta D}{\Delta T} = [\frac{(D-D_r)/D_r}{\Delta T}$$ (8)

$$\frac{\Delta D^*}{\Delta T} = [\frac{(D_1+D-D_r)/D_r}{\Delta T}]$$ (9)

where D, D_r, and ΔT are the same values for both Eq. 8 and 9. D_1 is positive, so D* is more sensitive to temperature than D.

MATERIALS AND METHODS

Materials

A potato (Anthony Farm Inc. No. 1, Scandinavia, WI), obtained from a local market in Urbana, IL, was used. A cylinder 25 mm in diameter and 60 mm in length was cored from the potato using a copper pipe with a sharp end. The sample was presoaked in water (the water was changed daily) at 20C for about four days before testing. This allowed a uniform moisture distribution to be obtained in the potato. During the presoaking period, the leakage of the sample holder was also tested. The moisture content as measured by the oven method (Standards, S358.2, ASAE 1992) was 82.88% (wb) before soaking and 83.56% (wb) after soaking.

Half Fourier Transform Scanning Techniques

A two dimensional Fourier transform spin-echo diffusion sequence was used to collect the MRI data (Fig. 1). There are two main approaches which can be used to reduce the data acquisition time of this sequence. One is the pulse flip angle method, and the other is the half Fourier transform method (Wehrli 1991). The flip angle method cannot be used for self-diffusion measurements with the current equipment, because the echo time for the small flip angle sequence is short. However, the diffusion time is even shorter than the echo time. Therefore, if the strength of the applied gradient is too low, then the b factor produced by this method is not strong enough to obtain the self-diffusion measurement.
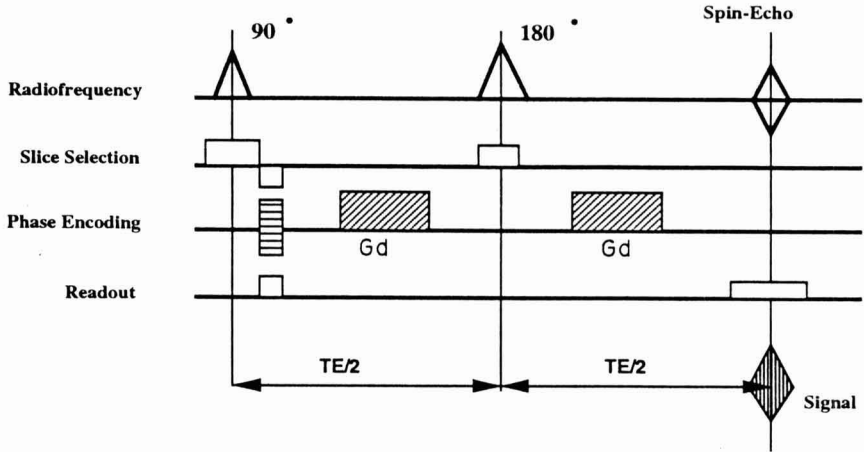
FIG. 1. 2DFT SPIN-ECHO DIFFUSION SEQUENCE
A bipolar diffusion gradient (Gd) was added to the phase encoding
direction to enhance diffusion weighting.

The half Fourier transform technique can be described using k-space. k-space is the spatial frequency domain in which data collection is performed (Fig. 2A). k_y is the phase encoding direction and k_x is the frequency encoding direction. The interval between two k lines in the k_y direction is the product of the repetition time and the number of scans. The interval between two k lines in the k_x direction is the sampling time divided by the number of frequency encoding steps. Since k-space and the image are the Fourier transform of one another, each line of the k-space contributes to the entire image. The center lines contribute most to the signal to noise ratio, and the peripheral lines contribute mainly to the spatial resolution (Wehrli 1991). The data acquisition speed in the phase encoding direction is much slower than in the frequency encoding direction. Therefore, data acquisition time can be reduced by collecting the half k-space (half-Fourier) in the phase encoding direction (Fig. 2B).

The data acquisition time was also reduced by using fewer phase encoding steps. The generalized series (GS) reconstruction method (Liang et al. 1992) was used to improve the image resolution. The GS technique allows for the reconstruction of low resolution images into high resolution images. With the GS technique, a full Fourier transform image (I_1) with the required spatial resolution is needed. I_1 is then built into the basic function of a generalized series model for reconstruction of the half Fourier transform image (I_2) with fewer phase encoding steps. Thus, image reconstructed by the GS method contains all the information in I_2, but has the same resolution as I_1. Therefore, data acquisition time is reduced while image resolution is enhanced.
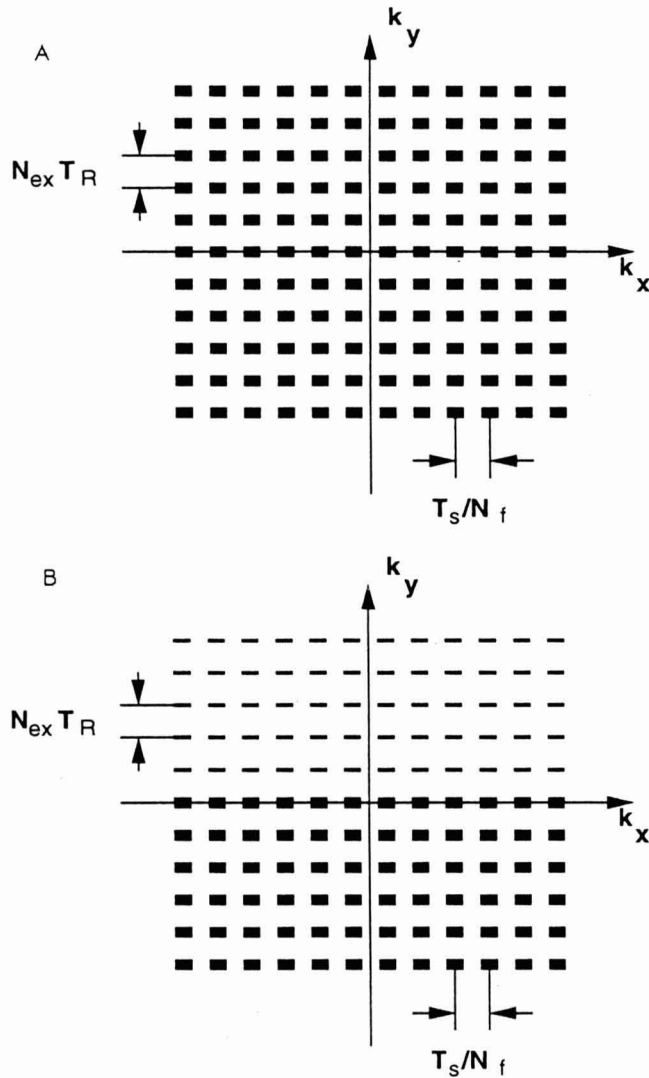
FIG 2. ILLUSTRATION OF k-SPACE

(A) is the k-space of the full Fourier transform and (B) is the k-space of the half Fourier transform. The parameters are k_y, the phase encoding direction, k_x, the frequency encoding direction, N_{ex}, the number of excitation steps, T_R, the repetition time, N_f, the number of frequency encoding steps, and T_S, the sampling time.

Experimental Setup

Data were acquired at the Biomedical Magnetic Resonance Laboratory at the University of Illinois. A 200 MHz instrument with a static magnetic field of 4.7 Tesla was used. The probe was 8 cm in diameter and had a radio frequency (RF) coil region 20 cm long.

The sample was placed in the center of the 45 mm diameter sample holder, which was centered in the probe. The heating system consisted of a water bath, pump, tubing, and thermocouples. The sample was heated by circulating the water through the sample holder. The water was in direct contact with the sample. Most of the signal intensity from the circulating water was attenuated because the water was moving. The signal intensity remaining from the circulating water was minimized by using a small pair of diffusion gradient pulses. The temperature difference between the inlet and outlet of the water bath was less than 1.5C when operated at 50C. The initial temperature of the sample was 20C, and the heating water temperature circulating past the sample was 50C. A proton density image of the potato was acquired using a full Fourier transform spin-echo sequence at room temperature with a repetition time (T_R) of 2000 ms and an echo time (T_E) of 40 ms. The average spin-lattice relaxation time of the potato was measured by the inversion-recovery method (Stark and Bradley 1988), and the average spin-spin relaxation time of the potato was measured by the CPMG method (Stark and Bradley 1988). Self-diffusion data were acquired at 1 min intervals beginning 1 min after the start of the processes for 4 min. The T_R was 700 ms, the T_E was 95 ms, the b factor produced by this sequence was 350 s/mm^2, the data acquisition time was about 10 s with 16 phase encoding steps.

Nonmagnetic thermocouples (copper-constantan) were used with a 1.21 mm outside insulated diameter around a pair of 0.25 mm diameter wires. The junction length of the thermocouple was 1 mm long. The thermocouples were implanted into the sample at radial depths of 3 mm, 6 mm, 9 mm, and 12 mm. Thermocouple data were acquired with a 21X micrologger at 2 s intervals simultaneously with the MRI data (Fig. 3). When using the thermocouples, more care was required in order to adjust (tuning and shimming) the magnetic field.

RESULTS AND DISCUSSION

From the proton density image of the potato, shown in Fig. 4, it is apparent that the tissue at the center of the potato (referred to as potato core) had a different structure and composition from the surrounding tissue. The core gave a higher signal intensity than the surrounding tissue. However, no difference in the diffusion coefficient between the different tissues was observed
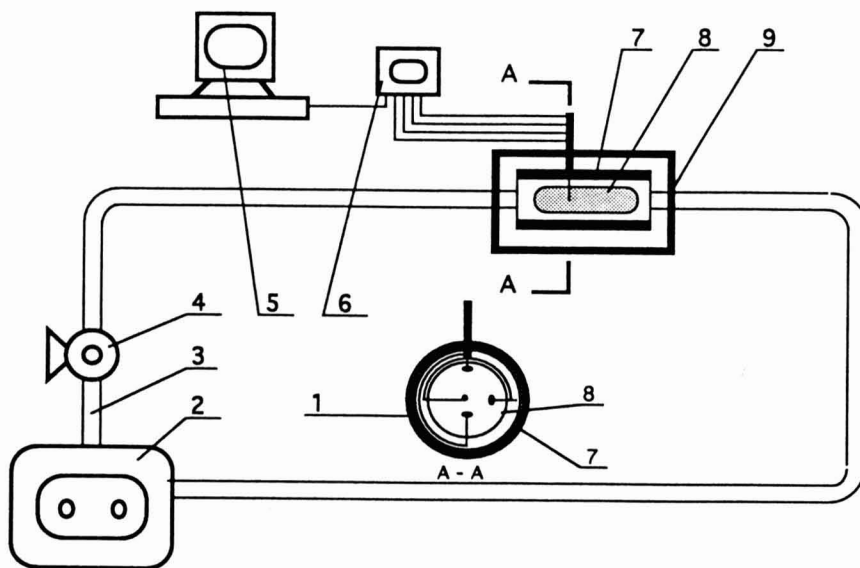
FIG. 3. EXPERIMENTAL SETUP SHOWING MRI, THERMOCOUPLE,
AND HEATING SYSTEMS
1. Cross section of sample holder and sample with thermocouple placement.
2. Water bath. 3. Tubing. 4. Pump. 5. Computer. 6. Micrologger.
7. Sample holder. 8. Sample plastic tube. 9. Magnet and probe.
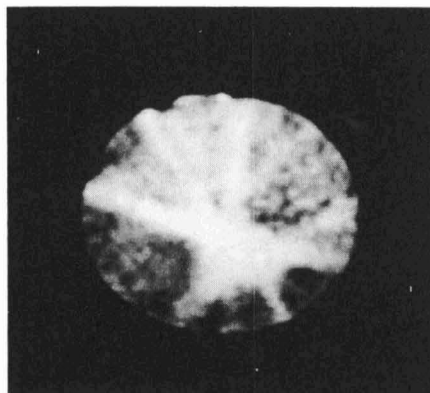
FIG. 4. TRANSVERSE SECTION PROTON DENSITY IMAGE
OF THE POTATO CYLINDER WITH REPETITION TIME
(T_R) OF 2000 ms, AND ECHO TIME (T_E) of 40 ms

at temperatures below 50C (Fig. 5). The average spin-lattice relaxation time was 1173 ms, and the average spin-spin relaxation time was 67 ms.

The average self-diffusion coefficient (D) of the potato at room temperature was 0.42×10^{-3} mm²/s obtained using imaging methods with a spatial resolution of 0.75 mm². The pseudo D* of the potato increased linearly with temperature over the tested temperature range, 20–50C (Fig. 6). The temperature coefficient (KT^2_r/E_a) (slope of Fig. 7) was 13.5%/°C. D* images with selected cross sectional profiles in the potato cylinder during heating are shown in Fig. 7. Temperature images, calculated by Eq. 5 based on the D* images during heating, showed transient temperature changes at 1, 2, 3, and 4 min after heating (Fig. 8). The brighter signals in these images correspond to higher temperatures.

MRI and thermocouple temperature profiles through the center of the potato cylinder are plotted in Fig. 9. The temperature gradients were larger at 1 min than at 2 min of heating. The results obtained by MRI are similar to the results measured by the thermocouples.
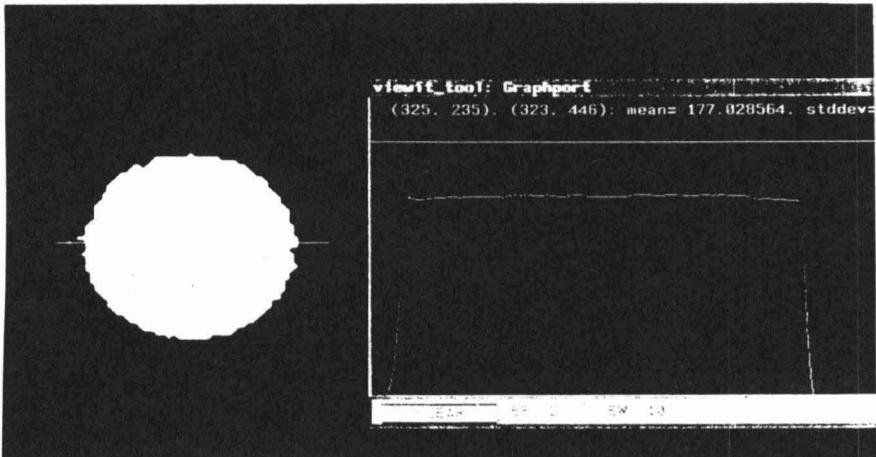
FIG. 5. TRANSVERSE SECTION SELF-DIFFUSION COEFFICIENT IMAGE OF THE POTATO CYLINDER AT 20C WITH REPETITION TIME (T_R) OF 700 ms, ECHO TIME (T_E) of 95 ms, AND b FACTOR OF 350 s/mm².
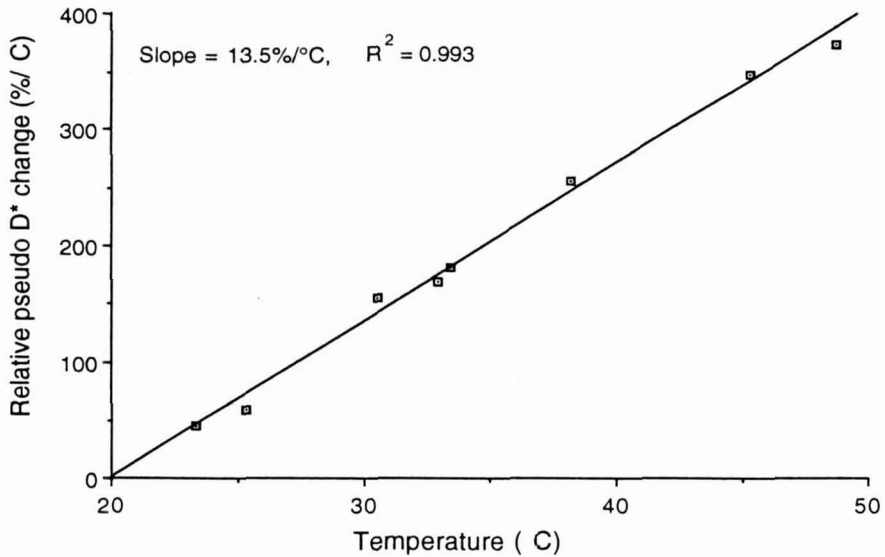
FIG. 6. RELATIVE CHANGE IN D* FOR THE POTATO AT 8
TEMPERATURES
The temperature coefficient (KT^2_r/E_a) is the slope of the regression
line. The activation energy E_a can be calculated from the
temperature coefficient at a given temperature, T_r.
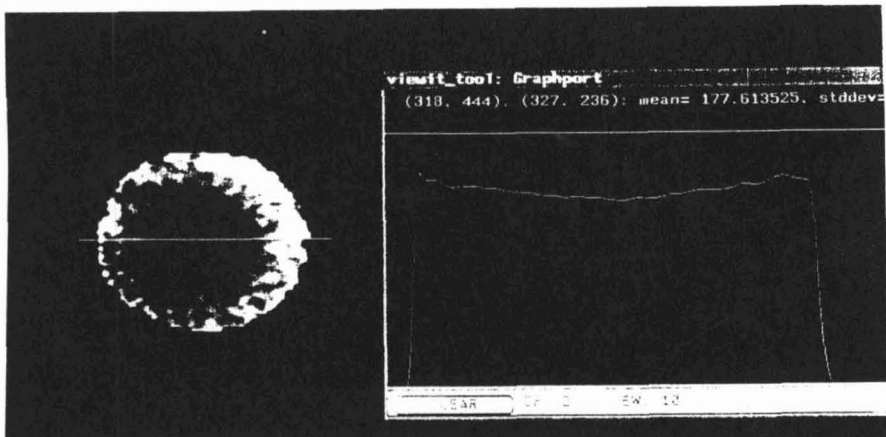
FIG. 7. PSEUDO SELF-DIFFUSION COEFFICIENT (D*) IMAGE OF
A SELECT CROSS-SECTIONAL PROFILE FOR THE POTATO
The initial temperature of the potato was 20C. This image was
collected 2 min after the start of heating with water at 50C.
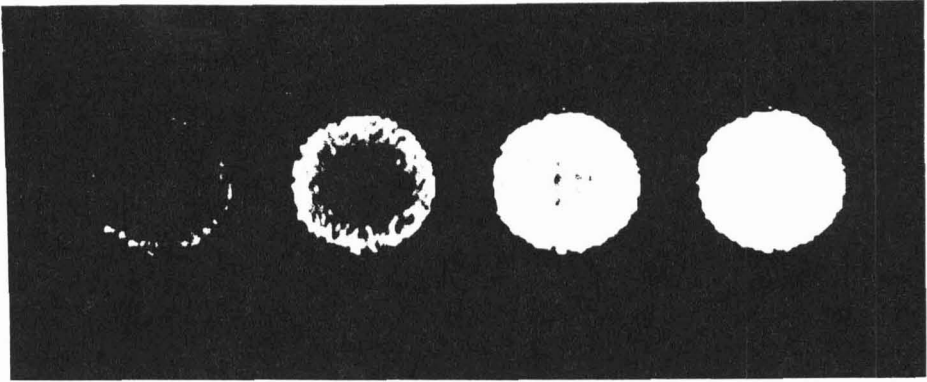
FIG. 8. 2D TEMPERATURE IMAGES OF A CYLINDRICAL POTATO DURING HEATING
The initial temperature of the potato was 20C and the heating water was 50C. The
first image on the left is after 1 min of the heating, and each subsequent image was
taken at 1 min intervals. The data acquisition time was about 10 s/image.
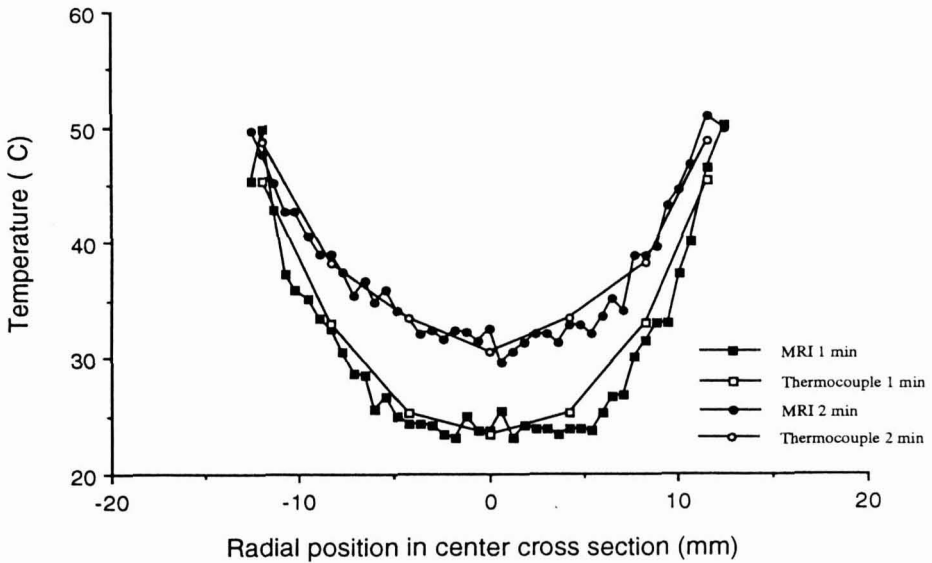
FIG. 9. MRI AND THERMOCOUPLE TEMPERATURE PROFILES IN A
CYLINDRICAL POTATO DURING HEATING AT 1 AND 2 MIN
The initial potato temperature was 20C and the potato was heated by
circulating water at 50C past the sample.

There were two main sources of error in the MRI measurements. One was
the error caused by the temperature changes in the sample during data
acquisition time. This error (e_1) is defined by Eq. 10:

$$e_1 = \frac{T_{max} - T_{min}}{2} \tag{10}$$

where e_1 is the error caused by data acquisition time, T_{min} is the temperature measured by thermocouple at the beginning of the acquisition, and T_{max} is the temperature measured by thermocouple at the end of the acquisition. For this experiment, this error was less than 0.32C. Compared to the error (0.30C) caused by temperature changes during data acquisition for agar gel (Sun *et al.* 1993), the error for this test was nearly the same. However, this does not mean that the half Fourier transform imaging techniques used for the potato did not improve the temperature mapping measurement resolution, since the temperature difference between the potato and the heating water was 30C, while the difference in the agar gel experiment was only 17C. The second source of error (e_2) was noise. The magnitude of this error was estimated as the variances of the nonlinear regression to the MRI data. The maximum average variation was 0.52C, which was less than the error (0.61C) for the agar gel (Sun *et al.* 1993). The total error ($e_1 + e_2$) of the MRI measurement was less than 0.84C with 0.75 mm² spatial area resolution (i.e., 0.55 mm resolution in the x direction and 1.36 mm resolution in the y direction). The variation between the MRI and thermocouple measurements was estimated as the square roots of the variances between the MRI and the thermocouple measurements. The average variation between MRI and thermocouple measurements was less than 0.5C.

NOMENCLATURE

b   Gradient factor s/mm²
D   Self-diffusion coefficient mm²/s
D*   Pseudo self-diffusion coefficient mm²/s
E_a Activation energy of molecular translational motion erg
K   Boltzmann constant erg/mol K
K(T)   A constant generated by MRI at a constant temperature
S   Signal intensity
T   Temperature, C
T_1 Longitudinal (spin-lattice) relaxation time ms
T_2 Transverse (spin-spin) relaxation time ms
T_E Echo time ms
T_R Repetition time ms
γ Gyromagnetic ratio 1/s
ρ Proton density

ACKNOWLEDGMENT

REFERENCES

ASAE. 1992. *ASAE Standards*, 39th Ed., American Society of Agricultural Engineers, 2950 Niles Road, St. Joseph, MI 69085-9659.

CUSSLER, E.L. 1984. Values of Diffusion Coefficient. *Diffusion: Mass Transfer in Fluid System*, Cambridge University Press, New York.

DICKINSON, R.J., HALL, A.S., HIND, A.J. and YOUNG, I.R. 1986. Measurement of changes in tissue temperature using MR imaging. J. Comput. Assisted Tomogr. *10*, 468–472.

HOWE, F.A. 1988. Relaxation times in paramagnetically doped agarose gel as a function of temperature and ion concentration. Magn. Reson. Imag. *6*, 919–270.

LE BIHAN, D. 1988. Intravoxel incoherent motion imaging using steady-state free precession. Magn. Reson. Med. *7*, 346–351.

LE BIHAN, D. 1991. Molecular diffusion nuclear magnetic resonance imaging. Magn. Reson. Q. *7*(1), 1–30.

LE BIHAN, D., DELANNOY, J. and LEVIN. R.L. 1989. Temperature mapping with MR imaging of molecular diffusion: application to hyperthermia. Radiology *171*, 853–857.

LIANG, Z.P., BOADA, F.E., CONSTABLE, R.T., HAACKE, E.M., LAUTERBUR, P.C. and SMITH, M.R. 1992. Constrained reconstruction methods in MR imaging. Rev. Magn. Reson. Med. *4*, 67–185.

PARKER, D.L., SMITH, V., SHELDON, O., CROOK, L.E. and FUSSELL, L. 1982. Temperature distribution measurements in two-dimensional NMR imaging. Med. Phys. *10*(3), 321–325.

RUAN, R.S. 1991. Studies of corn kernel steeping using microscopy NMR imaging. Ph.D. Thesis, University of Illinois, Urbana, IL 61801.

SIMPSON, J.H. and CARR, H.Y. 1958. Diffusion and nuclear spin relaxation in water. Physiol. Rev. *111*, 1201–1202.

STARK, D.D. and BRADLEY, W.G. 1988. *Magnetic Resonance Imaging*. The C.V. Mosby Co., St. Louis, MO.

SUITS, B.H. 1986. Nuclear magnetic resonance imaging of temperature profiles. J. Appl. Phys. *60*(10), 3772–3773.

SUN, X., LITCHFIELD, J.B. and S.J. SCHMIDT. 1993. Temperature mapping in a model food gel using magnetic resonance imaging. J. Food Sci. *58*, 168–172, 181.

TAYLOR, D.G. and BUSHELL, M.C. 1985. The spatial mapping of translational diffusion coefficient by the NMR imaging technique. Phys. Med. Biol. *30*(4), 345–349.

WEHRLI, F.W. 1991. *Fast-scan Magnetic Resonance Principles and Applications*, Raven Press, New York.

A RESOURCE TRACKING METHOD FOR
THE FOOD INDUSTRY

CANDELARIA BARCENAS

The Larsen Company
Cambria, Wisconsin

and

JOHN P. NORBACK

Food Science Department
University of Wisconsin
Madison, Wisconsin

ABSTRACT

Matrix Data Structure (MDS) and the Gozinto Procedure (GP) can be the basis for resource tracking and for costing systems used in the food industry. These methods have enjoyed great success and broad application among fabricators, but they have not been used much in process industries, including the food industry. While the main data entry requirement for such a system is to build accurate bills of material (BOM) for the intermediate and finished products, this is not sufficient to make a useful application in the food industry. Food and other process industries need such a system to convert between purchase units, batch units and sales units. This conversion problem *and the existence of unit operations that are* separation processes *have prevented the application of these methods in the industry. These two problems have led to many* ad hoc *methods for calculating costs and tracking resource use. The unit conversion problem (purchasing in pounds, kilograms or gallons of input materials, processing batches of intermediate products, and selling containers or cases of finished product) is solved by introducing a unit conversion matrix to the system. The problem of multiple counting the input material going into a separation process is solved by using dummy input material names for the BOM of the products coming out of the separation process. The solution to these problems have provided access to the structural power of MDS as an organizational tool and the application of GP to the matrix structure to obtain integrated, consistently computed information to support managers in the production planning and control activities.*

INTRODUCTION

Useful and important methodologies applied to materials management in fabrication industries include the model based on Matrix Data Structure (MDS) and Gozinto Procedure (GP). These computation procedures are at the heart of "Materials Requirements Planning" (MRP), and have been applied by fabricators since the early 1960's. The advantage gained by applying MRP is a consistent means of tracking resources as they aggregate into subassemblies and assemblies of subassemblies and so on. Besides determining amounts required and costs of these intermediate products, MRP solved the "time phasing of inventories" problem faced by fabricators—knowing how much inventory to have on hand and when it will be required. These methods have not been broadly used in the food industry because of the peculiarities of continuous manufacturing that make the computational model cumbersome and in some cases invalid.

The objectives of this work and of this article were to devise a means to make these methods valid and applicable in the food industry and to illustrate the power and usefulness of these methods in such process industry settings.

CURRENT SYSTEMS

Resource tracking and costing systems commonly used in the food industry are built on spreadsheets and data base programs. These software packages provide consistent calculations but the organization of these calculations is *ad hoc*—the user must set formulas to compute and retrieve desired information. For example, a formula is required to retrieve product unit cost, another to calculate total resource requirements for a given period of time, and a third to know total resource costs. These characteristics increase possibility of errors, are time consuming, and cause extra work to obtain integrated information for cost analysis. Resource management tracking and costing systems built to fit discrete manufacturing (parts and assemblies) do not always generate correct information for materials management in food industry settings. Generally, the food industry is a mix of discrete and continuous processes. A continuous manufacturing environment has some peculiarities not found in discrete processes. A system used in the food industry should accommodate to the peculiarities of the industry (Archer and Harrison 1992; Luber 1992; Phelan 1988).

The model for MDS and GP, when implemented on a computer, provides a flexible and consistent way of organizing the information. The user provides the bill of materials (BOM) information, the per unit resource costs and a desired production plan. The machine retrieves all materials management information useful for production planning and control. These minimal input requirements yield important organizational advantages when compared to the

use of some of the commonly used (spreadsheet based) resource tracking and costing systems.

Two problems occur when applying MDS and GP to resource control in the food industry. These problems have previously prevented the application of these powerful methods in food industry settings. The problems are:

(1)   The control of resources in the food industry is commonly organized on the bases of per batch of output. Batching is not only a custom but is often required by employed technology. This "per batch" approach avoids the difficulty of manipulating small numbers to obtain accurate net resource requirements for a given period of time. However, knowing the amount of input material required to prepare one batch of output does not immediately provide the amount of input materials in one sales unit of output. The batch unit must be converted to item unit. This is a tedious procedure if done piecemeal, but it can be done easily with the use of a conversion factor matrix integrated with the GP to allow computation of the amount of input required per item unit. This information is important for further production planning, costing, and labeling activities.

(2)   Food processing may include a separation process. A separation process, as its name implies, separates one input into two or more outputs. In this situation, the unmodified application of MDS and GP multiply counts the input material that is separated. The use of dummy inputs for each separated part solves this problem.

BACKGROUND AND THEORY FOR THE GOZINTO PROCEDURE

Most food industry enterprises are multiproduct, multilevel production processes. This characteristic makes it difficult to organize information to obtain integrated responses for production planning and control (Chung and Norback 1992). We illustrate how to organize Bill of Material (BOM) information into a matrix and to apply the Gozinto Procedure (GP) in this situation.

The BOM lists all the materials that are direct inputs to a product (Chase and Aquilano 1977; Mize *et al*. 1971). It is the basic set of information used to control resources, and to obtain accurate results for planning, costing and labeling. It is critical that accurate and reliable BOM data for intermediate and final products be used in the method.

After the initial stage of building the BOM for each product, the construction of the recipe matrix requires more time and attention than other decision support systems; however, with appropriate software, this step is an automatic consequence of the building the BOMs. MDS and GP allows quick,

computationally consistent, integrated responses to change in ingredients, food components, supplier costs, demand or any other variation that affect products and process. To demonstrate the application of MDS and GP in the food Industry, an example was developed using data from the dairy pilot plant of the Food Science Department at the University of Wisconsin. The example includes the BOM of four finished products.

THE RECIPE MATRIX

The Recipe Matrix (R) lists the products whose BOM are contained in the matrix (Fig. 1). It must show the direct resources for each BOM name to obtain an accurate total requirement matrix T when applying the GP. Note the small number of nonzero entries in this matrix. In our example, the finished products include whole milk (Archer and Harrison 1992), skim milk (Chase and Aquilano 1977), unflavored yogurt (Chung and Norback 1992), and strawberry yogurt (Luber 1992). The entries in rows 11 to 21 in the R matrix provide the number of pounds of ingredient i required to produce 100 lb of each output product. For example, to prepare one batch (100 lb) of whole milk requires 90 lb of raw milk, 10 lb of condensed skim milk and 0.0005 lb of vitamin D. Differentiation of resources is necessary while preparing different flavors of yogurt for the purposes of costing and production planning.

The entries in rows 1 to 10 in the R matrix provide the number of batches of intermediate product i required to manufacture a batch of output j. For a continuous processing industry like the dairy industry, the organization of the BOM in a matrix form shows that the total amount of output from a lower level operation is required as an input for the next level operation. This characteristic allows managers to establish a ratio of intermediate to finished product equal to one. This means that to make one batch of a finished product one batch of intermediate product is required. However, it is possible that a batch of intermediate product is partitioned to continue the simultaneous manufacture of two or more products. In this case, the relationships between the output batch from an operation and the next level batch outputs are less than one. For example, one batch (100 lb) of yogurt mix may be partitioned to manufacture 0.6 batch (60 lb) of unflavored yogurt and 0.4 batch (40 lb) of strawberry yogurt.

THE TOTAL REQUIREMENTS MATRIX

The Total Requirements Matrix (T) provides the total amount of input material i to manufacture one batch of finished or intermediate product j (Mize *et al.* 1971). This matrix is determined from the R matrix and requires no direct

(R)

		1	2	3	4	5	6	7	8	9	10	11	12	13	14	15	16	17	18	19	20	21
Whole Milk	1	0	0	0	0	0	0	0	0	0	0	0	0	0	0	0	0	0	0	0	0	0
Skim Milk	2	0	0	0	0	0	0	0	0	0	0	0	0	0	0	0	0	0	0	0	0	0
Unfl Yogurt	3	0	0	0	0	c	0	0	0	0	0	0	0	0	0	0	0	0	0	0	0	0
Strawb Yogurt	4	0	0	0	0	0	0	0	0	0	0	0	0	0	0	0	0	0	0	0	0	0
3 25% Milk Mix	5	1	0	0	0	0	0	0	0	0	0	0	0	0	0	0	0	0	0	0	0	0
2% Milk Mix	6	0	1	0	0	0	0	0	0	0	0	0	0	0	0	0	0	0	0	0	0	0
Cult'd Yog Mix	7	0	0	1	1	0	0	0	0	0	0	0	0	0	0	0	0	0	0	0	0	0
P-H 3 25% Mix	8	0	0	0	0	1	0	0	0	0	0	0	0	0	0	0	0	0	0	0	0	0
P-H 2% Mix	9	0	0	0	0	0	1	0	0	0	0	0	0	0	0	0	0	0	0	0	0	0
P-H Yog Mix	10	0	0	0	0	0	0	1	0	0	0	0	0	0	0	0	0	0	0	0	0	0
Recomb. Milk	11	0	0	0	0	0	0	0	90	48	80	0	0	0	0	0	0	0	0	0	0	0
Bag's Lid	12	20	20	0	0	0	0	0	0	0	0	0	0	0	0	0	0	0	0	0	0	0
Cup's Lid	13	0	0	200	200	0	0	0	0	0	0	0	0	0	0	0	0	0	0	0	0	0
5 Gallon Bag	14	20	20	0	0	0	0	0	0	0	0	0	0	0	0	0	0	0	0	0	0	0
8 Ounce Cup	15	0	0	200	200	0	0	0	0	0	0	0	0	0	0	0	0	0	0	0	0	0
Strawb Flavor	16	0	0	0	0.15	0	0	0.1	0	0	0	0	0	0	0	0	0	0	0	0	0	0
Vitamin A & D	17	0	0	0	0	0.005	0.005	0	0	0	0	0	0	0	0	0	0	0	0	0	0	0
Culture	18	0	0	0	0	0	0	0	0	0	10	0	0	0	0	0	0	0	0	0	0	0
Stored Sk Milk	19	0	0	0	0	0	0	0	10	54	30	0	0	0	0	0	0	0	0	0	0	0
Water	20	0	0	0	0	0	0	0	0	0	10	0	0	0	0	0	0	0	0	0	0	0
Raw Milk	21	0	0	0	0	0	0	0	0	0	0	1	0	0	0	0	0	0	0	0	0	0

Entries in rows 1 to 10 provide the number of batches of intermediate product I to manufacture one batch of output in column J.
Entries in rows 11 to 21 provide the amount of Input I to manufacture a batch of output in ccolumn J.

FIG. 1. THE RECIPE MATRIX

user inputs. The T matrix (Fig. 2) illustrates the amounts of all resources required to manufacture a unit (batch) of the intermediate and finished products. The information in this matrix is essential for the production planning and control activities.

The Unit Conversion Problem

An ordinary approach of tracking resources measures the input material going into a production line in units such as pounds, kilograms, gallons, etc. The entries in the ingredient rows in the T matrix (Fig. 2) tell us the amount of input material i required to manufacture a unit of output j. The mathematical expression of the entries in the ingredient rows ($i = 11,...21$) is as follows:

$$t_{ij} = \frac{Weight \ of \ ingredient \ material \ i}{Batch \ of \ output \ j}$$

For intermediate products the amount of product coming out of an operation is considered one batch of the output j. Therefore, the entries in all other rows ($i = 1,...10$) in the T matrix tell the number of batches of intermediate product i necessary to manufacture one batch of output j in the next level.

$$t_{ij} = \frac{Batches \ of \ intermediate \ product \ i}{Batch \ of \ intermediate \ product \ j}$$

This organization by batches is convenient for manufacturing and purchasing but not for marketing and costing or pricing because it does not gives us information per output (sales) unit basis. To make the computational results valid and useful in all circumstances it is required to convert batch amounts to container amounts. The per container amounts of the ingredient rows in the T matrix can be obtained by multiplying them by conversion factors that relate batches with the number of containers that can be filled with a batch. Thus, the entries in the purchased input material rows (11 to 21) in the T matrix will be changed to per unit of finished product j instead of per batch of product j. The relation is:

$$New \ t_{ij} = \frac{Weight \ of \ input \ i}{Batch \ of \ product \ j} \ x \ \frac{Batch \ of \ product \ j}{Number \ of \ containers} = \frac{Weight \ of \ input \ i}{Per \ container}$$

	1	2	3	4	5	6	7	8	9	10	11	12	13	14	15	16	17	18	19	20	21
Whole Milk 1	1	0	0	0	0	0	0	0	0	0	0	0	0	0	0	0	0	0	0	0	0
Skim Milk 2	0	1	0	0	0	0	0	0	0	0	0	0	0	0	0	0	0	0	0	0	0
Unfl. Yogurt 3	0	0	1	0	0	0	0	0	0	0	0	0	0	0	0	0	0	0	0	0	0
Strawb. Yogu 4	0	0	0	1	0	0	0	0	0	0	0	0	0	0	0	0	0	0	0	0	0
3.25% Milk Mi 5	1	0	0	0	1	0	0	0	0	0	0	0	0	0	0	0	0	0	0	0	0
2% Milk Mix 6	0	1	0	0	0	1	0	0	0	0	0	0	0	0	0	0	0	0	0	0	0
Cult'd Yog Mi 7	0	0	1	1	0	0	1	0	0	0	0	0	0	0	0	0	0	0	0	0	0
P-H 3.25% Mi 8	1	0	0	0	1	0	0	1	0	0	0	0	0	0	0	0	0	0	0	0	0
P-H 2% Mix 9	0	1	0	0	0	1	0	0	1	0	0	0	0	0	0	0	0	0	0	0	0
P-H Yogurt Mi 10	0	0	1	1	0	0	1	0	0	1	0	0	0	0	0	0	0	0	0	0	0
Recomb. Milk 11	90	46	60	60	90	46	60	90	48	60	1	0	0	0	0	0	0	0	0	0	0
Bag's Lid 12	20	20	0	0	0	0	0	0	0	0	0	1	0	0	0	0	0	0	0	0	0
Cup's Lid 13	0	0	200	200	0	0	0	0	0	0	0	0	1	0	0	0	0	0	0	0	0
5 Gallon Bag 14	20	20	0	0	0	0	0	0	0	0	0	0	0	1	0	0	0	0	0	0	0
8 Ounce Cup 15	0	0	200	200	0	0	0	0	0	0	0	0	0	0	1	0	0	0	0	0	0
Strawb. Flavo 16	0	0	0	0.15	0	0	0	0	0	0	0	0	0	0	0	1	0	0	0	0	0
Vitamin A & D 17	0.005	0.005	0	0	0.005	0.005	0	0	0	0	0	0	0	0	0	0	1	0	0	0	0
Culture 18	0	0	0.1	0.1	0	0	0.1	0	0	0	0	0	0	0	0	0	0	1	0	0	0
Stored Sk Mil 19	10	54	30	30	14	54	30	10	54	30	0	0	0	0	0	0	0	0	1	0	0
Water 20	0	0	10	10	0	0	10	0	0	10	0	0	0	0	0	0	0	0	0	1	0
Raw Milk 21	90	46	60	60	90	46	60	90	48	60	1	0	0	0	0	0	0	0	0	0	1

Entries in rows 1 to 10 provide total number of batches of Intermediate product I to manufacture one batch of output in column j.
Entries in rows 11 to 21 provide total amounts of input I to manufacture a batch of output in column j.

FIG. 2. THE TOTAL REQUIREMENTS MATRIX

The result of multiplying the ingredient rows times the conversion matrix provides the amount of ingredient i per unit of finished product j, the adjusted T matrix (Fig. 3). The entries in columns 12 to 21 are zero except the one's in the diagonal. These entries are not shown to reduce space. The ratio of weight of input i required to manufacture a finished product j is essential data when determining total resources to satisfy demand. The information is also important to track component content for labeling purpose as well as costing and pricing.

$(AT = AT2 + T1)$

		1	2	3	4	5	6	7	8	9	10	11	 21
Whole Milk	1	1	0	0	0	0	0	0	0	0	0	0	 0
Skim Milk	2	0	1	0	0	0	0	0	0	0	0	0	 0
Unfl. Yogurt	3	0	0	1	0	0	0	0	0	0	0	0	 0
Strawberry Yog.	4	0	0	0	1	0	0	0	0	0	0	0	 0
3.25% Milk Mix	5	1	0	0	0	1	0	0	0	0	0	0	 0
2% Milk Mix	6	0	1	0	0	0	1	0	0	0	0	0	 0
Cult'd Yog Mix	7	0	0	1	1	0	0	1	0	0	0	0	 0
P-H 3.25% Mix	8	1	0	0	0	1	0	0	1	0	0	0	 0
P-H 2% Mix	9	0	1	0	0	0	1	0	0	1	0	0	 0
P-H Yogurt Mix	10	0	0	1	1	0	0	1	0	0	1	0	 0
Recomb. Milk	11	4.5	2.3	0.3	0.3	4.5	2.3	0.3	4.5	2.3	0.3	1	 0
Bag's Lid	12	1	1	0	0	0	0	0	0	0	0	0	 0
Cup's Lid	13	0	0	1	1	0	0	0	0	0	0	0	 0
5 Gallon Bag	14	1	1	0	0	0	0	0	0	0	0	0	 0
8 Ounce Cup	15	0	0	1	1	0	0	0	0	0	0	0	 0
Strawb. Flavor	16	0	0	0	0.0007	0	0	0	0	0	0	0	 0
Vitamin A & D	17	0.0002	0.0002	0	0	0.0002	0.0002	0	0	0	0	0	 0
Culture	18	0	0	0.0053	0.0053	0	0	0.0053	0	0	0	0	 0
Stored Sk Milk	19	0.5	2.7	0.15	0.15	0.5	2.7	0.15	0.5	2.7	0.15	0	 0
Water	20	0	0	0.05	0.05	0	0	0.05	0	0	0.05	0	 0
Raw Milk	21	4.5	2.3	0.3	0.3	4.5	2.3	0.3	4.5	2.3	0.3	1	 1

Entries in rows 1 to 10 provide the number of batches of intermediate product i per batch of output in column j.
Entries in rows 11 to 21 provide the total amounts of input i per batch of output in column j.

FIG. 3. ADJUSTED MATRIX

The multiplication of the adjusted T matrix times the D matrix (Fig. 4) will provide input material requirements to accomplish demand forecast. The unit analysis, in this case, is as follows:

$$\frac{Weight\ of\ input\ i}{Unit\ of\ product\ j} \times \frac{Demand\ of\ product\ j}{Period\ of\ time} = \frac{Weight\ of\ input\ i}{Period\ of\ time}$$

In general, the amount of raw material i required to prepare a unit of finished product j is equal to the amount of input i required to produce a batch of finished product j divided by the number of packaging units that should be filled from the batch. An advantage of using the GP is that it makes it possible to control resources per unit item when different sizes of food containers are filled from one batch.

Separation Process Problem

The ordinary way of organizing the BOM into a matrix and applying GP will not produce valid results when there is a separation process. The Gozinto Procedure is an additive procedure that aggregates amounts of inputs required to obtain an output. A separation process does not combine inputs; in contrast, as its name implies, it separates the input material into two or more outputs. This splitting into parts makes the computation invalid so that it is no longer possible to track resources.

The separation process may occur at the beginning, middle or at the end of the production line. When the separated parts are intended as finished products of the process, the application of GP does not present major difficulties. In the other cases, the problem is to avoid multiple counts of the input to be separated. To be more specific, the entries in the traditional R matrix tell us the amount of input i needed to produce a unit of output j, but in a separation process an input i yields several outputs. If we use the separation input amount for more than one output, the input is multiply counted, causing a computational error.

To apply the GP when a separation process exists, some modifications to the R and T matrices must be done to enable tracking resources. The first change is to enlarge the matrices with rows and columns dedicated to dummy inputs in place of every separated input. The use of dummy inputs avoids multiple counting of the input amount to be separated. The T matrix will then show the amount of each dummy input needed to produce a unit of each separated product. Depending on the values of these entries and the demand for each of the separated products, one of the dummy inputs will have the maximum

input value in the net requirement matrix. This determines how much input material is required in order to meet target production of the separated products. The other dummy inputs may be ignored.

(D)

		P1
Whole Milk	1	100
Skim Milk	2	150
Unfl. Yogurt	3	300
Strawb. Yogur	4	325
3.25% Milk Mi	5	0
2% Milk Mix	6	0
Cult'd Yog Mi	7	0
P-H 3.25% Mi	8	0
P-H 2% Mix	9	0
P-H Yogurt Mi	10	0
Recomb. Milk	11	0
Bag's Lid	12	0
Cup's Lid	13	0
5 Gallon Bag	14	0
8 Ounce Cup	15	0
Strawb. Flavo	16	0
Vitamin A & D	17	0
Culture	18	0
Stored Sk Mil	18	0
Water	20	0
Raw Milk	21	0

Entries provide demand of finished products.

FIG. 4. DEMAND FORECAST MATRIX

To demonstrate the application of MDS and GP even when the production process involves separation, our original R matrix will be enlarged to produce skim milk and cream. To build an R matrix, which is consistent with the reasoning of the procedure, some steps should be followed. First, the required input amount to prepare one unit (pound, kilograms, batch, etc.) of each of the separated product must be known. In our example, from every unit of raw milk going into the separator, we obtain 65% skim milk and 35% cream. Therefore, preparing 1 lb of skim milk and 1 lb of cream requires processing 1.54 and 2.86 lb of raw milk, respectively.

Second, an equal number of rows and columns labeled dummy raw milk are added to the R matrix (Fig. 5). Entries in columns 14 – 25 are zero except the one's on the diagonal. These columns are not shown. The dummy inputs must be equal to the number of separated parts; thus, dummy raw milk 1 (row 23 and column 23) and dummy raw milk 2 (row 24 and column 24) are the new rows and columns in the R matrix. The raw milk required to produce finished products 1, 2, 3, and 4 is named raw milk in the R matrix (row 25 and column 25). The reason why both dummy raw milks must be differentiated from the raw milk used for the other finished products is that, at this stage, managers do not know the maximum dummy input requirement. The maximum dummy input depends not only on the input/output relationship in the T matrix (Fig. 6) but also on the demand for the separated parts (separated skim milk and separated cream must also be included in the demand matrix, 500 and 200 lb respectively).

Third, after the net requirement matrix (AT × D) is obtained, special attention must be given to the dummy rows (Fig. 7). For the purposes of production planning and cost analysis, the amount of dummy raw milk required to accomplish demand of separated products is the maximum dummy input (770 lb). Thus, the total amount of raw milk required to meet demand for finished product 1 to 4 and the separated products (11 and 12) equal to 1682.5 units. This amount is the result of adding row 23 (770 lb) to row 25 (912.5 lb). This 770 lb of raw milk is the amount required to obtain the production target of skim milk. The production target of cream is reached with 572 lb of the same input. This means that the separation of 770 lb of raw milk will yield the production target of skim milk as well as the cream's production target plus an excess of cream. The excess may be calculated as the difference between the two dummy raw milks divided by the amount of raw milk required to manufacture a pound of cream.

$$\frac{Dummy\ milk\ 1\ -\ Dummy\ milk\ 2}{raw\ milk\ for\ a\ unit\ of\ cream} = \frac{Excess\ of\ milk}{2.86} = Excess\ of\ cream$$

This solution to the problem applies when the separated parts can be considered as final or intermediate outputs of the production process that continue in the production line independently. An input to be separated at the beginning or middle of the production line can be tracked if this assumption applies. This procedure may also be applied to tracking waste stream from an operation.

		1	2	3	4	5	6	7	8	9	10	11	12	13	...25
Whole Milk	1	0	0	0	0	0	0	0	0	0	0	0	0	0	...0
Skim Milk	2	0	0	0	0	0	0	0	0	0	0	0	0	0	...0
Unfl. Yogurt	3	0	0	0	0	0	0	0	0	0	0	0	0	0	...0
Strawb. Yogurt	4	0	0	0	0	0	0	0	0	0	0	0	0	0	...0
3.25% Milk Mix	5	1	0	0	0	0	0	0	0	0	0	0	0	0	...0
2% Milk Mix	6	0	1	0	0	0	0	0	0	0	0	0	0	0	...0
Cult'd Yog. Mix	7	0	0	1	1	0	0	0	0	0	0	0	0	0	...0
P-H 3.25% Mix	8	0	0	0	0	1	0	0	0	0	0	0	0	0	...0
P-H 2% Mix	9	0	0	0	0	0	1	0	0	0	0	0	0	0	...0
P-H Yog. Mix	10	0	0	0	0	0	0	1	0	0	0	0	0	0	...0
Septsed. Skim	11	0	0	0	0	0	0	0	0	0	0	0	0	0	...0
Septed. Cream	12	0	0	0	0	0	0	0	0	0	0	0	0	0	...0
Recomb. Milk	13	0	0	0	0	0	0	0	90	46	60	0	0	0	...0
Bag's Lid	14	20	20	0	0	0	0	0	0	0	0	0	0	0	...0
Cupp's Lid	15	0	0	200	200	0	0	0	0	0	0	0	0	0	...0
5 Gallon Bag	16	20	20	0	0	0	0	0	0	0	0	0	0	0	...0
8 Ounce Cup	17	0	0	200	200	0	0	0	0	0	0	0	0	0	...0
Strawb. Flavor	18	0	0	0	0.15	0	0	0	0	0	0	0	0	0	...0
Vitamin A & D	19	0	0	0	0	0.005	0.005	0	0	0	0	0	0	0	...0
Culture	20	0	0	0	0	0	0	0	0	0	0.1	0	0	0	...0
Stored Sk Milk	21	0	0	0	0	0	0	0	10	54	30	0	0	0	...0
Water	22	0	0	0	0	0	0	0	0	0	10	0	0	0	...0
Dummy Milk 1	23	0	0	0	0	0	0	0	0	0	0	1.54	0	0	...0
Dummy Milk 2	24	0	0	0	0	0	0	0	0	0	0	0	2.86	0	...0
Raw Milk	25	0	0	0	0	0	0	0	0	0	0	0	0	1	...1

Entries in rows 1 to 13 provide number of batches of intermediate product i to manufacture a batch of product in column j.
Entries in rows 14 to 25 provide the amounts of input i required to manufacture a batch of output in column j.

FIG. 5. THE RECIPE MATRIX

There is also difficulty in pricing products that used the output from a separation process. The cost of the dummy input resources is arbitrary and must be assigned by the user. The Gozinto procedure allows tracking of these costs throughout the process after the resource unit cost is established.

		1	2	3	4	5	6	7	8	9	10	11	12	13	... 25
Whole Milk	1	1	0	0	0	0	0	0	0	0	0	0	0	0	... 0
Skim Milk	2	0	1	0	0	0	0	0	0	0	0	0	0	0	... 0
Unfl. Yogurt	3	0	0	1	0	0	0	0	0	0	0	0	0	0	... 0
Strawb. Yogurt	4	0	0	0	1	0	0	0	0	0	0	0	0	0	... 0
3.25% Milk Mix	5	1	0	0	0	1	0	0	0	0	0	0	0	0	... 0
2% Milk Mix	6	0	1	0	0	0	1	0	0	0	0	0	0	0	... 0
Cult'd Yog. Mix	7	0	0	1	1	0	0	1	0	0	0	0	0	0	... 0
P-H 3.25% Mix	8	1	0	0	0	1	0	0	1	0	0	0	0	0	... 0
P-H 2% Mix	9	0	1	0	0	0	1	0	0	1	0	0	0	0	... 0
P-H Yog. Mix	10	0	0	1	1	0	0	1	0	0	1	0	0	0	... 0
Septed. Skim	11	0	0	0	0	0	0	0	0	0	0	1	0	0	... 0
Septed. Cream	12	0	0	0	0	0	0	0	0	0	0	0	1	0	... 0
Recomb. Milk	13	4.5	2.3	0.3	0.3	4.5	2.3	0.3	4.5	2.3	0.3	0	0	1	... 0
Bag's Lid	14	1	1	0	0	0	0	0	0	0	0	0	0	0	... 0
Cupp's Lid	15	0	0	1	1	0	0	0	0	0	0	0	0	0	... 0
5 Gallon Bag	16	1	1	0	0	0	0	0	0	0	0	0	0	0	... 0
8 Ounce Cup	17	0	0	1	1	0	0	0	0	0	0	0	0	0	... 0
Strawb. Flavor	18	0	0	0	0.0007	0	0	0	0	0	0	0	0	0	... 0
Vitamin A & D	19	0.0002	0.0002	0	0	0.000	0.0002	0	0	0	0	0	0	0	... 0
Culture	20	0	0	0.0053	0.0053	0	0	0.0053	0	0	0	0	0	0	... 0
Stored Sk Milk	21	0.5	2.7	0.15	0.15	0.5	2.7	0.15	0.5	2.7	0.15	0	0	0	... 0
Water	22	0	0	0.05	0.05	0	0	0.05	0	0	0.05	0	0	0	... 0
Dummy Milk 1	23	0	0	0	0	0	0	0	0	0	0	1.54	0	0	... 0
Dummy Milk 2	24	0	0	0	0	0	0	0	0	0	0	0	2.86	0	... 0
Raw Milk	25	4.5	2.3	0.3	0.3	4.5	2.3	0.3	4.5	2.3	0.3	0	0	1	... 1

Entries in rows 1 to 13 provide total number of batches of intermediate product i to manufacture one batch of product in column j.
Entries in rows 14 to 25 provide total amounts of input i to manufacture one unit of product in column j.

FIG. 6. THE ADJUSTED MATRIX

Whole Milk	1	100
Skim Milk	2	150
Unfl. Yogurt	3	300
Strawb. Yogurt	4	325
3.25% Milk Mix	5	100
2% Milk Mix	6	150
Cult'd Yog. Mix	7	625
P-H 3.25% Mix	8	100
P-H 2% Mix	9	150
P-H Yog. Mix	10	625
Septed. Skim	11	500
Septed Cream	12	200
Recomb. Milk	13	912.5
Bag's Lid	14	250
Cupp's Lid	15	625
5 Gallon Bag	16	250
8 Ounce Cup	17	625
Strawb. Flavor	18	0.2438
Vitamin A & D	19	0.0625
Culture	20	0.3125
Stored Sk Milk	21	547.75
Water	22	31.25
Dummy Milk 1	23	770
Dummy Milk 2	24	572
Raw Milk	25	912.5

Entries in rows 1 to 13 provide net requirements of product j to meet demand.
Entries in rows 14 to 20 provide net requirements of input i to meet demand.

FIG. 7. NET REQUIREMENTS MATRIX

CONCLUSION

A model based on MDS and GP can be the basis for the resource tracking and costing system to be used in the food industry. The main requirement for the system to fit the peculiarities of the industry is to build accurate BOM for the intermediate and finished products. The system automatically organizes the BOMs in the recipe matrix and applies GP to obtain the total requirement matrix. This matrix is then algebraically combined with the conversion factor, cost, demand and inventory matrices to obtain the desired information. The problems and their solutions discussed in this paper have proved the power of MDS to organize and store information and the application of GP to manipulate the information retrieving integrated responses.

REFERENCES

ARCHER, G. and HARRISON, M. 1992. Out of the manufacturing black hole. Accountancy *102*(1182), 97–98.

CHASE, R.B. and AQUILANO, N.J. 1977. *Production and Operation Management*, 5th Ed., Richard D. Irwin, Homewood, IL.

CHUNG, H.C. and NORBACK, J.P. 1992. Batching decisions in a multi-staged food manufacturing process. J. Food Process Engineering *15*(2), 99–114.

LUBER, A. 1992. How to identify a true process industry. Prod. Inventory Manage. *12*(2), 16–177.

MAY, R.G., MULLER, G.G. and WILLIAMS, T.H. 1977. *A New Introduction to Financial Accounting*, 2nd Ed., Prentice Hall, Englewood Cliffs, NJ.

MIZE, J.H., WHITE, C.R. and BROOKS, G.H. 1971. *Operation Planning and Control*, Prentice Hall, Englewood Cliffs, NJ.

PHELAN, S.A. 1988. A packaged MRP solution for process manufacturing. Manuf. Sys. *6*(10), 65–66.

TREATMENT OF POULTRY CHILLER WATER BY FLOCCULATION[1]

KENG C. NG, CHARLES C. HUXSOLL and LEE S. TSAI

Western Regional Research Center, Agricultural Research Service
U.S. Department of Agriculture
800 Buchanan St., Albany, California 94710

ABSTRACT

A laboratory study was conducted to assess the efficiency of using a combination of flocculating substances to remove organic constituents from poultry chiller water. Rice bran in combination with commercial flocculant AP-273 (polyelectrolyte) removed 60% and 72% of chemical oxygen demand (COD) from low and high COD samples, respectively. Addition of granular activated carbon to the flocculant mixture increased COD removal to about 75%, respectively, from the same samples. Turbidity (suspended particles) of the chiller water was reduced by more than 90% using flocculant AP-273 plus rice bran. Chlorine demands were also greatly reduced. Soluble inorganic mineral content was not reduced by the combined flocculating substances. The residues collected after flocculation could be used as a feed ingredient, or as an organic fertilizer. Flocculation of chiller water would be a beneficial pretreatment to further recycling processes or to microfiltration of chiller water for reuse.

INTRODUCTION

Poultry processing uses large quantities of fresh water, resulting in excessive amounts of wastewater. For economic reasons, the poultry industry has been engaged in studies to recycle this wastewater. Organic materials suspended in the processing water are of special concern to the processor,

---

because of great difficulties encountered when attempting to reduce them to a level that will permit reuse of the water (Rogers 1978). One unit operation requiring substantial quantities of water is the carcass chiller. In modern poultry processing plants, the live birds are slaughtered, defeathered, eviscerated, cleaned, chilled and then packed under a federal inspection program supervised by personnel of the USDA meat and poultry inspection service. In order to ensure quality and wholesomeness of poultry products, one of the regulations is that the eviscerated carcasses must be cooled to 4C (40F) or lower within prescribed time limits depending on the weight of the bird (USDA 1976). In the United States these requirements are most commonly complied with by immersion chilling of carcasses in a flow-through tank called a chiller, containing water at near-freezing temperature. During the operation, solids and microbial buildup in the chiller is minimized by providing a water overflow. Regulations require 0.5 gallon of chiller water overflow per bird for chicken processing and one gallon of overflow per bird for turkey processing (USDA 1976). Recycling chiller water would save substantial amount of water and greatly reduce pollution. Therefore, a laboratory study was conducted to determine the efficiency of flocculation for removing organic matter from poultry chiller water, for improving chlorine efficiency and to determine its feasibility as part of further recycling processes.

The principles of coagulation and flocculation have been previously investigated and discussed (Purchase 1971). Solid particles suspended in water have like electrical charges, usually negative, which cause the particles to repel each other. When a neutralizing agent is added to the water, the surface charges on the particles are eliminated, and the particles are drawn together (coagulated) by the normal process of attraction. When an appropriate organic polyelectrolyte is added to the water, it will neutralize the surface charges of the particles and form chemical bridges between the suspended coagulated particles (Michaels 1954). The particles then agglomerate and form a precipitating floc. The process of flocculation is common in water and waste treatment operations.

Current practice in water treatment uses ionic polyelectrolytes as flocculants, to both neutralize the charge and provide the chemical bridge. Early use of flocculants in water treatment included natural organic materials, especially starches (Michaels 1954).

In the present study, we investigated the effectiveness of using a combination of polyacrylamide polyelectrolyte with other natural materials that would flocculate the colloidal particles in chiller water and would be suitable for incorporation into an added-value chicken-feeding ration.

MATERIALS AND METHODS

Poultry Chiller Water

A poultry chiller system usually consists of one or a number of stainless steel tanks with a semi-circular cross section of a radius between 3 to 5 ft. The length of the tank depends in part upon the processing capacity. If the plant operates with two or more chilling tanks, the first tank, which receives the warm carcasses, is referred to as prechiller and the following tank(s) as chiller(s). During operation, carcasses are lifted out from the prechiller and transported by a conveyer belt to the near end of the next chiller to be further cooled. In this experiment, water samples were collected from a nearby medium-size plant that operated with a single chiller about 5 ft wide, 4 ft high and 30 ft long. The chiller holds about 3500–4000 gallons of fresh refrigerated well water and ice. Water is kept at about 1C by periodic addition of ice. Production rate was 60–70 birds/min and the carcass residence time in the chiller was 50–60 min. At the steady state of operation the chiller contained about 3000–3500 carcasses. Water was vigorously circulated in the tank by pumping the icy water from near the carcass exit end, and returning it near the carcass entry side, a daily (8 h) water overflow (0.5 gal/bird) of about 15,000 gal or more using fresh well water for makeup. In the summer season, the plant runs on an 8-h shift, starting at 0600 h in the morning. Water samples from the plant were collected from the middle of the chiller into two, 1-gal amber-colored glass containers. Six water samples, one on each of 6 processing days, representing between 3 to 5 h of operating time, were collected between 0900 and 1100 h. A sample of the fresh well water used to fill and replenish the chiller was also collected from the fresh water in-flow with each sampling of the chiller water. Additionally, two 10-gal water samples for flocculant treatment, one on each of two processing days, representing 3 and 5 h of operation, respectively, were collected in black plastic containers. All samples were held in ice from the time of collection to the time of evaluation.

Analytical Procedures

Chemical analysis of the well and chiller waters was performed in accordance with the Standard Methods of the Examination of Water and Wastewater of the American Public Health Association (APHA *et al.* 1985). Turbidity of water was determined on a 15-ml sample using a Model DRT-150

Turbidity meter (H-F Instrument Co., Fredomia, NY). Residual chlorine in solution was determined by the DPD (N,N-diethyl-p-phenylenediamine) ferrous titrimetric method, which accounts for free and combined available chlorine or total residual available chlorine. Chlorine demand of water is defined as the difference between added and residual chlorine after a specific period of contact time. A stock sodium hypochlorite solution containing 4.0% chlorine as chlorine source was used in this experiment. Chemical oxygen demand (COD) in a 20-ml sample was determined by a dichromate reflux method. The amount of potassium dichromate consumed by the organic matter was determined, and the amount of oxidizable organic matter was calculated in terms of its oxygen equivalent. If the COD values of the samples were too high, dilution samples were prepared according to APHA procedures. Conductivity of a 50-ml water sample was measured using a Model CDM3 conductivity meter (Radiometer Co., Copenhagen, Denmark). The total residue of chiller water, or fresh well water, was determined by evaporating the sample in a 90-mm diameter porcelain evaporating dish. Due to the high fat contents of the chiller water samples, a well-mixed 100-ml sample was evaporated to near dryness in a steam bath and then dried to a constant weight in a vacuum oven at 75–80C to obtain the total residue weight. Total filterable residue in the chiller water, or in the fresh well water, is assumed as the material that passes through a 300-ml Millipore funnel with ground glass base and 1 μm Millipore filter paper. In this test, a 100 ml filtrate was evaporated to near dryness in a weighed dish and then dried to constant weight in a vacuum oven to obtain total filterable residue weight. Total nonfilterable residue was calculated from difference between the total residue and the total filterable residue. Water pH was measured by a Corning 150 pH meter with a temperature compensating device.

Flocculant Treatment

Separan AP-273 (Dow Chemical Co., Midland, Mich.) is a food-grade polyacrylamide flocculant, made up of relatively large molecules that possess electrostatic properties that would attract particles suspended in water. The flocculant brings the organic particles together forming a heavy agglomerate which settles out of suspension and is easily removed by filtration. To facilitate flocculation, several natural occurring materials were also combined with the polyacrylamide flocculant. The materials and corresponding levels were: 0.2% rice bran; 0.2% Celite; 0.2% rice bran + 0.5% granular activated carbon (12-20 mesh).

Three liters of the chiller water were placed in a 4-L beaker on a magnetic stirring plate. The naturally occurring materials described above were added and gently mixed for 5–10 min. One ppm of the finely powdered flocculant AP-273 was slowly dispersed in the water and then gently mixed for another 5-10 min.

During mixing the suspended particles gradually formed an agglomerate that slowly settled out of suspension. After flocculation was completed, a water sample from each treatment was filtered through a 125-mm diameter Buchner funnel using S&S 604 filter paper (Schleicher & Schuell Co.), which is an open texture rough paper with large porosity and particle retention up to 45 μm. All flocculant-treated samples were run in duplicate. The filtered waters were then analyzed for their COD, turbidity, chlorine demand and conductivity.

RESULTS AND DISCUSSION

Fresh well water used for the poultry processing and water taken from the chiller tank are characterized in Table 1. The well water used in this particular poultry processing plant had a pH ranging from 7.1–7.2, which is only slightly alkaline. Alkalinity of many well or surface waters is primarily due to carbonate, bicarbonate and hydroxide contents. The pH of most water supplies in California ranges from 6.5 to 8.5 (Water Quality of East Bay 1991).

The well water had high conductivity values in the range of 140–270 μS (microsiemens), indicating high concentration of ionized constituents. Solutions of most organic acids, bases and salts are relatively good conductors, while solutions of nondissociating organic compounds are poor conductors. The high conductivity values of the well water together with the pH values of 7.1– 7.2, indicate that dissolved salts are likely the main cause of the high conductivity. Masri (1986) reported a high sodium, magnesium and calcium in samples from the same general area. The conductivity of most potable waters in the United States ranges from 5–150 μS, and the Public Health Service of California recommends a maximum level of 90 μS (Water Quality of East Bay 1991).

The filterable and nonfilterable solids refer to the residue of solid matter suspended or dissolved in water respectively. Water with a high residue content is generally of inferior palatability and may induce an unfavorable physiological reaction upon consuming. For these reasons, a desirable limit of 500 mg total residue per liter is set for drinking water (APHA *et al.* 1985). The well water samples in this test had a low total residue contents of 21–62 mg/L; (range: 6–12 mg/L filterable, and, 15–50 mg/L nonfilterable). Turbidity of the well water is caused by suspended filterable solids. Turbidity-free water is difficult to obtain. Most water supplies set the turbidity limit at 5 NTU (Nephelometer turbidity units). The well water had lower turbidity values of 3.0–3.5 NTU.

Chlorine demand is the quantity of chlorine that is reduced or converted to inert or less active form of chlorine by organic substances in the water. The organic substances in well water induced the rapid loss of chlorine (6–10 ppm at initial contact time).

TABLE 1.
CHARACTERISTICS OF WELL WATER AND POULTRY CHILLER WATERS

No. of Sampling	pH at 25 C	Turbidity (NTU)	Conductivity µS	C.O.D. mg/L	Chlorine demand 1 C, PPM	Filterable solids, mg/L	Nonfilterable solids, mg/L
				Well Water			
1	7.1	3.2	210	50	9	8	28
2	7.1	3.3	220	60	10	8	30
3	7.1	3.5	270	75	10	12	50
4	7.2	3.2	210	60	10	8	29
5(a)	7.1	3.0	140	36	6	6	15
6	7.1	3.3	210	50	9	8	26
Range	7.1-7.2	3.0-3.5	140-270	36-75	6-10	6-12	15-50
				Chiller Water			
1	7.2	453	1230	1590	193	989	419
2	7.3	462	1255	1685	194	1094	420
3(b)	7.4	465	1300	2472	195	1200	423
4	7.2	450	1235	1587	194	969	419
5(a)	7.1	230	900	1500	140	780	100
6	7.2	458	1280	1663	194	1027	422
Range	7.1-7.4	230-465	900-1300	1500-2472	140-195	780-1200	100-423

Note: Values were based on water samples collected on each of 6 different days. Chlorine demand was determined at initial contact time.

a) Well sample was collected two days after the first rain storm in the fall of the year. Chiller water sample was collected on the same day with a low daily output of the plant.

b) Chiller sample was collected during malfunction of the chiller recirculating pump and overflow system was temporarily interrupted.

The biochemical oxygen demand (BOD) test is widely employed in water quality evaluation and wastewater treatment, but the test is lengthy (5 days), and prone to difficulties in selecting the right kind of microorganism. Therefore, the relatively simpler and faster chemical oxygen demand (COD) test was used in this study. Under strong oxidizing conditions, COD is a measure of the oxygen equivalent of the organic matter contents in the water. It is carbon and hydrogen (not nitrogen) that is oxidized by the dichromate in the test; thereby, ammonium ion is not oxidized. The COD value of the well water was mostly contributed by the carbon content in the organic matter of the residue (filterable and nonfilterable solids).

The well water sample No. 5, which was collected 2 days after the first heavy rain storm in the fall of that year, had lower test values for all parameters except pH. The storm water seems to have a diluent effect on the chemical constituents in the well water, especially following a lengthy consecutive six-year drought in California. Under normal conditions the well water used by the processing plant is relatively of good quality, although high in salt content, and is approved by the Public Health Service for use as poultry chiller water.

The characteristics of the chiller water, as indicated in Table 1, show values that are many times higher than those for the fresh well water in every parameter analyzed, except for the pH, which remained the same. Sample No. 3, which was collected during malfunction of the recirculating pump of chiller and when the overflow system was temporarily interrupted, had the highest values for each of the parameters analyzed. Chiller sample No. 5 had the lowest test values due to low daily output of the plant, corresponding with the date of water sample collection.

Tsai et al. (1987) reported that the filterable and nonfilterable solids in chiller water were lowest at the beginning of each day run and then increased rapidly as more carcasses were introduced into the chiller. After 5–6 h of operation a plateau was reached and equilibrium established between solids removed by the overflow water and solid gained from incoming carcasses. Based on this information, two chiller water samples representing 3 and 5 h operation, with high and low COD values, were used for the flocculation study.

The control samples (Table 2), which represent the chiller water without flocculant treatments, were filtered through S&S 604 filter paper. Due to the high content of fat in the chiller water, the filter paper clogged rapidly, especially for the sample with high COD values, in this test. It took 3–4 filtering runs for each sample in order to collect enough filtrate to run chemical analyses. Therefore, for practical purposes, the initial parameter values of chiller water were used as control to evaluate the efficiencies of the flocculation. In this study the efficiency of flocculation was judged by the amount of organic matter (COD) removed from the sample. Table 2 indicates that an average of 42% and 45% of COD, respectively, was removed by flocculant AP-273 from two water

TABLE 2.
INFLUENCE OF DIFFERENT FLOCCULANT TREATMENTS ON COD REMOVAL FROM POULTRY CHILLER WATERS

							Flocculant Treatments			
Chiller Water	Control		AP-273		AP-273 + 0.2% Rice Bran		AP-273 + 0.2% Rice Bran + 0.5 activated carbon		AP-273 + 0.2% Celite	
	Final COD	% COD Removal	Final COD	% COD Removal	Final COD	% COD Removal	Final COD	% COD Removal	Final COD	% COD Removal
Initial			562	43.3	340	65.7	280	74.8	660	33.5
COD	754	23.8	658	33.7	358	63.9	276	72.2	650	34.5
(mg/L)	757	23.8	539	45.7	400	59.7	302	69.6	640	35.5
992			543	45.3	463	53.3	228	77.0	655	34.0
Average		23.8	575.5	42.0	390.3	60.7	271	72.7	651.3	34.4
SD			55.9	5.6	54.6	5.5	31.2	3.6	8.5	0.85
Initial			823	48.0	398	74.8	342	78.4	880	44.4
COD	1358	14.3	975	38.4	488	69.2	321	79.7	984	37.8
(mg/L)	1355	14.3	842	46.8	392	75.2	336	78.8	965	39.0
1582			876	44.6	441	72.1	325	79.4	973	38.5
Average		14.3	879	44.5	429.8	72.8	331	79.0	950.5	39.9
SD			67.7	4.3	44.5	2.8	9.7	0.59	47.6	3.9

Note: All flocculant-treated samples, except control, were run in duplicate. All samples were filtered through a S&S 604 filter paper. Values indicated were based on duplicate analysis of the filtrate of each sample.

SD - Standard deviation

samples with low and high COD values. COD removal was improved to 45%
and 64% by the addition of 0.2% rice bran to the flocculant in the low and high
COD chiller waters, respectively. In another experiment with the same water
samples, in which rice bran was replaced by Celite 505 (diatomaceous earth) in
the presence of the flocculant, the COD removal was lowered by 18% and 10%,
respectively. Lillard (1978) filtered poultry chiller water through diatomaceous
earth in a pressure leaf filter to remove organic matter without flocculation. The
disadvantage of this process is that it could produce large amounts of poultry
waste mixture and might also create a pollution and discharge problem. The
lowering of COD by about 75% in both samples was achieved by the addition
of 0.2% rice bran + 0.5% granular activated carbon (GAC) to the flocculant.
It was also noted that the efficiency of flocculation was improved in samples
with high initial COD values.

Table 3 indicates that the turbidity (suspended particles) of chiller waters,
with NTU values of 280 and 400, were reduced by 75% and 83%, respectively,
using flocculant AP-273. Turbidity was reduced by 90% and 94%, respectively,
through the addition of 0.2% rice bran to enhance flocculation. Rice bran
appeared to adsorb the suspended particles, which were then flocculated by
AP-273. When GAC was additionally included in the flocculant mixture, at least
95% of suspended matter was removed from both water samples. The removal
of suspended particles, in chiller water, would be a beneficial pretreatment to
any filtering process, and especially to prevent potential clogging and tedious
cleaning of the microfilter after use (Hart et al. 1988, 1990).

Figure 1 shows chlorine demand of the chiller water sample with COD
1582 mg/L was decreased by 38% at initial contact time when using flocculant
AP-273 + 0.2% rice bran and was further decreased to about 56% by the
addition of GAC to the flocculant mixture. The use of GAC for the removal of
organics in solution is not new. In Europe, GAC has been used for years to
remove organic traces associated with taste and odors, as well as for color
removal. GAC is a very effective agent for the adsorption of finely suspended
substance in water onto its convoluted surface (McCreary and Aboeyink 1980;
Wilcox et al. 1983). Poultry chiller water has a faster rate of chlorine
disappearance (high chlorine demand) in presence of chicken skin or muscle
tissue. This is due to the reaction of chlorine with leached organic materials
from the tissue or the reaction of chlorine with the tissue (Masri 1986). Table
3 shows 95% of suspended matter was removed by adding GAC in the
flocculant mixture. This indicates that most active organic materials, which
could have reacted with chlorine to form chlorinated organic compounds, were
adsorbed by GAC. Rice bran also adsorbs suspended materials in chiller water
but is not as effective as GAC. There was no change in chlorine demand as the
contact time with the water increased. In contrast, an increase of contact time
resulted in an increase of chlorine demand in experiments with chiller water

TABLE 3.
EFFECT OF FLOCCULANT TREATMENTS ON CONDUCTIVITY AND TURBIDITY OF POULTRY CHILLER WATERS

Chiller Water	Control	Flocculant Treatments		
Initial Conductivity (μS)		AP-273	AP-273 + 0.2% Rice Bran	AP-273 + 0.2% Rice Bran + 0.5% Activated Carbon
640 (COD 992 mg/L)		635	645	638
		638	645	638
	641	640	650	640
	638	637	652	635
Average	639.5	638	648	638
1450 (COD 1582 mg/L)		1443	1432	1443
		1440	1432	1443
	1440	1438	1444	1432
	1442	1440	1455	1430
Average	1441	1440	1441	1437
Initial Turbidity (NTU)				
280 (COD 992 mg/L)		71	26	12
		70	26	12
	195	70	28	13
	196	70	26	12
Average	195.5	70.3	26.5	12.3
400 (COD 1582 mg/L)		67	24	10.5
		67	24	10.5
	289	66	24	10.0
	291	67	23	10.0
Average	290	66.8	23.8	10.1

Note - Values were based on duplicate analysis of the filtrates from the flocculated and control samples indicated in Table 2.
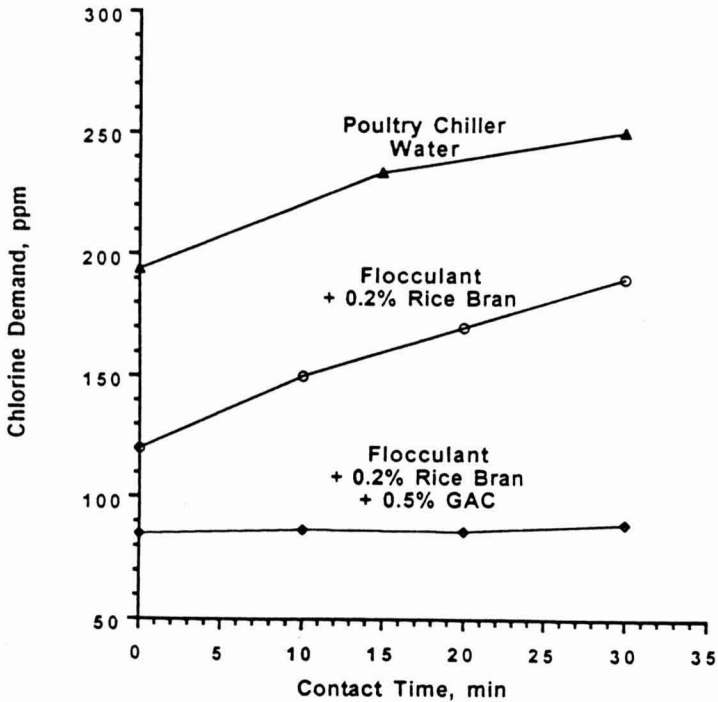
FIG. 1. INFLUENCE OF FLOCCULANT TREATMENTS ON
CHLORINE DEMAND OF POULTRY CHILLER WATER
WITH COD 1582 mg/L AT 1C
GAC = granular activated carbon.

without the use of flocculants (Masri 1986). Some organic compounds in chiller water appear to require longer contact time to react with chlorine (Masri 1986).

Lack of change in conductivity (Table 3) with the addition of rice bran, or rice bran plus GAC to the flocculant AP-273, would indicate that no soluble inorganic minerals were removed by flocculation.

No attempt was made in this study to determine the cost of flocculating poultry chiller water with AP-273 or any other appropriate flocculant. In general, the cost depends on the level of flocculant use. The required amount in this study was extremely small, ranging from 0.5 to 1.0 mg/L. Thus, the beneficial effects may well justify the cost. By contrast, the cost of GAC is relatively high, and the benefits obtained from its use may require further cost justification.

CONCLUSIONS

Flocculation assisted in the removal of 42% and 45% of the COD from poultry chiller water with COD of 992 mg/L and 1582 mg/L, respectively. COD removal was improved to 45% and 64% by the addition of rice bran with flocculant AP-273 for the above samples, respectively. Addition of GAC improved COD removal to 75% in both samples. Efficiency of flocculation was relatively higher in chiller water with higher COD values.

Chlorine demand of the chiller water was decreased by over 56% with the addition of GAC to flocculant AP-273 plus rice bran. Turbidity of the chiller water was reduced by more than 90% when rice bran was used in the flocculation. However, soluble inorganic minerals were not removed by this treatment.

The residue collected after flocculation contained mostly rice bran, chicken blood, fat and body tissue, which may be usable as feed ingredients (without GAC), or as an organic fertilizer after drying.

Flocculation of the poultry chiller water would be a beneficial pretreatment to further recycling processes or to microfiltration with pores less than a half micron in diameter, which will satisfactorily remove the organic matter and the microorganisms when recycling chiller water.

REFERENCES

APHA, AWWA and WPCF. 1985. Standard Methods for the Examination of Water and Wastewater, 16th Ed. APHA, AWWA and WPCF, Washington, D.C.

HART, M.S., HUXSOLL, C.C., TSAI, L.S. and NG, K.C. 1988. Preliminary studies of microfiltration for food processing water reuse. J. Food Prot. 51(4), 269–276.

HART, M.S. et al. 1990. Microfiltration of chicken process waters for reuse: Plant studies and projected operating costs. J. Food Proc. Eng. 12, 191–210.

LILLARD, H.S. 1978. Improving quality of bird chiller water for recycling by diatomaceous earth filtration and chlorination. J. Food Sci. 43(5), 1528–1531.

MASRI, M.S. 1986. Chlorinating poultry chiller water: The generation of mutagens and water reuse. Food Chem. Toxic 24, 923–930.

McCREARY, J.J. and ANOEYINK, V.L. 1980. Granular activated carbon in water treatment. J. Am. Water Works Assoc. 69, 437–444.

MICHAELS, A.S. 1954. Aggregation of suspensions by poly-electrolytes. Ind. Eng. Chem. *46*, 1485–1490.

PURCHASE, D.B. 1971. *Industry Filtration of Liquid*, CRC Press, Cleveland, OH.

ROGERS, C.J. 1978. Recycling of water in poultry processing plants. Technical report EPA-600/ 2-78-039, U.S. Environmental Protection Agency, Cincinnati, OH.

TSAI, L.S., MAPES, C.J. and HUXSOLL, C.C. 1987. Aldehydes in poultry chiller water. Poultry Sci. *52*, 983–989.

USDA. 1976. Meat and Poultry Inspection Regulations. Animal and Plant Inspection Service, Meat and Poultry Program. U.S. Dept. of Agric., Washington, D.C.

Water Quality Report of East Bay Municipal Utility District. 1991. Oakland, CA 94623.

WILCOX, D.F., CHANG, E., DICKSON, K.L. and JOHANSSON, K.R. 1983. Microbial growth associated with granular activated carbon in a pilot water treatment facility. Appl. Environ. Microbiol. *46*, 406–416.

INACTIVATION OF *SACCHAROMYCES CEREVISIAE* IN APPLE JUICE BY SQUARE-WAVE AND EXPONENTIAL-DECAY PULSED ELECTRIC FIELDS

QINGHUA ZHANG[1], ADELMO MONSALVE-GONZÁLEZ[1], BAI-LIN QIN[1], GUSTAVO V. BARBOSA-CÁNOVAS[1,3] and BARRY G. SWANSON[2]

[1]*Department of Biological Systems Engineering*
[2]*Department of Food Science and Human Nutrition*
Washington State University, Pullman, WA 99164-6120

ABSTRACT

With equivalent electrical energy input, inactivation of microorganisms by pulsed electric fields depends on pulse waveform. Exponential-decay and square-wave pulsed electric fields were selected to treat Saccharomyces cerevisiae *suspended in apple juice. A parallel-plate static treatment chamber with 25 ml volume and 0.95 cm electrode gap was used. Peak electric field and pulse electric energy input were 12 kV/cm and 260 Joules per pulse for both waveforms. Both waveforms were found effective in the microbial inactivation. However, inactivation of* S. cerevisiae *treated with square-wave pulses was greater than yeast treated with exponential-decay pulses. For the purpose of food pasteurization, square-wave pulsed electric fields may result in significant energy savings compared to exponential-decay pulses.*

INTRODUCTION

Pulsed electric field (PEF) treatments inactivate microorganisms in food without significant adverse effect on the flavor and taste caused by traditional thermal pasteurization processes (Dunn and Pearlman 1987; Grahl *et al.* 1992; Pothakamury *et al.* 1994; Zhang *et al.* 1994). The lethal effects of PEF are related to electric field intensity, number of pulses and pulse duration (Hülsheger *et al.* 1981; Castro *et al.* 1993), and by the temperature of fluid medium being treated (Dunn and Pearlman 1987; Jayaram *et al.* 1992).

To ensure a nonthermal operation and conserve energy, electric pulse waveform is a PEF operation parameter to be investigated. While most of the previously conducted studies are based on exponential-decay pulses, square-wave

[3]Author to whom correspondence should be addressed.

pulsed electric fields also inactivate microorganisms (Sale and Hamilton 1967). Comparison of the microbial inactivation effects of PEF waveforms is lacking.

There are many possible electrical waveforms. Practical high voltage pulses are generated as exponential-decay, square-wave, and bell-shaped waveforms. Exponential-decay pulses are generated simply by charging and discharging a capacitor. The electric field declines exponentially from the peak value. Square-wave pulses are generated by a series of capacitor-inductor units emulating a transmission line (Valencia 1987) or by a switch-chopping circuit. Bushnell *et al.* (1991) proposed the use of a pulse forming network to generate square-wave high voltage pulses to treat pumpable foods. Bell-shaped pulses are generated by pulse compression technology using saturable inductor switches (Chu and Valencia 1987).

Exponential-decay pulses are widely used due to the simplicity of the circuit. Although the circuits are more complex, the square and bell-shaped waveforms are potentially more energy efficient.

In this study, the effect of exponential-decay and square-wave PEF on the inactivation of *Saccharomyces cerevisiae* is compared. Except for the difference in waveforms, apple juice samples treated with pulsed electric fields of both waveforms were subjected to equivalent treatment conditions, including peak electric field intensity, energy input and fluid temperature.

MATERIALS AND METHODS

Generation of Pulsed Electric Fields

A disk-shaped parallel plate static treatment chamber (Zhang *et al.* 1994) of 25 ml volume and 0.95 cm gap was used to convert the high voltage pulses into high intensity pulsed electric fields.

Exponential-decay pulses were generated by a high voltage pulse generator (Fig. 1), where a 40 kV dc power supply charged a 5.58 μF capacitor bank. The ignitron trigger circuit generates a signal actuating the ignitron, which discharges the capacitors through the fluid inside the treatment chamber. A series resistor of 0.2 Ω and a parallel resistor of 58.6 Ω were selected to adjust the overall load resistance. Apple juice was selected as the food media, and exhibited an electric resistance of 22 $\pm$ 2 Ω in the temperature range of 4 to 10C.

High voltage square-wave pulses were generated by a pulse forming network (PFN) illustrated in Fig. 2. The PFN is essentially a transmission line emulated by a number of inductor-capacitor units. The characteristic impedance of the PFN is:

$$Z_0 = \sqrt{\frac{L}{C}} \qquad (1)$$

where L and C are the inductance and capacitance of discrete elements, respectively. When the characteristic impedance equals the resistance of the selected food, the peak voltage at the right hand side of the ignitron drops to half of the charged capacitor voltage. To obtain an equivalent peak value of voltage applied to the food, the charging voltage of the PFN was set to twice that of the exponential-decay pulse generator.
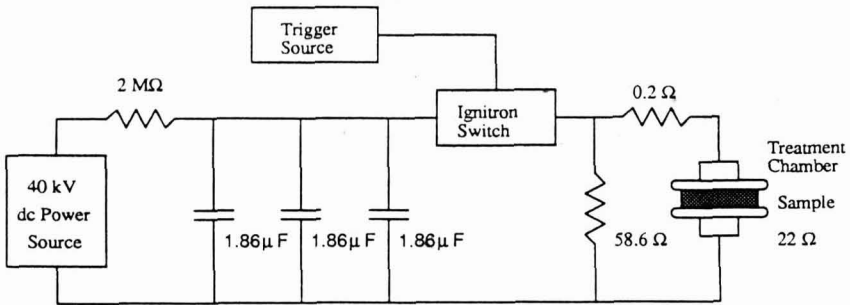
FIG. 1. EXPONENTIAL-DECAY HIGH VOLTAGE PULSE GENERATOR CIRCUIT
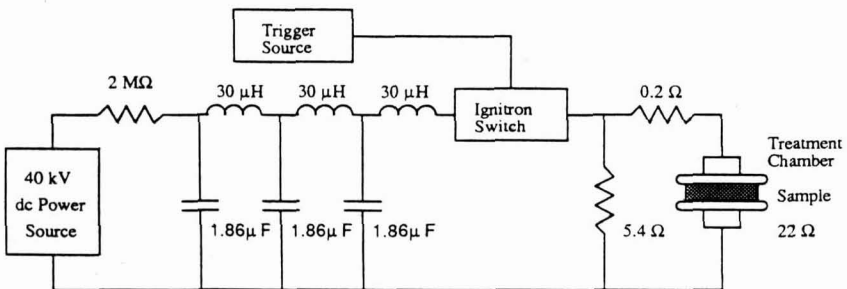
FIG. 2. LAYOUT OF A PULSE FORMING NETWORK OF THREE
CAPACITOR-INDUCTOR UNITS

The electrical energy stored in the capacitor bank can be calculated as:

$$E = \frac{1}{2}CV^2 \tag{2}$$

where V is the voltage of charge. The energy stored in the PFN was four times that of the exponential-decay pulse generator as a result of doubling the voltage charge. To ensure an equivalent amount of electrical energy received by the food, a parallel resistor of 5.4 Ω was inserted to reduce the overall load resistance of the PFN circuit.

Voltage and current waveforms in the food were recorded digitally. Output from a voltage divider and a Rogowski current pickup coil were monitored with an HP54501A digital oscilloscope at a sampling rate of 100 MHz and 8 bit vertical resolution. Communication between the oscilloscope and the computer was via an IEEE-488 bus. To minimize external interference the oscilloscope and computer were placed in a high voltage shielding room.

Typical waveforms of high voltage pulses are illustrated in Fig. 3. The charging voltages for the exponential-decay and square-wave pulses were 12 kV and 24 kV, respectively. Peak electric fields were 12 kV/cm for both waveforms.

Energy input to the food material was computed from the voltage and current measurement as:

$$E_M = \int_0^{400\mu s} vidt \tag{3}$$
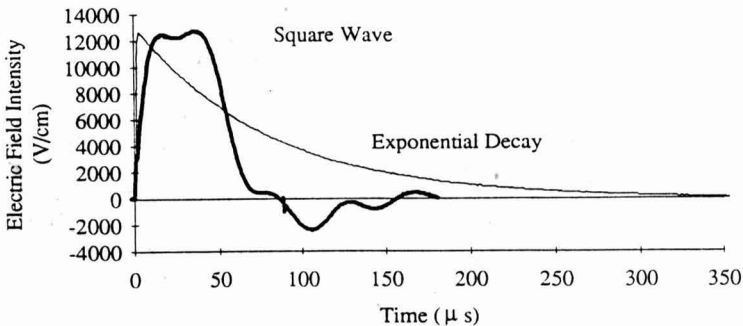
FIG. 3. TYPICAL WAVEFORMS USED IN THIS STUDY
The exponential-decay and square-wave pulse treatments were equivalent in peak electric field of 12 kV/cm.

Typical energy inputs are plotted in Fig. 4. Each exponential-decay pulse delivered total energy of 277.4 J and each square-wave pulse delivered 276.2 J. Food treated with exponential-decay or square-wave pulses received equivalent peak electric field and the energy. Considering 8 kV/cm as the threshold electric field for *S. cerevisiae* (Jacob *et al.* 1981), the energy effective for microbial inactivation was 170 J/pulse and 260 J/pulse for the exponential and square-wave pulses, respectively. Therefore, square-wave pulses are potentially more energy effective than the commonly used exponential-decay pulses.

Microbial Inactivation

Saccharomyces cerevisiae (ATCC 16664) were cultured in yeast malt broth (DIFCO 0711-01-9), continuously agitated in a temperature control shaker (Model MSB-3322A-1, GS Blue Electric, Blue Island, IL) until reaching an absorbance of 210 Klett units (early stationary phase) with a viable count of 80 $\times$ 10^6 cfu/ml. Cells were chilled on ice for 5 min and transferred to a sterile disposable centrifuge tube, centrifuged at 4000 g at 5C for 15 min and the supernatant discarded. The pellet was resuspended and washed with an equal volume of chilled broth and centrifuged at 4000 g at 5C for 15 min. This resuspension and centrifugation procedure was repeated twice. The resultant
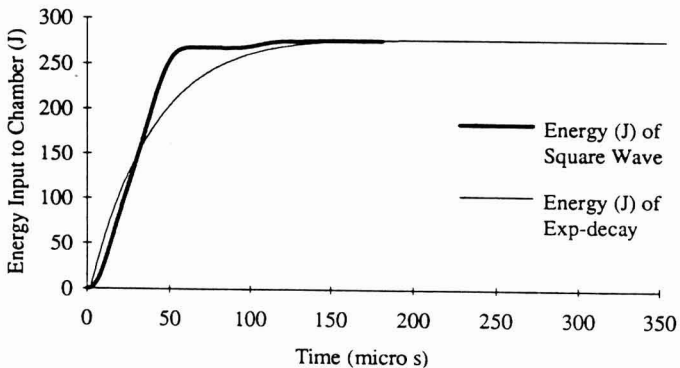
FIG. 4. TYPICAL ACCUMULATED ENERGY RECEIVED BY THE APPLE JUICE WITHIN THE STATIC TREATMENT CHAMBER
The energy of the exponential-decay pulse was 277.4 J/pulse. The energy of square pulse was 276.2 J/pulse.

pellet was resuspended in an equal volume of sterile 20% glycerol and frozen at −30C until further use. Individual frozen pellets of *S. cerevisiae* were activated according to ATCC guidelines and suspended in apple juice at 4C for 30 min before treatment. A recovery test were performed for 6 h with 30 min sample interval at 4C and no change in yeast viability was observed.

The treatment chamber was filled each time with apple juice at a temperature between 4 to 10C. The electrodes were precooled to 4C before filling. Gas bubbles were eliminated before application of PEF. Time between pulses was controlled to keep the electrode temperature below 8C. Cooling water temperature was set at 4C. After each batch of apple juice, the treatment chamber was washed with 70% sterile alcohol solution and sterile distilled water.

Inactivation of yeast was reported as survival fractions

$$S = \frac{V_s}{V_u} \tag{4}$$

where V_u and V_s are viabilities before and after PEF treatment.

The viability of the *S. cerevisiae* before and after treatments was assayed by counting colony forming units (cfu). Each frozen pellet was hydrated into 40 ml apple juice. While filling the treatment chamber with 25 ml apple juice, a 1 ml aliquot of apple juice was taken from the 40 ml batch to assay yeast viability in untreated apple juice. This untreated sample was serially diluted with appropriate broth, 1 ml of the dilution plated on potato dextrose agar without acid and incubated for 72 h. After PEF treatment a 1 ml aliquot of apple juice was taken from the treatment chamber and serially diluted with appropriate broth; a 1 ml portion of the dilution was plated on potato dextrose agar without acid and incubated for 72 h. The dilution for the viable counts was selected to achieve 25–100 cfu/plate. Each count was calculated from a mean of four plates. Apple juice was treated with 12 kV/cm PEF for a selected number of pulses, 1, 3, 6, 9, 15, and 20. Each treatment was triplicated.

RESULTS AND DISCUSSION

Pulsed electric fields with both exponential-decay and square waveforms inactivated *S. cerevisiae*. Figure 5 illustrates the survival fraction of *S. cerevisiae* as a function of the number of pulses at 12 kV/cm with exponential-decay and square-waveforms. Survival fraction of inoculated apple juice treated by square-wave pulses is significantly smaller than survival fraction of inoculated apple juice treated by exponential-decay pulses (F = 10.66, F_c = 5.05, α = 0.05). Square-wave pulses resulted an average of 60% more
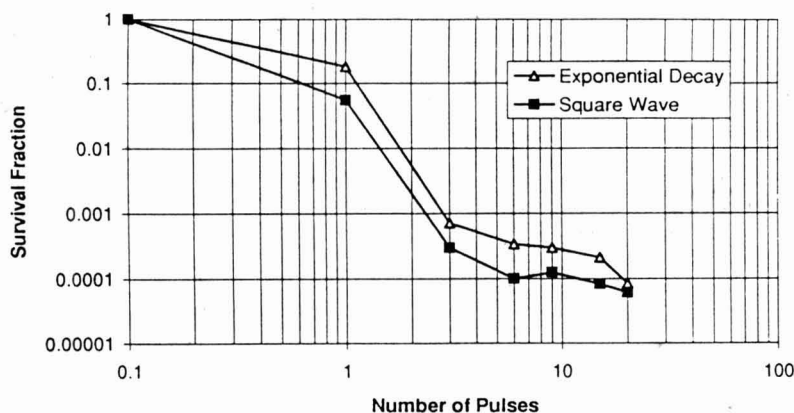
FIG. 5. SURVIVAL FRACTION OF *S. CEREVISIAE* AFTER PEF TREATMENT IN THE
WAVEFORMS OF EXPONENTIAL-DECAY AND SQUARE-WAVE
Electric field strength is 12 kV/cm. Pulse width is 90 μs for exponential-decay pulses and
60 μs for square-wave pulses. Each data point represents an average of three samples.

inactivation than exponential-decay pulse waveform with the equivalent electric field and energy. At 20 pulse treatment, however, both waveforms resulted in similar microbial inactivation.

To achieve microbial inactivation, applied electric field needs to be greater than the critical electric field for a particular microorganism (Castro *et al.* 1993). Jacob *et al.* (1981) determined the critical electric field for inactivation of *S. cerevisiae* to be 8 kV/cm at 21C using 20 μs pulses, in a 0.9% NaCl solution with an initial *S. cerevisiae* concentration of 2500 cfu/ml.

When the electric field (E) is below the 8 kV/cm critical electric field (Castro *et al.* 1993), energy delivered to the food is not utilized and implies unnecessary heating to the food. The total energy delivered by a square-wave pulse was 276.2 J. The amount of energy, when E > 8 kV/cm, was 252.2 J per pulse. The energy efficiency for the square-wave pulse treatment was 91%. On the other hand, the amount of energy for an exponential-decay pulse, when E > 8 kV/cm, was 176.5 J and the total energy was 277.4 J per pulse. Energy efficiency for the exponential-decay pulse treatment was 64%. This energy efficiency analysis was confirmed by the experimental microbial inactivation results.

For many microorganisms, survival fraction (*s*) is related to the number of pulses (*n*) and electric fields (*E*) by an empirical equation (Hülsheger *et al.* 1981).

$$s = \left[\frac{n\tau}{t_c}\right]^{(E-E_c)} k \tag{5}$$

where t_c and E_c are the critical treatment time and critical electric field, τ is the pulse width, and k is an empirical constant. For a fixed electric field, a pulse width and a treatment temperature, survival fraction (*s*) relates to the number of pulses (*n*) linearly in a log-log fashion as

$$\log(s) = -\frac{E-E_c}{K}\log(n) + \log(\tau_c) - \log(t_c) \tag{6}$$

Figure 5 illustrates that there is no reduction in survival fraction after four log cycles of inactivation, a fact that is not described by Eq. (6). This phenomenon could be related to two hypotheses, the protection mechanism and the regeneration mechanism. An initial concentration test was designed to reveal whether microbial survival fraction is affected by initial inoculation of yeast.

Figure 6 presents PEF microbial inactivation as a function of initial microbial load. Initial concentrations of *S. cerevisiae* were set at 10^6, 10^5, and 10^4 cfu/ml, and treatments were selected at an electric field of 25 kV/cm and a pulse width of 25 μs. The initial concentration of *S. cerevisiae* was inversely correlated with survival fraction under the selected treatment conditions, suggesting that initial inoculation does affect the survival fraction with the same pulsed electric field treatment. With the same pulse treatment and initial inoculation, Matsumoto *et al.* (1991) demonstrated that agitation in the treatment chamber resulted in increased inactivation. The effect of initial inoculation and agitation are secondary evidence of cluster type of protection mechanism. We also observed visible precipitation for 10^6 and higher initial yeast concentrations in inoculated apple juice. A high speed microphotography is recommended to obtain direct evidence of cluster protection mechanism.

CONCLUSIONS

Pulse waveform affects microbial inactivation by pulsed electric fields. Square-wave pulses demonstrated a higher rate of microbial inactivation on *S. cerevisiae* than exponential-decay pulses. Increased initial *S. cerevisiae* inoculation load resulted in lower microbial inactivation.
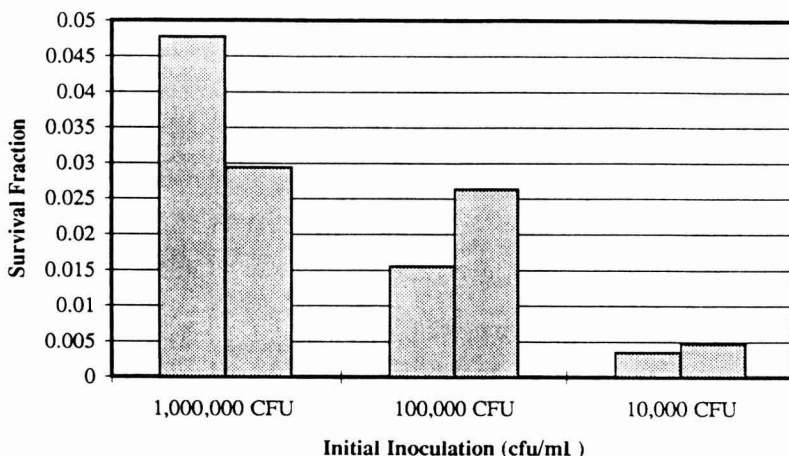
FIG. 6. EFFECT OF INITIAL CONCENTRATION ON THE INACTIVATION
OF *S. CEREVISIAE*
Electric field strength was 25 kV/cm, and apple juice temperature was 7C.

ACKNOWLEDGMENT

REFERENCES

CASTRO, A.J., BARBOSA-CÁNOVAS, G.V. and SWANSON, B.G. 1993. Microbial inactivation of foods by pulsed electric fields. J. Food Processing Preservation *17*, 47–73.

BUSHNELL, A.H., DUNN, J.E., LA COSTA, R., CLARK, R. W. and MAR, D. 1991. High pulsed voltage systems for extending the shelf life of pumpable food products. U.S. Pat. 5,048,404.

CHU, E.Y. and VALENCIA, V.I. 1987. Saturable inductor switch and pulse compression power supply employing the switch. U.S. Pat. 4,707,619.

DUNN, J.E. and PEARLMAN, J.S. 1987. Methods and apparatus for extending the shelf life of fluid food products. U.S. Pat. 4,695,472.

GRAHL, T., SITZMANN, W. and MÄRKL, H. 1992. Killing of microorganisms in fluid media by high-voltage pulses. DECHEMA Biotechnol. Conf. Ser., *5B*, 675–678.

HÜLSHEGER, H., POTEL, J. and NIEMANN, E.G. 1981. Killing of bacteria with electric pulses of high field strength. Radiat. Environ. Biophys. *20*, 53–65.

JACOB, H.E., FORSTER, W. and BERG, H. 1981. Microbiological implications of electric field effects. II. Inactivation of yeast cells and repair of their cell envelope. Z. Allg. Mikrobiol. *21*, 225–233.

JAYARAM, S., CASTLE. G.S.P. and MARGARITIS, A. 1992. Kinetics of sterilization of *Lactobacillus brevis* by the application of high voltage pulses. Biotech. Bioeng. *40*(11), 1412–1420.

MATSUMOTO, Y., SATAKE, T., SHIOJI, N. and SAKUMA, A. 1991. Inactivation of microorganisms by pulsed high voltage applications. Conference Record of IEEE Industrial Applications Society Annual Meeting, pp. 652–659.

POTHAKAMURY, U.R., MONSALVE-GONZÁLEZ, A., BARBOSA-CÁNOVAS, G.V. and SWANSON, B.G. 1994. Inactivation of *Escherichia coli* and *Staphylococcus aureus* in model foods by pulsed electric field technology. Food Preservation 2000 Proceedings, Natick, MA.

SALE, A.J.H. and HAMILTON, W.A. 1967. Effects of high electric fields on microorganisms. I. Killing of bacteria and yeasts. Biochim. Biophys. Acta *148*, 781–788.

VALENCIA, V.I. 1987. Symmetrically charged pulse-forming circuit. U.S. Pat. 4,684,820.

ZHANG, Q., MONSALVE-GONZÁLEZ, A., BARBOSA-CÁNOVAS, G.V. and SWANSON, B.G. 1994. Inactivation of *E. coli* and *S. cerevisiae* by pulsed electric fields under controlled temperature conditions. Trans. ASAE *37*(2), 581–587.

AUTHOR INDEX

SUBJECT INDEX

F
N
P PUBLICATIONS IN
FOOD SCIENCE AND NUTRITION

Journals

JOURNAL OF FOOD LIPIDS, F. Shahidi

JOURNAL OF RAPID METHODS AND AUTOMATION IN MICROBIOLOGY,
   D.Y.C. Fung and M.C. Goldschmidt

JOURNAL OF MUSCLE FOODS, N.G. Marriott and G.J. Flick, Jr.

JOURNAL OF SENSORY STUDIES, M.C. Gacula, Jr.

JOURNAL OF FOODSERVICE SYSTEMS, C.A. Sawyer

JOURNAL OF FOOD BIOCHEMISTRY, J.R. Whitaker, N.F. Haard and H. Swaisgood

JOURNAL OF FOOD PROCESS ENGINEERING, D.R. Heldman and R.P. Singh

JOURNAL OF FOOD PROCESSING AND PRESERVATION, D.B. Lund

JOURNAL OF FOOD QUALITY, J.J. Powers

JOURNAL OF FOOD SAFETY, T.J. Montville

JOURNAL OF TEXTURE STUDIES, M.C. Bourne

Books

MEAT PRESERVATION: PREVENTING LOSSES AND ASSURING SAFETY,
   R.G. Cassens

S.C. PRESCOTT, M.I.T. DEAN AND PIONEER FOOD TECHNOLOGIST,
   S.A. Goldblith

FOOD CONCEPTS AND PRODUCTS: JUST-IN-TIME DEVELOPMENT, H.R. Moskowitz

MICROWAVE FOODS: NEW PRODUCT DEVELOPMENT, R.V. Decareau

DESIGN AND ANALYSIS OF SENSORY OPTIMIZATION, M.C. Gacula, Jr.

NUTRIENT ADDITIONS TO FOOD, J.C. Bauernfeind and P.A. Lachance

NITRITE-CURED MEAT, R.G. Cassens

POTENTIAL FOR NUTRITIONAL MODULATION OF AGING, D.K. Ingram *et al.*

CONTROLLED/MODIFIED ATMOSPHERE/VACUUM PACKAGING OF
   FOODS, A.L. Brody

NUTRITIONAL STATUS ASSESSMENT OF THE INDIVIDUAL, G.E. Livingston

QUALITY ASSURANCE OF FOODS, J.E. Stauffer

THE SCIENCE OF MEAT AND MEAT PRODUCTS, 3RD ED., J.F. Price and
   B.S. Schweigert

HANDBOOK OF FOOD COLORANT PATENTS, F.J. Francis

ROLE OF CHEMISTRY IN THE QUALITY OF PROCESSED FOODS,
   O.R. Fennema, W.H. Chang and C.Y. Lii

NEW DIRECTIONS FOR PRODUCT TESTING OF FOODS, H.R. Moskowitz

PRODUCT TESTING AND SENSORY EVALUATION OF FOODS, H.R. Moskowitz

ENVIRONMENTAL ASPECTS OF CANCER: ROLE OF MACRO AND MICRO
   COMPONENTS OF FOODS, E.L. Wynder *et al.*

FOOD PRODUCT DEVELOPMENT IN IMPLEMENTING DIETARY
   GUIDELINES, G.E. Livingston, R.J. Moshy, and C.M. Chang

SHELF-LIFE DATING OF FOODS, T.P. Labuza

ANTINUTRIENTS AND NATURAL TOXICANTS IN FOOD, R.L. Ory

UTILIZATION OF PROTEIN RESOURCES, D.W. Stanley *et al.*

VITAMIN B_6: METABOLISM AND ROLE IN GROWTH, G.P. Tryfiates

POSTHARVEST BIOLOGY AND BIOTECHNOLOGY, H.O. Hultin and M. Milner

Newsletters

MICROWAVES AND FOOD, R.V. Decareau

FOOD INDUSTRY REPORT, G.C. Melson

FOOD, NUTRITION AND HEALTH, P.A. Lachance and M.C. Fisher

FOOD PACKAGING AND LABELING, S. Sacharow

UNITED STATES POSTAL SERVICE™

Statement of Ownership, Management, and Circulation
(Required by 39 U.S.C. 3685)

1. Publication Title	2. Publication No.	3. Filing Date
Journal of Food Process Engineering	0 1 4 5 - 8 8 7 6	Oct. 1, 1994

4. Issue Frequency	5. No. of Issues Published Annually	6. Annual Subscription Price
Quarterly	4	$132.00

7. Complete Mailing Address of Known Office of Publication *(Street, City, County, State, and ZIP+4) (Not Printer)*
2 Corporate Drive, POB 374
Trumbull, Fairfield, Connecticut 06611-0374

8. Complete Mailing Address of Headquarters or General Business Office of Publisher *(Not Printer)*
2 Corporate Drive, POB 374
Trumbull, Connecticut 06611-0374

9. Full Names and Complete Mailing Addresses of Publisher, Editor, and Managing Editor *(Do Not Leave Blank)*
Publisher *(Name and Complete Mailing Address)*
John J. O'Neil
2 Corporate Drive, POB 374
Trumbull CT 06611

Editor *(Name and Complete Mailing Address)*
Dr. Dennis P Heldman
253 Agricultural Engineering, Missouri University
Columbia, MO 65211

Managing Editor *(Name and Complete Mailing Address)*
Dr. R. Paul Singh
Dept. of Agricultural Engineering
University of California, Davis, CA 95616

10. Owner *(If owned by a corporation, its name and address must be stated and also immediately thereafter the names and addresses of stockholders owning or holding 1 percent or more of the total amount of stock. If not owned by a corporation, the names and addresses of the individual owners must be given. If owned by a partnership or other unincorporated firm, its name and address as well as that of each individual must be given. If the publication is published by a nonprofit organization, its name and address must be stated.) (Do Not Leave Blank.)*

Full Name	Complete Mailing Address
Food & Nutrition Press, Inc.	2 Corporate Drive, POB 374, Trumbull, CT 06611
John J. O'Neil	53 Stonehouse Road, Trumbull, CT 06611
Michael J. Tully	3 N. Slope, Union Gap, Clinton, NJ 08809
Kathryn & Christopher Ziko	8 Maria Alicia Dr., Huntington, CT 06484
John J. O'Neil, Jr.	115 Maureen St., Stratford, CT 06497

11. Known Bondholders, Mortgagees, and Other Security Holders Owning or Holding 1 Percent or More of Total Amount of Bonds, Mortgages, or Other Securities. If none, check here. ☐ None
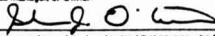
Full Name	Complete Mailing Address
None	

13. Publication Name	14. Issue Date for Circulation Data Below
Journal of Food Process Engineering	11-10-93,1-3-94,3-4-94,6-16-94,9-23-94

15.

Extent and Nature of Circulation	Average No. Copies Each Issue During Preceding 12 Months	Actual No. Copies of Single Issue Published Nearest to Filing Date
a. Total No. Copies *(Net Press Run)*	400	400
b. Paid and/or Requested Circulation (1) Sales Through Dealers and Carriers, Street Vendors, and Counter Sales *(Not Mailed)*	0	0
(2) Paid or Requested Mail Subscriptions *(Include Advertisers' Proof Copies/Exchange Copies)*	252	257
c. Total Paid and/or Requested Circulation *(Sum of 15b(1) and 15b(2))*	252	257
d. Free Distribution by Mail *(Samples, Complimentary, and Other Free)*	53	53
e. Free Distribution Outside the Mail *(Carriers or Other Means)*	0	0
f. Total Free Distribution *(Sum of 15d and 15e)*	53	53
g. Total Distribution *(Sum of 15c and 15f)*	305	310
h. Copies Not Distributed (1) Office Use, Leftovers, Spoiled	95	90
(2) Return from News Agents	0	0
i. Total *(Sum of 15g, 15h(1), and 15h(2))*	400	90
Percent Paid and/or Requested Circulation *(15c / 15g x 100)*	83%	83%

16. This Statement of Ownership will be printed in the Vol. 17, No.4 **issue of this publication.** ☐ Check box if not required to publish.

17. Signature and Title of Editor, Publisher, Business Manager, or Owner

John J. O'Neil, Publisher *[signature]* Date: October 1, 1994

I certify that all information furnished on this form is true and complete. I understand that anyone who furnishes false or misleading information on this form or who omits material or information requested on the form may be subject to criminal sanctions *(including fines and imprisonment)* and/or civil sanctions *(including multiple damages and civil penalties).*

Instructions to Publishers

1. Complete and file one copy of this form with your postmaster on or before October 1, annually. Keep a copy of the completed form for your records.

2. Include in items 10 and 11, in cases where the stockholder or security holder is a trustee, the name of the person or corporation for whom the trustee is acting. Also include the names and addresses of individuals who are stockholders who own or hold 1 percent or more of the total amount of bonds, mortgages, or other securities of the publishing corporation. In item 11, if none, check box. Use blank sheets if more space is required.

3. Be sure to furnish all information called for in item 15, regarding circulation. Free circulation must be shown in items 15d, e, and f.

4. If the publication had second-class authorization as a general or requester publication, this Statement of Ownership, Management, and Circulation must be published; it must be printed in any issue in October or the first printed issue after October, if the publication is not published during October.

5. In item 16, indicate date of the issue in which this Statement of Ownership will be printed.

6. Item 17 must be signed.

Failure to file or publish a statement of ownership may lead to suspension of second-class authorization.

PS Form 3526, October 1994 *(Reverse)*

GUIDE FOR AUTHORS

Typewritten manuscripts in triplicate should be submitted to the editorial office. The typing should be double-spaced throughout with one-inch margins on all sides.

Page one should contain: the title, which should be concise and informative; the complete name(s) of the author(s); affiliation of the author(s); a running title of 40 characters or less; and the name and mail address to whom correspondence should be sent.

Page two should contain an abstract of not more than 150 words. This abstract should be intelligible by itself. The main text should begin on page three and will ordinarily have the following arrangement:

Introduction: This should be brief and state the reason for the work in relation to the field. It should indicate what new contribution is made by the work described.

Materials and Methods: Enough information should be provided to allow other investigators to repeat the work. Avoid repeating the details of procedures that have already been published elsewhere.

Results: The results should be presented as concisely as possible. Do not use tables *and* figures for presentation of the same data.

Discussion: The discussion section should be used for the interpretation of results. The results should not be repeated.

In some cases it might be desirable to combine results and discussion sections.

References: References should be given in the text by the surname of the authors and the year. *Et al.* should be used in the text when there are more than two authors. All authors should be given in the Reference section. In the Reference section the references should be listed alphabetically. See below for style to be used.

RIZVI, S.S.H. 1986. Thermodynamic properties of foods in dehydration. In *Engineering Properties of Foods*, (M.A. Rao and S.S.H. Rizvi, eds.) pp. 133–214, Marcel Dekker, New York.

MICHAELS, S.L. 1989. Crossflow microfilters ins and outs. Chem. Eng. *96*, 84–91.

LABUZA, T.P. 1982. *Shelf-Life Dating of Foods,* pp. 66–120, Food & Nutrition Press, Trumbull, CT.

Journal abbreviations should follow those used in *Chemical Abstracts.* Responsibility for the accuracy of citations rests entirely with the author(s). References to papers in press should indicate the name of the journal and should only be used for papers that have been accepted for publication. Submitted papers should be referred to by such terms as "unpublished observations" or "private communication." However, these last should be used only when absolutely necessary.

Tables should be numbered consecutively with Arabic numerals. The title of the table should appear as below:

TABLE 1.

ACTIVITY OF POTATO ACYL-HYDROLASES ON NEUTRAL LIPIDS,
GALACTOLIPIDS AND PHOSPHOLIPIDS

Description of experimental work or explanation of symbols should go below the table proper. Type tables neatly and correctly as tables are considered art and are not typeset. Single-space tables.

Figures should be listed in order in the text using Arabic numbers. Figure legends should be typed on a separate page. Figures and tables should be intelligible without reference to the text. Authors should indicate where the tables and figures should be placed in the text. Photographs must be supplied as glossy black and white prints. Line diagrams should be drawn with black waterproof ink on white paper or board. The lettering should be of such a size that it is easily legible after reduction. Each diagram and photograph should be clearly labeled on the reverse side with the name(s) of author(s), and title of paper. When not obvious, each photograph and diagram should be labeled on the back to show the top of the photograph or diagram.

Acknowledgments: Acknowledgments should be listed on a separate page.

Short notes will be published where the information is deemed sufficiently important to warrant rapid publication. The format for short papers may be similar to that for regular papers but more concisely written. Short notes may be of a less general nature and written principally for specialists in the particular area with which the manuscript is dealing. Manuscripts that do not meet the requirement of importance and necessity for rapid publication will, after notification of the author(s), be treated as regular papers. Regular papers my be very short.

Standard nomenclature as used in the engineering literature should be followed. Avoid laboratory jargon. If abbreviations or trade names are used, define the material or compound the first time that it is mentioned.

EDITORIAL OFFICE: DR. D.R. HELDMAN, COEDITOR, *Journal of Food Process Engineering*, Food Science/Engineering Unit, University of Missouri-Columbia, 235 Agricultural/Engineering Bldg., Columbia, MO 65211 USA; or DR. R.P. SINGH, COEDITOR, *Journal of Food Process Engineering*, University of California, Davis, Department of Agricultural Engineering, Davis, CA 95616 USA.

CONTENTS